Effects and Possible Mechanisms of Some Phytochemicals on *Drosophila* Models of Alzheimer's Disease

Major in Entomology

Department of Agricultural Biotechnology, Seoul National University

Xue Wang

ABSTRACT

Alzheimer's disease (AD) is the most common type of presenile and senile dementia in developed and developing countries. The human β-amyloid (Aβ) cleaving enzyme (BACE-1) is a key enzyme responsible for amyloid plaque production, which implicates the progress and symptoms of AD. In this study, a fluorescence resonance energy transfer (FRET)-based enzyme assay was used to identify the BACE-1 inhibitory constituents from methanol extracts from the rhizomes of turmeric, *Curcuma longa* L. (Zingiberaceae), and the whole blue licorice (Korean mint) plant, *Agastache rugosa* (Fisch. & C.A. Mey.) O. Kuntze (Lamiaceae). The active constituents were determined to be the curcuminoids, diarylalkyls curcumin (CCN), demethoxycurcumin (DMCCN) and bisdemethoxycurcumin (BDMCCN) from *C. longa* rhizomes, and the *O*-methylated flavone, acacetin, and the oleanane triterpenoids, maslinic acid and oleanolic acid from whole *A. rugosa* plants. BDMCCN exhibited the strongest inhibitory activity toward BACE-1 with IC_{50} 17 μM, which was 20 and 13-fold more potent than those of CCN and DMCCN, respectively. Quantitative structure–activity relationship of the curcuminoids indicates that structural characteristics, such as degrees of saturation, types of carbon

skeleton and functional group, and hydrophobicity rather than molecular weight appear to play a role in determining inhibitory potency of curcuminoids on BACE-1. Acacetin was a 4.0-fold and 5.5-fold more potent inhibitor of BACE-1 than oleanolic acid and maslinic acid, respectively. Overall, these compounds were significantly less potent inhibitors of BACE-1 than a positive control, the cell-permeable isophthalamide, BACE-1 inhibitor IV.

To assess the neuro-protective ability of the curcuminoids and acacetin, the *Drosophila melanogaster* models of AD were constructed and characterized by phenotypes, histological analysis, and reverse transcription polymerase chain reaction (RT-PCR). *Drosophila* model system overexpressed BACE-1 and its substrate amyloid precursor protein (APP) in compound eyes and entire neurons. Overexpression of APP/BACE-1 resulted in the progressive and measurable defects in morphology of eyes and locomotion. The feeding, climbing activity, lifespan, and morphological changes in fly eyes were also evaluated. Remarkably, supplementing diet with either BDMCCN, CCN, and acacetin rescued APP/BACE-1-expressing flies and kept them from developing both eye morphology (dark deposits, ommatidial collapse and fusion, and the absence of ommatidial bristles) and behavioral (motor abnormalities) defects.

Acacetin's mechanisms of action on transgenic *Drosophila* model of AD were also determined. The real-time RT-PCR analysis revealed that acacetin reduced both the human *APP* and *BACE-1* mRNA levels in the transgenic flies, suggesting that it plays an important role in the transcriptional regulation of human *BACE-1* and *APP*. Western blot analysis revealed that acacetin reduced Aβ production by interfering with BACE-1 activity and APP synthesis, resulting in a decrease in the levels of the APP carboxy-terminal fragments and the APP intracellular domain. Therefore, the protective effect of acacetin on Aβ production is mediated by transcriptional regulation of *BACE-1*

and *APP*, resulting in decreased APP protein expression and BACE-1 activity. Acacetin also inhibited APP synthesis, resulting in a decrease in the number of amyloid plaques.

In conclusion, *C. longa* rhizome-derived curcuminoids and whole *A. rugosa* plant-derived acacetin are potential therapeutics or lead compounds for the prevention or treatment of AD. The anti-AD action of these compounds provides an indication of at least one of the pharmacological actions of *C. longa* and *A. rugosa*. Detailed tests are needed to understand how to improve the anti-AD potency and stability of the compounds isolated from *C. longa* and *A. rugosa* for eventual commercial development.

Key words: Alzheimer's disease, *Drosophila melanogaster*, BACE-1, *Curcuma longa*, *Agastache rugosa*, curcuminoid, acacetin, mechanisms of action

Student number: 2009-23972

INTRODUCTION

Alzheimer's disease (AD) is the most common cause of presenile and senile dementia in developed and developing countries (Ferri *et al.,* 2005; Kalaria *et al.,* 2008). Worldwide, the number of people with dementia was estimated to be 35.6 million in 2010; this figure is expected to reach 115.4 million by 2050 (Prince and Jackson, 2009). The major histopathological hallmarks of AD are neurofibrillary tangles (NFTs) composed of hyperphosphorylated tau protein filaments, and extracellular senile plaques, which are deposits of β-amyloid (Aβ) generated via sequential proteolytic processing of the transmembrane amyloid precursor protein (APP) by two enzymes in the amyloidogenic processing pathway, namely β-secretase (β-amyloid (Aβ) precursor cleavage enzyme or BACE-1) and γ-secretase (Hardy and Selkoe, 2002; Suk and Checler, 2002; Baptista *et al*., 2014).

AD is currently treated using acetylcholinesterase (AChE) inhibitors (Birks, 2006) and *N*-methyl-D-aspartate (NMDA) receptor antagonists (Molinuevo *et al.,* 2005; Danysz and Parsons, 2012). However, these treatments have serious side effects and do not stop the disease process or prevent neuronal degeneration (Molinuevo *et al.,* 2005; Thompson *et al.,* 2004; Paris *et al.,* 2011). BACE-1 is considered a primary target for preventing and treating AD (Cole and Vassar, 2007; Ghosh *et al.,* 2008; Manicini *et al.,* 2011). Many peptidomimetics and heterocyclic compounds have been evaluated as BACE-1 inhibitors (Thompson *et al*., 2005; John, 2006; Orhan, 2012); however, none of these have been successfully developed as anti-AD drugs. Therefore, there is a pressing need to develop new improved anti-AD agents.

Natural compounds from plant extracts have been suggested as alternative sources for

anti-AD drugs. This approach is appealing, in part, because plants are sources of bioactive secondary metabolites that are perceived by the general public as relatively safe, and that act on multiple, novel target sites (Rate, 2001; Raskin *et al.,* 2002). Certain plant preparations and their constituents are regarded as potential sources for commercial anti-AD products to prevent or treat AD. Plant-derived BACE-1 and AChE inhibitors have been well documented by Orhan (2012) and Mukherjee *et al*. (2007), respectively. Recently, plants in the family Zingiberaceae have drawn attention because they contain anti-AD principles (Lee *et al.,* 2010; Caesar *et al.,* 2012). The rhizomes of turmeric, *Curcuma longa* L., are not only important as a spice or flavoring, but they have also been prescribed for indigestion, hepatitis, jaundice, diabetes, atherosclerosis, and bacterial infection (Tang and Eisenbrand, 1992; Araújo and Leon, 2001; Kuhn and Winston, 2001). Previous studies have shown that a methanol extract from the whole blue licorice (Korean mint) plant, *Agastache rugosa* (Fisch. & C.A. Mey.) O. Kuntze (Lamiaceae), possessed human BACE-1 inhibitory activity. Historically, this plant species has been used to treat cholera, vomiting, and miasma (Zielinska and Matkowski, 2014). No previous studies have investigated the potential use of *A. rugosa* for managing AD, although the phytochemistry and bioactivity of plants in the genus *Agastache* have been well documented by Zielinska and Matkowski (2014).

In this study, an assessment was made of the BACE-1 inhibitory activity of the three curcuminoids [curcumin (CCN), demethoxycurcumin (DMCCN), and bisdemethoxycurcumin (BDMCCN)] isolated from *C. longa* rhizomes, as well as acacetin, maslinic acid, and oleanolic acid, extracted from the whole *A. rugosa* plants, using a fluorescence resonance energy transfer (FRET) enzyme assay. Trans-human *APP* and *BACE-1* genes *Drosophila* were constructed based on UAS-GAL4 system and

characterized that could be used as models of AD. The effects of the two curcuminoids (CCN and BDMCCN) and acacetin on feeding, climbing, eclosion rate, life span, and morphological changes in the compound eyes of flies which express human *APP* and *BACE-1* genes within the developing nervous system and compound eyes were assessed. The quantitative structure–activity relationship (QSAR) of the curcuminoids also are discussed. In addition, the morphological changes in the compound eyes of the transgenic flies were examined using light microscopy and scanning electron microscopy (SEM). Finally, the possible mechanism underlying the anti-AD actions of acacetin was elucidated using real-time quantitative reverse transcription polymerase chain reaction (qRT-PCR) and western blot analyses.

LITERATURE REVIEW

1. Alzheimer's disease

1.1. Introduction of Alzheimer's disease

AD is a type of dementia that is characterized by causing problems with memory, thinking, and behavior. These symptoms usually develop slowly, and as the time goes on, they will get worse and interfere with daily life. AD was first described in 1906 by a German physician Alois Alzheimer. In 1910, Emil Kraepelin, a German psychiatrist who worked with Dr. Alzheimer, first named "Alzheimer's Disease" in the eighth edition of his book Psychiatrie (Hippius, 2003). AD accounts for 60–70% of dementia cases (Burns and Lliffe, 2009; WHO, 2015), and vascular disease is the second most common cause, accounting for 10%. Other dementia and conditions, including dementia with Lewy bodies, Parkinson's disease, mixed dementia, frontotemporal lobar degeneration, Creutzfeldt-Jakob disease, and normal pressure hydrocephalus, account for the remaining 13% (Alzheimer's Association, 2014).

1.2. Pathological hallmarks of Alzheimer's disease

There are two hallmarks of AD, amyloid plaques and neurofibrillary tangles (NFTs) (Fig. 1). Amyloid plaques are abnormal cluster of peptide fragments (Aβ), built up between nerve cells, whereas NFTs are found inside the neurons and are abnormal collections of protein tau (Silbert, 2007). Normal tau proteins can stabilize microtubules. However, abnormal hyperphosphorylated tau protein separate from the microtubules and collection to generate NFTs.

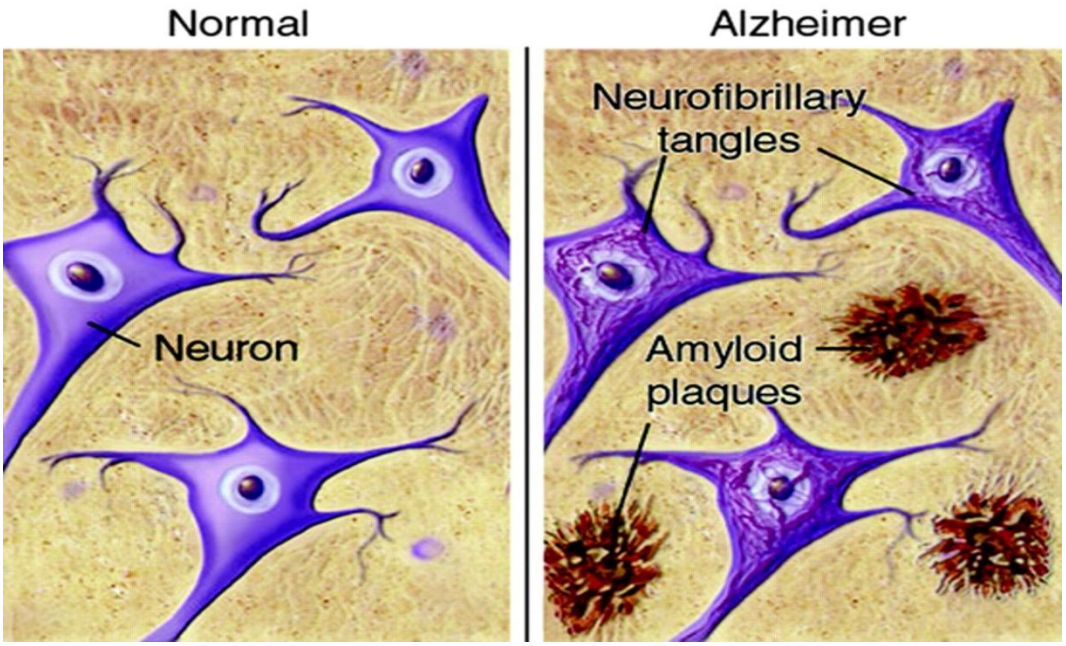

Fig. 1. Neuropathological hallmarks of Alzheimer's disease.

1.3. Epidemiology and worldwide death rate of Alzheimer's disease

In 2009, the 5.6 million people worldwide are living with AD and another dementia. The number is expected to grow sharply to 65.7 million in 2030 and 115.4 million in 2050 (Prince *et al.*, 2009). The prevalence rate of dementia was estimated to be 5–8% in people with the age over 60 years old, 15–20% in people over age 75, and 25–50% in people over age 85 (Duthey, 2013). The regional prevalence in individuals over the age of 60 years are 6.4% in North America, 5.4% in Western Europe, and 4.6% in Latin America, followed by 4.0% in China and Western Pacific regions and 1.6% in Africa (Qui *et al*., 2009). The prevalence of dementia in developed countries is higher than in developing countries that maybe due to the exposure rate to cerebrovascular risk factor like smoking, obesity, hypertension and diabetes (Ferri *et al*., 2005; Rizzi *et al*., 2014). The incidence of AD is related to both age and gender. As described by Alzheimer's Association (2014), more women are suffering AD and other dementias than men, and about two-third of Americans with AD are women about 3.2 million and 1.8 million are men. The reason of

this phenomenon is not simply due to the higher life span of women than men. The mitochondria in young females are protected from Aβ toxicity, release less apoptogenic signals, and form less reactive oxygen species indicating estrogenic action may be important in protecting cells against Aβ toxicity (Viña and Lloret, 2010).

1.4. Risk factors and causes for Alzheimer's disease

The most prime risk factor of AD are age, family history, and genetics. Some no-genetic factors also influence the evidence of AD.

1.4.1. Age

Advancing age is the greatest well-known risk factor for AD. Most people get AD after age 65, the evidence of AD is nearly doubles every 5 years after 65 years old, that means the prevalence higher than 25% in people with age over 90 (Qiu *et al*., 2009). The age-dependent hypothesis of AD has been established. In this hypothesis, advancing age leads to the normal synaptic dysfunction of brain, and this induces the normal cognitive decline, however, three factors including initiating injury, chronic neuroinflammatory responses, and altered brain cell physiology divert the normal brain decline into the pathophysiology of AD, leading to the major brain dysfunction and neuronal loss and final causing the onset of AD (Herrup, 2010).

1.4.2. Family history and genetic factors

AD can be divided into two major categories, sporadic late-onset AD and early-onset familial AD (FAD), causing about 5–7% (Finder, 2010). This AD generally affects individuals with the age below the age of 60, and the symptoms may appear between people age 30 and 40 (Duthey, 2013; Binetti, 2009). Certain genes mutated in the family history and developed the abnormal characteristics that lead the onset of FAD. These genes have a strong influence on the evidence of their children. If one parent has FAD, each child possesses a 50% chance of inheriting AD, and if two parents with FAD, all the children will develop to AD in their adulthood. There are many genetic mutation

associated with AD (Duthey, 2013) (Table 1). There are three genes are known to be associated with early-onset FAD including *PSEN1*, *APP* and *PSEN2*. *APP* mutation induces the early-onset FAD at age 40-65 with the duration 9-16 years, *PSEN1* and *PSEN2* mutations leads to the early-onset FAD at age 35–55 and 45–88 with the duration 5.8–6.8 and 4.4–10.8 years, respectively (Binetti, 2009).

Table 1. Main genes mutations associated with Alzheimer's disease

Gene	Main alteration	Presumed mechanism
APP	Mutation	Autosomal dominant, mostly early onset
Presenilin 2	Mutation	Autosomal dominant, mostly early onset
Presenilin 2	Mutation	Autosomal dominant, mostly early onset
Apolipoprotein-E	Common variant	Familial and sporadic, late onset
Sortilin-related receptor, L (DLR class) A-repeats containing	Common variant	Familial and sporadic, late onset
Clusterin	Common variant	Sporadic, late onset
Phosphatidylinositol binding clathrin assembly protein	Common variant	Sporadic, late onset
Complement component (3b/4b) receptor 1	Common variant	Sporadic, late onset
Bridging integrator 1	Common variant	Sporadic, late onset

1.4.3. Nongenetic factors

Cerebrovascular disease, blood pressure, type 2 diabetes, body weight, plasma lipid levels, metabolic syndrome, smoking, and traumatic brain injury can be nongenetic risk for AD (Reitza and Mayeux, 2014). However, some nongenetic factors are protective for AD. These factors include diet, physical activity, and intellectual activity. Diets high in fruit, vegetable and fish, low in red meat, and intake of wine can reduce the incidence of AD (Scarmeas *et al.,* 2009). That may be because the antioxidants are high in this diet inducing the suppressing of neuronal damage. In addition, high content vitamin E in fruits and vegetables can reduce apoptosis and Aβ-associated lipid peroxidation (Butterfield *et al*., 2002). Physical exercise may improve brain health, affecting the cognition by increasing cerebral blood flow, glucose utilization, and oxygen extraction (Reitza and Mayeux, 2014). Intellectual activities, such as reading, learning, and game playing, are benefit for cognitive function (Reitza and Mayeux, 2014).

1.5. Market and cost of Alzheimer's disease

The costs of AD include direct costs (such as hospital resources, drugs, family payments to caregivers, social and medical service) and indirect costs (such as loss of income by patient or reduction from family members) (Castro *et al*., 2010). The worldwide costs of AD were sharply increase form 315 billion USD in 2005 to 422 billion USD in 2009 and 604 billion USD in 2010 (Wimo *et al*., 2013). Over 70% worldwide cost is contributed to developed countries such as North America and Europe. The remaining lower than 30% was cost by low income countries, and this cost accounts for about 1% of the world's gross domestic product, varying from 1.24, 0.50, 0.35, and 0.24% in high, high middle, low middle, and low income countries, respectively (Wimo *et al*., 2010). The total costs of one people with dementia are 38 times higher in higher income countries than in low income countries, and the direct costs of social service are 120 times higher. Informal and social costs account almost 84%, whereas medial costs are much low, contributing about 16% of total costs, indicating the medication options for AD is limited (Wimo *et al*., 2010).

1.6. Treatments for Alzheimer's disease

Until now, there is no cure for AD, and no treatments can stop or reverse its symptoms. However, there are some medication that can alleviate some symptoms and slow down the pathogenetic process. There are two kinds of U. S. Food and Drug Administration (FDA) approved treatments for AD. They are four AChE inhibitors (e.g., tacrine, donepezil, galanthamine, and rivastigmine) and the uncompetitive NMDA receptor antagonist (e.g., memantine) (Parsons *et al*., 2013). Tacrine was the first AChE inhibitor approved in 1993, however, is rarely used today due to the associated side effects, such as possible liver damage (Schneider, 2013). Donepezil is approved to treat all stage, whereas galantamine and rivastigmine are used to treat mild to moderate stage of AD. The AChE inhibitors are approved to treat AD by increasing levels of acetylcholine, which is a chemical message involved in memory, thinking, and judgment. However, there are some side effects, including nausea, vomiting, anorexia, and loss of appetite (Schneider, 2013). The NMDA receptor antagonist acts by regulating the activity of glutamate, which is a chemical involved in information processing, storage, and retrieval. However, side effects appears including fatigue, constipation, confusion, headache, and dizziness (Burock and Naqvi, 2014).

1.7. Hypotheses involved in the pathological processing of Alzheimer's disease

1.7.1. Cholinergic hypothesis of Alzheimer's disease

The cholinergic hypothesis first emerged over decades. The hypothesis states that the dysfunction of acetylcholine induces to the cognitive decline in the central nervous system associated with AD. Furthermore, this cholinergic hypothesis proposes the loss of cholinergic neurons in the basal forebrain and decrease of neurotransmission in the areas of cerebral cortex and others learning and memory-related function areas (particularly, the hippocampus) are responsible for memory and cognitive deficits observed in AD (Francis *et al*., 1999). Recent studies suggested choline acetyltransferase and/or AChE activity was not affected in the brain of patients who had mild cognitive impairment (MCI) or early stage of AD, that led some challenges to the cholinergic hypothesis (Terry and

Buccafusco, 2003). Cholinergic abnormalities in aged and AD have a wide range including acetylcholine release, choline transport, nicotinic and muscarinic receptor expression, axonal transport, and neurotrophin support, which contribute to cognitive dysfunctions in aging and AD. This cholinergic dysfunctions may also conduce to noncognitive abnormalities in AD (Terry and Buccafusco, 2003). The changes in cholinergic neurons occurred in the aged and early AD brain are compared with healthy young neuron (Fig. 2). These changes include choline uptake, inadequate in the expression of nicotinic and muscarinic receptors, breakdown of acetylcholine release, deficits in axonal transport, and dysfunctional neurotrophin support (e.g., NGF receptor) (Terry and Buccafusco, 2003). The FAD approved drug AChE inhibitors have been developed based on this hypothesis.

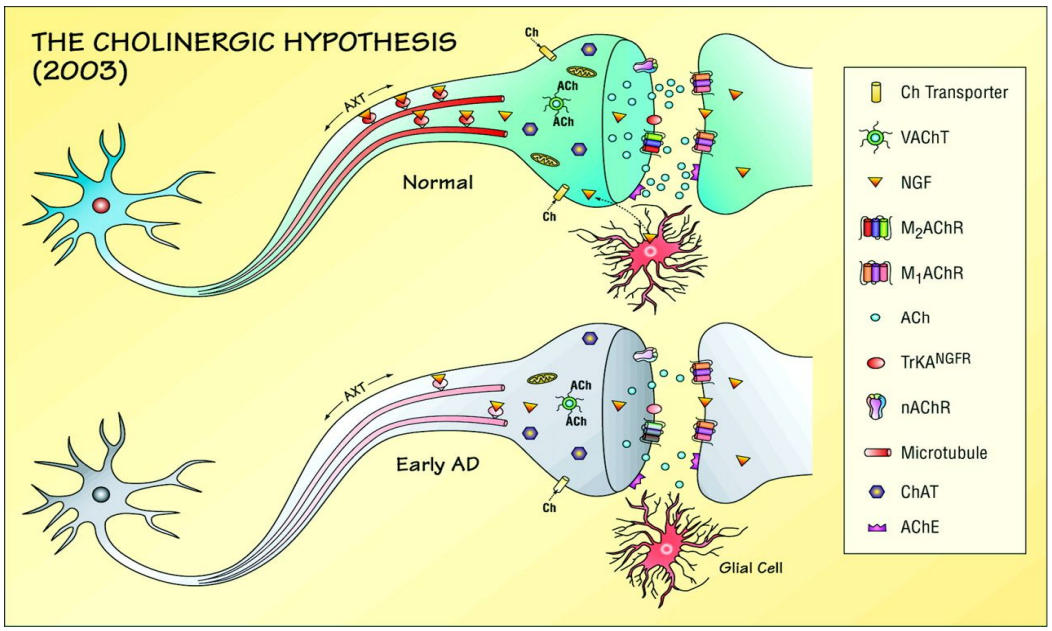

Fig. 2. Cholinergic hypothesis of Alzheimer's disease. Schematic representation of the known and proposed changes in cholinergic neurons that occur in the aged and early Alzheimer's disease (AD) brain compared with healthy young neurons.

1.7.2. Amyloid cascade hypothesis of Alzheimer's disease

In 1991, Selkoe (1991) first completed the amyloid cascade hypothesis of AD, and this hypothesis was similarly improved, as described by Hardy and Allsop (1991). This hypothesis plays an important role in explaining the pathogenesis and etiology of AD. Since senile plaque and NFTs are the major hallmarks of AD, Aβ is the main constitute of SPs and the initial pathological event in AD. In the amyloid cascade hypothesis, the mutations in *APP*, *presenilin 1* (*PSEN1*), and *presenilin 2* (*PSEN2*) genes induce to the formulation and accumulation of Aβ, leading to the neuronal dysfunction and death. Finally, it gives rise to AD (Fig. 3) (Reitz, 2012).

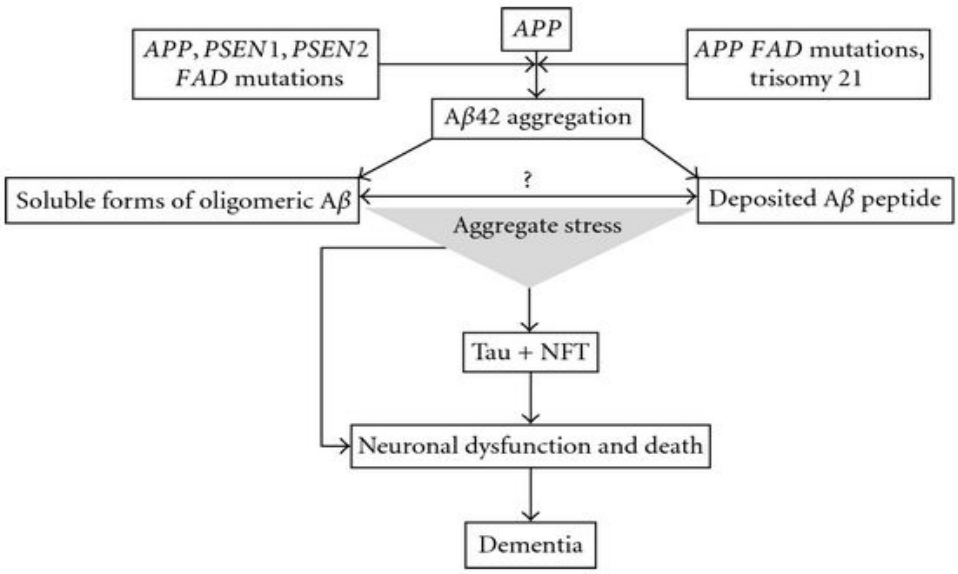

Fig. 3. Amyloid cascade hypothesis of Alzheimer's disease.

1.7.3. Tau hypothesis

Tau protein is a kind of microtubule-associated protein (MAP) that are observed mostly in neurons (Cleveland *et al*., 1977). Normal tau protein stabilizes microtubules trough four tubulin binding domains located at the C-terminus of the molecule (Kolarova *et al*., 2012). Microtubules take an important role in diverse cellular processes including cell division, cell morphogenesis, and intracellular trafficking (Drubin and Nelson, 1996; Goodson *et al*., 1997). However, the tau hypothesis suggests that abnormal phosphorylation or abundant of tau induce normal tau protein transformation into paired helical filament-tau and NFTs, resulting in the neuron cell dysfunction or death and finally leading to AD (Fig. 4) (Mohandas *et al*., 2009; de Paula *et al*., 2009).

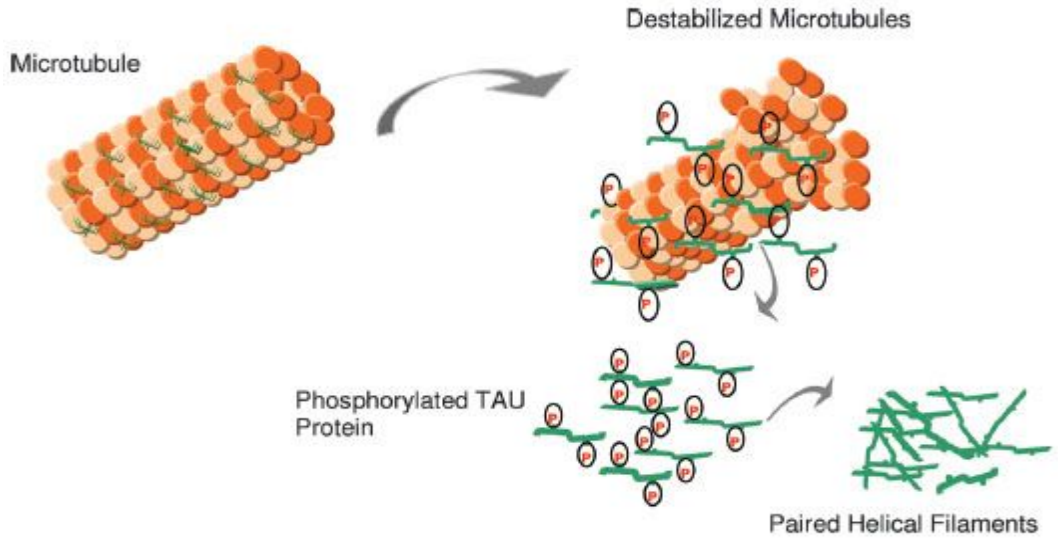

Fig. 4. Tau hypothesis of Alzheimer's disease.

2. Amyloid precursor protein and its proteolytic products

2.1. Basic knowledge of amyloid precursor protein

APP is a transmembrane protein that takes an important factor in the pathogenesis of AD. *APP* gene containing 18 exons is located on the chromosome 21 in humans (Zhang *et al*., 2012). Alternative splicing of transcripts from APP exon 7 that encodes a Kunitz protease inhibitor (KPI) domain, exon 8 that codes for OX-2 antigen, and exon 15 results in three main isoforms of gene products, APP695, APP751 and APP770 that consist of 695, 751, and 770 amino acids, respectively. APP751 and APP770 are larger isoforms expressed in most tissue and contain a 56 amino acid KPI domain within extracellular regions. Compared with APP751, APP770 contains OX-2 antigen domain. The APP 695 isoform does not contain the KPI and OX-2 domains that mainly expressed in neurons (Zhang *et al*., 2011; Evin and Li, 2012). There are two homologues of APP identified and named as APP-like protein 1 and 2 (APPLP1 and APPLP2), APLP1 is only expressed in the brain and is only found in mammals, while APLP2 is similar to APP expressed in all the tissues (Zhang *et al*., 2011). The schematic structure of APP protein is given in Fig. 5. APP contains an *N*-terminal globular domain, or E1 domain that contains heparin- and metal-binding sites. An acidic domain is connected to this, followed by KPI domain (except in APP695) and OX-2 domain (only in APP771) and carbohydrate domain (also named as E2 glycosylated domain) that contains also heparin- and metal-binding sites. APP is anchored through a transmembrane domain (TMD), followed by a cytosolic domain (CD). The Aβ region was composed of extracellular domain and membrane-spanning domain (Fig. 5) (Evin and Li, 2012).

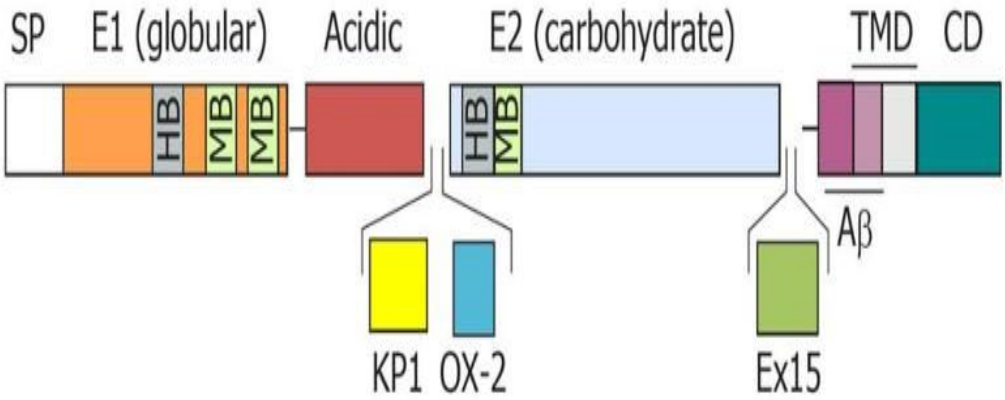

Fig. 5. Schematic diagram of APP. KPI; SP: signal peptide; E1: ectodomain 1; E2: ectodomain 2; TMD: transmembrane domain; CD: cytosolic domain; OX-2: domain with homology to OX-2 leukocyte antigen; Ex 15: exon 15 product; HB: heparin-binding domain; MB: metal ion-binding domain.

2.2. APP proteolytic processing

There are two processing pathways included in APP processing: amyloidogenic pathway and non-amyloidogenic pathway. There are several secretases (α-, β-, and γ-secretase) involved in these two pathways (Zhang *et al*., 2011). In the non-amyloidogenic pathway, APP is cleaved by α-secretase with the cleavage site within the Aβ domain and produces a large soluble ectodomain of APP (APPsα) and APP C-terminal fragment (APP-CTFα). APP-CTFα is followed cleaved by γ-secretase to generate P3 and APP intracellular domain (AICD). APPsα can regulate neural stem cell proliferation and initial for early CNS development (Caille *et al*., 2004). Besides, APPsα takes an important role in neuronal plasticity and survival (Fig. 6) (Furukawa *et al*., 1996). In amyloidogenic pathway, firstly, APP is cleaved by β-secretase and releases a large soluble ectodomain of APP (APPsβ) and APP C-terminal fragment (APP-CTFβ), then further cleaved by γ-secretase to generate toxic Aβ (Fig. 6) (Meraz-Ríos *et al*., 2014).

APPsβ is different from APPsα by missing the Aβ 1-16 region at its carboxyl-terminus. The APPsβ takes a role as a death receptor 6 ligand and adjust neuronal cell death and axonal pruning (Nikolaev *et al*., 2009) and can rescue gene expression of transthyretin and Klotho without rescuing the essential function of APP in mice (Li *et al*., 2010).

The α-secretase and β-secretase other cleavage products are APP-CTFα and APP-CTFβ, respectively. The function of APP-CTFs have been less known due to they are intermediate products (Zhang *et al*., 2011). It was reported that over-expression of APP-CTFβ was cytotoxic and cause neuronal degeneration that may be due to the interference of APP signal transduction (Yankner *et al*., 1989). Recently, APP-CTFβ was reported to regulate cell surface delivery of γ- secretases by direct binding of enzyme-substrate (Liu *et al*., 2009). As the substrate of γ- secretases, APP-CTFα may be have similar effects as APP-CTFβ (Zhang *et al*., 2011). AICD is a γ- secretases cleavage product, an important function of AICD is to facilitate the interaction of APP with various cytosolic factors that regulate APP's intracellular trafficking and/or signal transduction function, and these are controlled by the AICD phosphorylation state (Zhang *et al*., 2011).

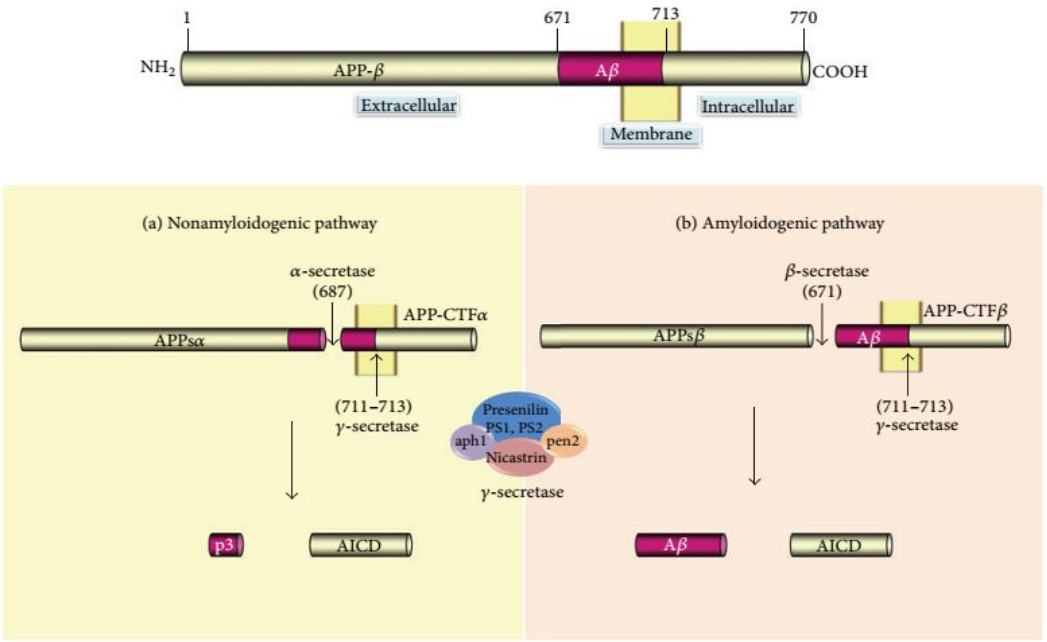

Fig. 6. Schematic diagram of APP processing. The non-amyloidogenic pathway involves α-secretase, while the amyloidogenic pathway involves β-secretase, and then subsequently cleaved by γ-secretase.

3. BACE-1 (β-Secretase 1)

3.1. Basic knowledge of BACE-1

B-site APP cleaving enzyme-1 (BACE-1) is also called β-secretase 1, memapsin 2, and aspartyl protease 2. It is a responsible enzyme for the production of 42-residue amyloid beta peptide (Aβ42) involved in APP amyloidogenic processing pathway (Mancini *et al.,* 2011). Aβ aggregates to form senile amyloid plaque which is one histopathological hallmark of AD. In 1999, β-secretase was identified as the transmembrane aspartic protease BACE-1 which forms a new branch of pepsin family that together with its homologue BACE-2 (Citron, 2004a). BACE-1, the major β-secretase, is a type I membrane-associated aspartyl protease of 501 amino acids, whereas BACE-2 is a single transmembrane aspartyl protease with 518 amino acids (Sun *et al*., 2005). BACE-1 gene maps on chromosome 11, while BACE-2 gene is on chromosome 21 (Cheon *et al*., 2008). BACE-1 and BACE-2 are a new family of transmembrane aspartic proteases, that are most closed to the pepsin family, which expressed few in humans. They are more distantly related to the retroviral aspartic protease, which contain the HIV protease, mouse Moloney leukaemia virus, and Rous sarcoma virus (Fig. 7) (Citron, 2004a). The active catalytic domain resides of BACE-1 are within the lumen of acidic intracellular compartments, such as endosomes and trans-golgi network, and it has highest expression level in the neurons of CNS. BACE-2 was identified that harbors about 64% amino acid that are conserved to BACE-1. Moreover, compared with BACE-1, BACE-2 is not high expressed in neurons, and it predominately cleaves APP within the Aβ domain (Vassar, 2014). The function of BACE-2 is controversial, but it appears to have no important role in APP processing pathway, so it is not regarded as a target for AD drug development (Citron, 2004b).

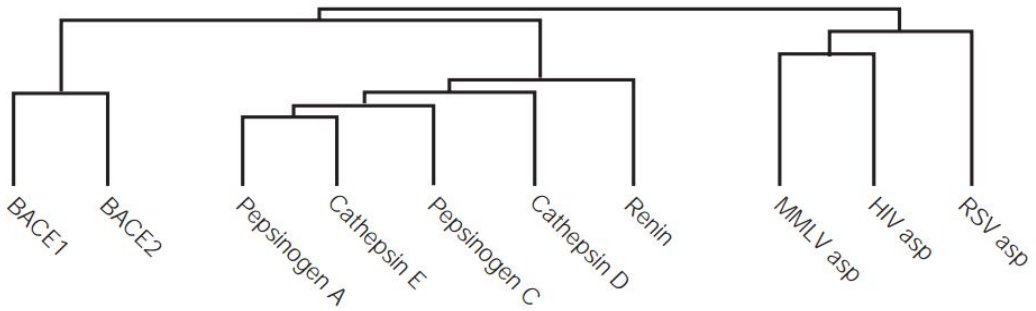

Fig. 7. Evolutionary tree showing the relationship between BACE-1, BACE-2, and other aspartic protease.

3.2. BACE-1 structure and catalytic mechanism

Since BACE-1 is a major target for AD treatment and drug development, previous study have reported that numerous structures of BACE-1 complexes (Hong *et al*., 2000; Patel *et al*., 2004). The active site of BACE-1 is characterized by the presence of hydrophilic and small hydrophobic pocket and covered by a flexible antiparallel β-hairpin named as a flap, which is considered to regulate substrate approach to the active site and assembles the substrate in the correct geometry for the catalytic process (Shimizu *et al*., 2008; Mancini *et al*., 2011). BACE-1 shows high activity in acidic pH 4.0–4.5, and this pH is usually applied for *in vitro* assay (Mancini *et al*., 2011). BACE-1 shows enzymatic activity by a general acid-base mechanism that is common to aspartyl protease. Aspartyl protease is characterized by two aspartic acids, to BACE-1, they are Asp_{32} and Asp_{228} (Mancini *et al*., 2011). The catalytic mechanism of BACE-1 is present in Fig. 8. The protonated Asp_{32} and the carbonyl oxygen of the cleavage bond form a hydrogen bond, and the non-protonated Asp_{228} correlates with lytic water. The tetrahedral intermediate collapses induction of the release of two peptidic products, and the enzyme is restored for

another cycle of catalysis (Fig. 8) (Mancini *et al*., 2011).

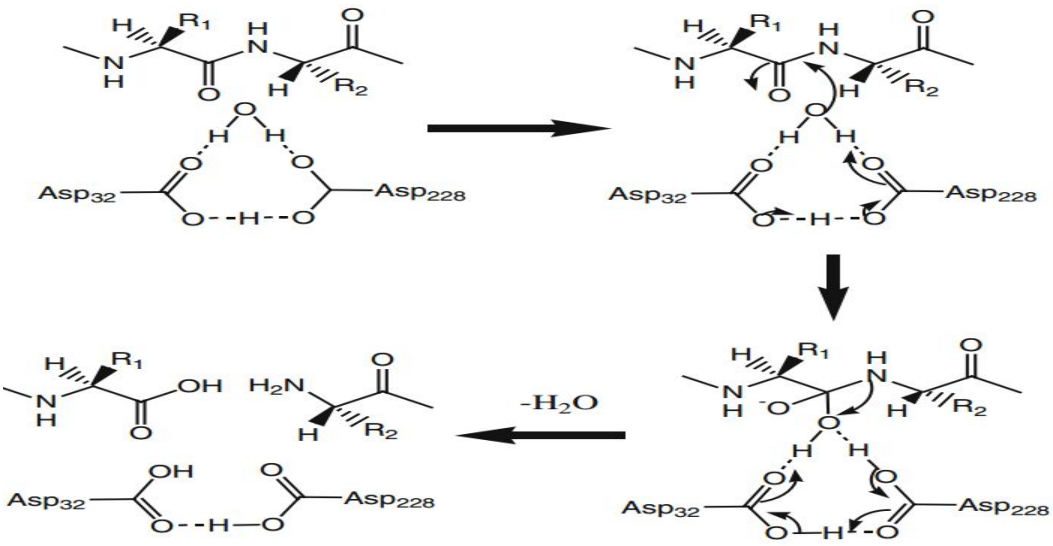

Fig. 8. Schematic representation of BACE-1 catalytic mechanism.

3.3. *In vitro* BACE-1 FRET assay principle

In most common assay method utilized to study BACE-1 inhibitory activity *in vitro* is the FRET assay. FRET is sensitive and is easily applied in high-throughput screening (HTS) for BACE-1 inhibitory compounds. FRET assay principle is shown in Fig. 9. The synthetic peptide with a fluorophore (donor group) and a quencher (acceptor group) was used as the substrates. In the uncleaved substrate, the fluorescence is quenched due to intramolecular resonance energy transfer from the donor group to quenching group. When the substrate is cleaved by BACE-1, the fluorescence is not quenched due to the disturbance of the energy transfer, and the fluorescent signal can be measured. The increase fluorescent signal is linearly related to the rate of proteolysis. While BACE-1 is

inhibited by an inhibitor, this fluorescent signal is be reduced. According to this, HTS of BACE-1 inhibitory compounds was performed.

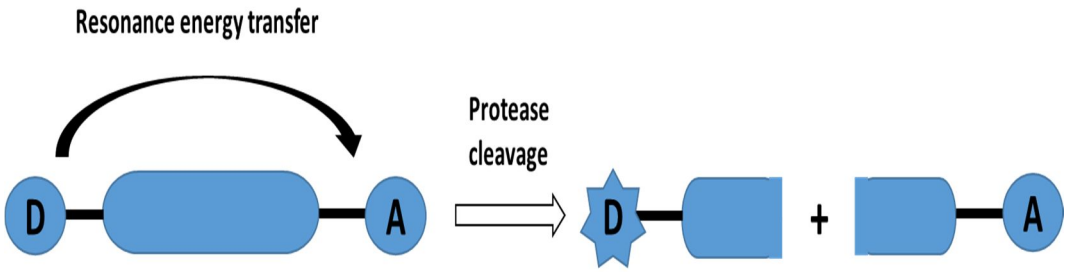

Fig. 9. Fluorescence resonance energy transfer assay principle. D: donor group; A: acceptor group.

3.4. BACE-1 inhibitors

In the amyloidogenic pathway, BACE-1 is a required enzyme for the production of Aβ. Development of BACE-1 inhibitors is considered as the therapeutic agents. BACE-1 inhibitors can be divided into two groups, peptidic and peptidomimetic inhibitors and non-peptide compounds, including synthetic inhibitors and natural compounds. The first generation BACE-1 inhibitors were peptidomimetics, which are very potent inhibitors *in vitro*, mainly due to the large open active site of BACE-1 having high affinity to binding polypeptide substrate (Vassar, 2014). However, these peptides are not potent inhibitor against BACE-1 *in vivo*, because of the poor oral bioavailability and blood-brain-barrier (BBB) penetration (Silvestri, 2009). However, small-molecular inhibitors with small molecular weight (MW), good penetrability to BBB, and high oral bioavailability have been developed and shown improved pharmacological characteristics. The second generation BACE-1 inhibitors possess improved pharmacological characteristic; however,

they were the substrates of P-glycoprotein, the ATP-dependent drug efflux pump for xenobiotics in the BBB, so were unable to achieve enough concentration in the brain (Probst *et al*., 2012). Recently, the third generation BACE-1 inhibitors with small MW and high potent inhibitory activity have been developed and were reported to have good brain penetration and can reduce cerebral Aβ in preclinical animal models. Several of these potent BACE-1 inhibitor drugs have been developed in human clinical trials (Table 2) (Vassar, 2014), and most are in the first clinical phase. Lilly was among the first to develop and test the bioavailability of non-peptide BACE-1 inhibitor in human. Drug LY2886721 was test in phase 2, but stopped due to abnormal liver biochemistry. RG7129 was developed and test by Roche. However, in October 2013, RG7129 was terminated due to the liver toxicity. It is still not clear that it is effective for the prevention or treatment in AD patients, although BACE-1 inhibitors are now in human clinical trials test for the safety and efficacy.

Table 2. Small molecular BACE-1 inhibitors in clinical trials

Company	Drug	Phase
AstraZeneca/Lilly	AZD3293	Phase 2/3
CoMentis	CTS-21166	Phase 1
Eisai/Biogen Idec	E2609	Phase 2
High Point	HPP854	Phase 1
Janssen/Shionogi	……	Phase 1
Lilly	LY2886721	Phase 2*
Merck	MK-8931	Phase 2/3
Novartis	…….	Phase 1
Pfizer	PF-05297909	Phase 1
Roche	RG7129	Phase 1**
Takeda	TAK-070	Phase 1
Vitae/Boehringer Ingelheim	VTP-37948	Phase 1

*Terminated due to abnormal liver biochemistry.

**Removed from pipeline.

4. *Drosophila* as a model for Alzheimer's disease

4.1. Advantages of *Drosophila* as a model for human disease

The fruit flies *Drosophila* have been used in genetic research for over a century (Morgan, 1910). They have low chromosomes which are 3 pairs of autosomes named no. 2, 3 and 4 chromosome, and 1 pair of sex chromosome. It is one of the first organisms with the fully sequenced genome (Adams *et al*., 2000). Fly genome reveals about 60%

genes that are conserved with human genome, and about 75% of disease-related genes in human have functional orthologs in the fly (Pandey and Nichols, 2011). Recently, *Drosophila* has been used as a powerful genetic model to study human neurological and neurodegenerative disorders including AD, Huntington's disease, Parkinson's disease, amyotrophic lateral sclerosis, and other polyglutamine disease (Iijima-Ando and Iijima, 2010). *Drosophila* has been used widely as a human disease model organism in biomedical research due to their advantages such as very rapid life cycle with 10 to 12 days at 25^{o}C; short life with 2–3 months; easy and inexpensive to culture in laboratory conditions; each female can produce large number of embryos; and they can be genetically modified in numerous manners such as UAS-GAL4 system and P-element. The advantages and disadvantages of *Drosophila* used as a model to research neurodegenerative disorder such as AD are listed in Table 3 (Prüßing *et al*., 2013).

Table 3. Advantages and disadvantages of using *Drosophila* as a model organism for neurodegenerative diseases like Alzheimer's disease

Advantage	**Disadvantage**
No ethical problems/no restrictions according to animal protection laws	Brain anatomy, cardiovascular system and respiration systems differs substantially from humans
Easy and cheap to maintain in large quantities, time and cost effective handling	No easy measure of complex behavior
Genetic manipulation is fast and inexpensive (3 month, < $ 500 per transgene)	Only basic measures of cognitive decline
Plethora of available resources/stocks (e.g. genome-wide RNAi-library)	Sometimes poor conservation of proteins/protein function
Short generation time (~10 days), short life span (2–3 month), easy to use for screens	Maintenance as living cultures only, no permanent conservation (e.g. frozen stocks) possible
Fully sequenced and annotated genome	Less complex and adaptive immune system as in vertebrates
Good conservation of basic signaling pathways and cellular processes in general	Effects of drugs on the organism might differ strongly (e.g. conversion of pro-toxins to toxins in liver)
Low redundancy/reduced number of paralogous genes compared to vertebrates	
Probably best analyzed/understood multi-cellular organism	
More complex organism compare to *Caenorhabditis elegans* and yeast	
Balancer chromosomes allow the maintenance of mutations/trangenes without genotyping	

4.2. *Drosophila* models of Alzheimer's disease

4.2.1. Ortholog of human APP, α-secretase, and β-secretase, and the component of γ-secretase in *Drosophila*

Drosophila has a human APP ortholog, APP-like protein (dAPPl) (Luo *et al*., 1992), and γ-secretase complex (Periz and Fortini, 2004). The dAPPl harbors characteristic domain with human APP, but the domain related to Aβ peptide is significantly different (Luo *et al*., 1992). The ortholog of human α-secretase is Kuzbanian (Kuz) in *Drosophila* that can cleave dAPPl (Carmine-Simmen *et al*., 2009). The β-secretase-like enzyme was also identified in *Drosophila*, which shares 25% conservation to human BACE-1 and 28% conservation to human BACE-2, but with low β-secretase activity (Yagi *et al*., 2000; Carmine-Simmen *et al*., 2009). There is no endogenous Aβ identified in *Drosophila*, however, overexpression of β-secretase-like enzyme induces the cleavage of dAPPl to generate a fragment that is related to Aβ peptide, and these peptides aggregate and result in age-dependent neurodegeneration and behavioral deficits (Carmine-Simmen *et al*., 2009). The dAPPl deficient flies show behavioral deficits which can be rescued by human *APP* transgene, suggesting a functional conservation between human APP and dAPPl (Luo *et al*., 1992). The comparison of APP, α-secretase, β-secretase, and the component of γ-secretase complex and as tau in human and *Drosophila* is illustrated in Fig. 10 (Iijima-Ando and Iijima, 2010).

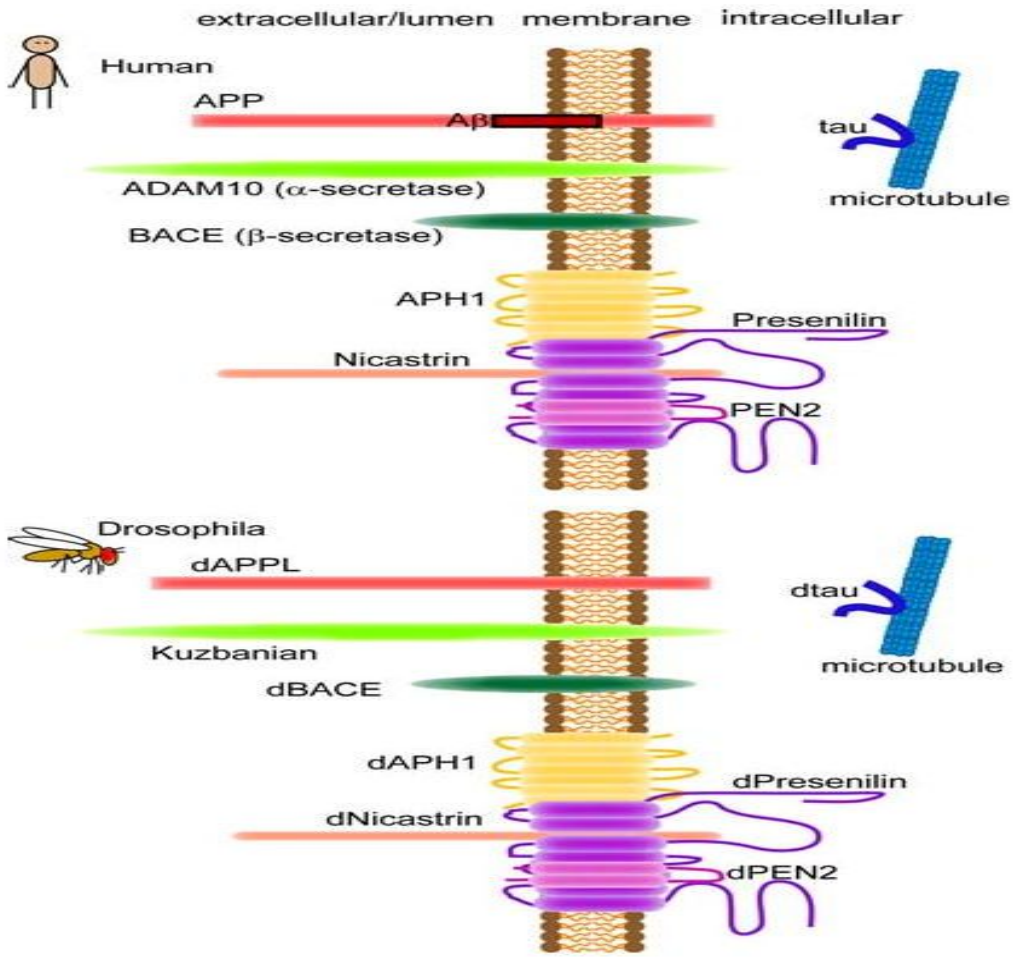

Fig. 10. Schematic illustration of APP, α-secretase, β-secretase, the component of γ-secretase complex, and tau in human and *Drosophila*.

4.2.2. Gal4-UAS system and *Drosophila* models of Alzheimer's disease

Gal4-UAS system, a fly geneticist's Swiss army knife, was used widely for target genes expression in *Drosophila* specific tissue (Duffy, 2002). Gal was identified in the yeast *Saccbaromyces cerevisiae* as a regulator of genes, which encodes a protein with 881 amino acid, and induce by galactose (Duffy, 2002). The drive line Gal4 was inserted in

the downstream of a *Drosophila* endogenous promoter. It binds to upstream activating sequence (UAS) to activating expression of target gene downstream. Variety of Gal4 can induce target gene expressed in specific tissue. The *glass multimer reporter* (GMR) driver and *elav* driver are used frequently, which drive target genes expressed in retinal and pan-neuronal system (Fig. 11).

AD *Drosophila* models can be realized through two ways. One way is by modeling amyloid toxicity and another way is by modeling tauopathies. Amyloid toxicity in *Drosophila* is realized by overexpression of Aβ and co-expression of human APP and BACE-1. The most used methods of modeling tauopathies are expression of human wild type and mutant tau, and co-expression Aβ42 and human tau. Until now, the frequently used AD *Drosophila* models are listed in Table 4 (Mhatre *et al*., 2013). Also, the culture medium, condition, and sexuality that applied in *Drosophila* models of AD in previous studies are given in Table 5.

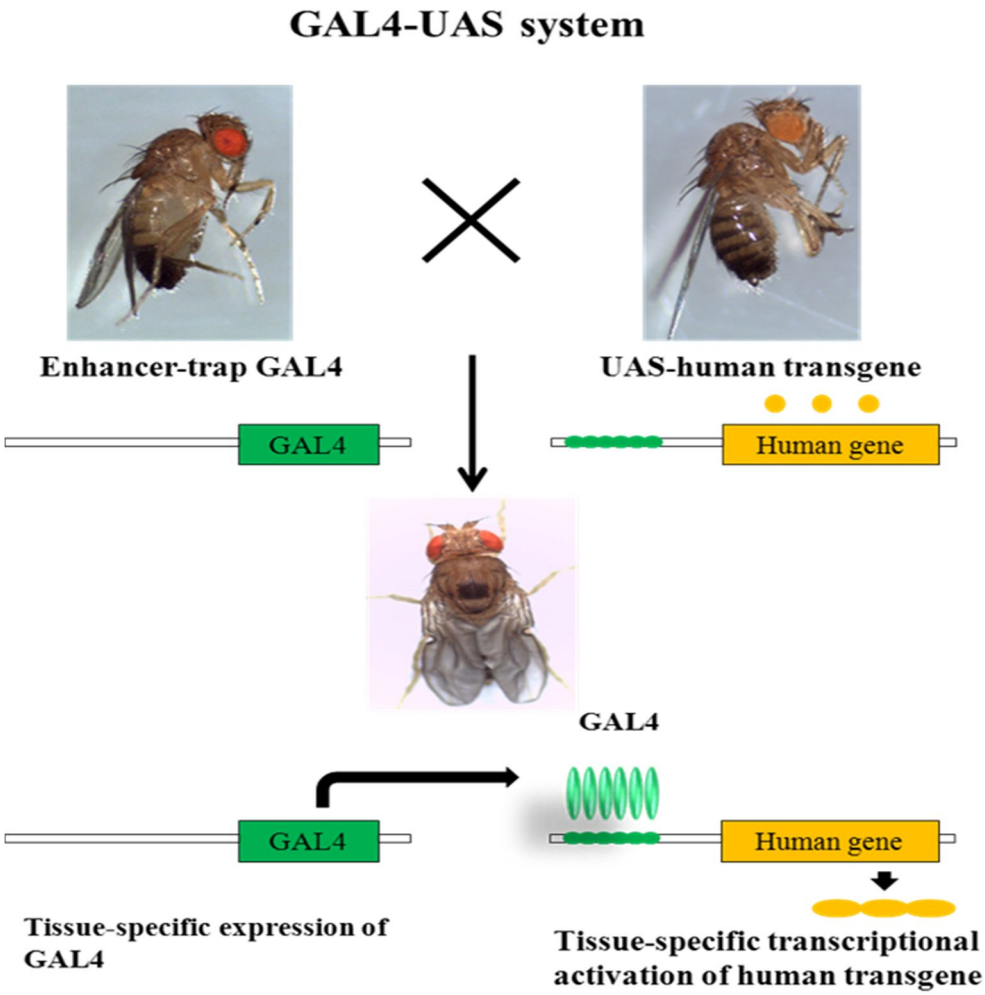

Fig. 11. Gal4-UAS system in *Drosophila*.

Table 4. Transgenic *Drosophila* models of Alzheimer's disease

Transgene	Expression pattern	Salient observation
Aβ42	Eye	Rough eye phenotype
Aβ42	Pan-neuronal	Locomotor and learning deficits, amyloid formation, progressive neurodegeneration, reduced lifespan, and mitochondrial mislocalization
Aβ42 artic mutation	Inducible pan-neuronal	Reduced lifespan, neuronal dysfunction
hAβPP and hAβPP Swedish mutant	Wing disc	Blistered wing phenotype
hAβPP C-terminal fragment	Eye	Rough eye phenotype
hAβPP, hBACE, and DPsn	Eye	Age-dependent degeneration of photoreceptor neuron, amyloid formation
hAβPP, hBACE, and DPsn	Ubiquitously	Semilethality, ectopic wing vein formation
hAβPP and hBACE	Pan-neuronal	Behavioral deficit, amyloid formation, age-dependent decrease in learning associated neuronal structure, memory deficits
hTau (0N3R)/wt-hTau	Sensory neurons	Axonal loss

hTau (0N4R) and mutant tau	Pan-neuronal	Reduced lifespan, age-dependent vacuolization, degeneration of cholinergic neurons, nearly complete loss of learning associated neuronal structure
hTau (0N3R)	Larval motor neurons	Synaptic dysfunction and reduce mitochondria
hTau (0N4R)	Glial cells	Reduced lifespan, glial and neuronal cell death, NFTs; synergistic effect with neuronal and glial expressing
hTau (0N4R)	Eye	Rough eye phenotype, NFTs
hTau (0N4R) mutant tau, and phosphorylation-incompetent tau, and pseudo-phosphorylated tau	Eye	Rough eye, loss of notum bristle phenotype
hTau (0N4R) and Aβ42	Eye	Rough eye phenotype
hTau (0N4R) and Aβ42	Pan-neuronal	Vacuolization
hTau (0N4R) and Aβ42	Motor neurons	Reduce lifespan, behavioral deficit, neuronal dysfunction

Table 5. Culture medium, condition, and sexuality that applied in *Drosophila* models of Alzheimer's disease

Fly medium	Temperature /humidity Compound Treatment time	Flies sexuality	References
Standard medium	25°C/70% -	WT: male and female Learning : male and female Climbing: male and female	Iijima *et al*. (2004)
Without compound: Standard medium. β, γ-secretase inhibitor: add to standard medium. Until eclosion: standard medium. Post eclosion: 50 mL vial containing 7 mL agar (20 g agar, 20 sugar in 1L water) and yeast past. Curcumin in 95% ethanol to con. 10 mg/mL then diluted into yeast paste to final concentration. of 1, 10, and 100 μg/g yeast paste.	29°C /no information From embryonic stage Until eclosion: 26°C/70% Post eclosion: 29°C/70% From post eclosion	No information No information	Greeve *et al*. (2004) Caesar *et al*. (2012)

γ-secretase inhibitor add to standard medium.	25°C/60%	From embryonic stage	Learning: male Court ship behavior training: male Climbing: no information Life span: no information	Chakraborty *et al*. (2011)
Without compound: standard medium. Until eclosion: instant food + Congo red/ Post eclosion: standard medium with 500 mg streak of yeast paste containing compound.	29°C/no information	From embryonic stage	No information	Crowther *et al*. (2005)
KSOP1009 hexane extract mix with standard medium to final concentration. 5 and 50 μg/mL.	29°C/no information	From embryonic stage	Male	Hong *et al*. (2011)
Standard medium addition compound.	25 °C/70%	From embryonic stage	Male	Wang *et al*. (2014)
Standard medium addition compound.	29 °C/60%	From embryonic stage	Male	Wang *et al*. (2015)

5. *Curcuma longa*

The rhizomes of *C. longa* are not only important as a spice or flavoring, but they have also been prescribed for indigestion, hepatitis, jaundice, diabetes, atherosclerosis, and bacterial infection in India, China, and other Asian countries (Tang and Eisenbrand, 1992; Araújo and Leon, 2001; Kuhn and Winston, 2001). The main curcuminoids in the rhizomes of *C. longa* extracts are three different diarylheptanoids, CCN, DMCCN, and BDMCCN. Usually, commercially available curcurmin consists of the mixture of these three curcuminoids. CCN is the principal curcuminoid. It has a broad range of biological activities including anti-inflammation, antioxidation, anti-HIV, anticancer, chemoprevention, antibacterial, antifungal, antiprotozoal, nematocidal, antivenom, and antitumor activities (Araújo and Leon, 2001; Çıkrıkçı *et al*., 2008; Itolawa *et al*., 2008). CCN has a potential role in the prevention and treatment of AD. Recently, there are some researches focused on the mechanisms of action of CCN in AD and pathology. It has been proposed to alleviate Aβ toxicity in transgenic human Aβ and human tau flies by reducing the pre-fibrillar/oligomeric species of Aβ (Caesar *et al*., 2012). The modes of action of CCN in AD include delayed degradation of neurons, decreased Aβ plaque, anti-inflammatory, antioxidant, decreased microglia formation, and metal-chelation (Mishra and Palanivelu, 2008).

6. *Agastache rugosa*

A. rugosa is an important traditional medicine in China, Korea, and Japan that is native to East Asia. It contains monoterpenoids, sesquiterpenoids, phenylpropanoids, terpenoids, penolic compounds, phenolic acids, and lignans (Zielińska and Matkowski, 2014). *A. rugosa* has various biological activities in both *in vitro* and animal models. These pharmacological activities include antimicrobial, antiviral, antimutagenic, antioxidant activity, and cytotoxic properties (Zielińska and Matkowski, 2014). It has been used to treat of summer cold, summer flu, headache, nausea, vomiting, stomachache, and dyspepsia in Chinese and Korean traditional medicine (Zheng *et al*., 2013). Besides, *A. rugosa* has been reported possess effect of anti-skin wrinkle through fermentation

process of the lactic acid (Kim *et al*., 2015). Historically, this plant species has been used as an agent for the treatment of cholera, vomiting, and miasma (Zielinska and Matkowski, 2014). No previous studies, however, have investigated the potential use of *A. rugosa* for managing AD, although the phytochemistry and bioactivity of plants in the genus *Agastache* have been well documented by Zielinska and Matkowski (2014).

7. Perspectives

In the amyloidogenic processing pathway of APP, BACE-1 is the key therapeutic target for AD that initiated the production of Aβ which is the composition of amyloid plaque that is one of the hallmarks of AD. It is over 16 years since the first discovery of BACE-1 (Vassar *et al*., 2014). During the past decade, a wide variety of BACE-1 inhibitors have been developed for treatment of AD. BACE-1 inhibitors have been developed into third generation (Vassar *et al*., 2014). The first generation inhibitors are peptide-based transition state analogs which are very potent *in vitro* to inhibit BACE-1, however, they don't have *in vivo* pharmacological functions, due to their large molecular and low bioavailability (Caesar *et al*., 2012). So, a new classes of small BACE-1 inhibitor with small molecular weight, better pharmacokinetics, and good plasma membrane permeability were developed (Evin *et al*., 2011). However, most second generation BACE-1 inhibitors cannot reach high concentration in the brain because they are substrates of P-glycoprotein (Marques *et al*., 2013). Recently, third-generation small molecular BACE-1 inhibitors have been developed with improved pharmacological characteristics, and some drugs have been in process of human clinical trials to test safety and efficacy (Vassar *et al*., 2014).

Initial research reported BACE-1 knockout mice were to be normal, however, recent studies suggest that BACE-1 takes a role in synaptic function (Kandalepas *et al*., 2013). Many subtle neuronal phenotypes have been uncovered in BACE-1 knockout mice. These subtle neuronal phenotypes may be present mechanism-based toxicities of BACE-1 inhibitors in human. Any of subtle abnormal phenotypes should be considered during the drugs development in human clinical trials. Although several third generation BACE-1

inhibitors have entered the human clinical trials, two have been stopped due to the side effects, and there are very little information about their process been reported (Vassar *et al*., 2014). The identification and characterization of natural product-derived BACE-1 inhibitors are becoming urgent. Natural products, particular traditional Chinese medicine, have been used for human healthy for a long time because of their safety properties. Recently, it has been reported that curcuminoids from rhizome of *C. longa* (Wang *et al*., 2014) and acacetin, oleanolic acid, and maslinic acid from whole *A. rugosa* plants (Wang *et al*., 2015) possessed potent BACE-1 inhibitory activity. These two plant species are widely used as traditional Chinese medicine in Asia. In addition, the neuroprotective effects of CCN, BDMCCN, and acacetin on trans human *APP* and *BACE-1* genes *Drosophila* models of AD have been also reported (Wang *et al*., 2014; Wang *et al*,. 2015). Especially, acacetin can inhibit *BACE-1* and *APP* both in mRNA and protein levels, as well as APP processing that were elucidated by real-time RT-PCR and western blot analyses (Wang *et al*., 2015). Although curcuninoids and acacetin showed potent neuroprotective effects in *Drosophila* models of AD, the more researches are necessary for *in vivo* assay such as utilization of mice models. These natural product-derived materials could be useful as sources of potential therapeutics or lead compounds for prevention or treatment of AD drugs development.

CHAPTER I

BACE-1 Inhibitory Phytochemicals Identified in *Curcuma longa* Rhizomes and Whole *Agastache rugosa* Plants

INTRODUCTION

In amyloidogenic pathway of APP, BACE-1 is a required enzyme for the production of Aβ. Besides AChE, it is also considered as a key therapeutic target to prevent and treat AD (Ghosh *et al*., 2008; Mancini *et al*., 2011). The first generation BACE-1 inhibitors, peptidomimetics, are very potent inhibitors *in vitro*. Due to the poor oral bioavailability, and BBB penetration (Silvestri, 2009), these peptidomimetics are not potent inhibitor against BACE-1 *in vivo*. Small-molecular inhibitors with small MW, good penetrability to BBB and high oral bioavailability were developed and showed improved pharmacological characteristics. Therefore, the BACE-1 inhibitory compounds with small MW and good penetrability from natural products are urgently needed. Particularly, traditional Chinese medicinal plants have been reported to have functions in dementia disease treatment (Gao *et al*., 2013). Various compounds were isolated form these plants possessing inhibitory activity against human BACE-1 (Zhang, 2012).

In this study, three BACE-1 inhibitory curcuminoids were isolated from *C. longa* rhizome (CCN, DMCCN, and BDMCCN), and flavonoid, acacetin, and two triterpenoids, maslinic acid and oleanolic acid, extracted from the whole *A. rugosa* plants, based on FRET enzyme assay. The BACE-1 inhibitory activities of these phytochemicals were assessed in comparison with two positive control, the cell-permeable isophthalamide, BACE-1 inhibitor IV (Vassar, 2014) and the natural BACE-1 inhibitor, EGCG (Jeon *et al*., 2003).

MATERIALS AND METHODS

1.1. Materials and reagents

The seven commercially-available organic pure curcuminoids, acacetin, maslinic acid, and oleanolic acid examined in this study are listed in Table 6, along with their sources. For the QSAR analysis, values of MW, hydrophobic parameter (log *P*), and steric effects for the test curcuminoids were obtained from ChemDraw Ultra 10.0 (Cambridge Soft Corporation, Cambridge, MA, USA) and recorded in Table 6. Molecular refraction (MR) was used as the parameter for describing steric effects. Epigallocatechin gallate (EGCG) and Inhibitor IV were purchased from Sigma-Aldrich (St. Louis, MO, USA) and Merck (Darmstadt, Germany), respectively. Recombinant human BACE-1 and fluorogenic peptide substrate Mca-SEVNLDAEFRK (Dnp) RR-NH_2 were purchased from R&D system (Minneapolis, MN, USA). All of the other chemicals and reagents used in this study were of analytical grade quality and available commercially.

Table 6. Values of physical parameters of four curcuminoids, maslinic acid, oleanolic acid, and acacetin examined in this study

Compound	MW[a]	log *P*[b]	MR[c]	Source
CCN	368	2.92	104	S-A[d]
DMCCN	338	3.08	98.78	S-A[d]
BDMCCN	308	3.32	92.10	S-A[d]
Tetrahydrocurcumin	372	2.73	100.63	S-A[d]
Maslinic acid	472	7.87	135.08	S-A[d]
Oleanolic acid	456	9.06	133.6	S-A[d]
Acacetin	284	3.15	74.64	S-C-B[e]

[a] Molecular weight.

[b] Hydrophobic parameter expressed as the log of the octanol/water partition coefficient.

[c] Parameter for steric effects as described using molecular refraction.

[d] Purchased from Sigma-Aldrich (St. Louis, MO, USA).

[e] Santa Cruz Biotechnology (Dallas, Texas, USA).

1.2. Plants

The rhizomes of *C. longa* and whole *A. rugosa* plants were purchased from Boeun medicinal herb shop, Kyoungdong market (Seoul Yangnyeongsi, Republic of Korea (ROK)). Voucher specimens (CL-R1 and AR-WP-01) were deposited in the Research Institute for Agriculture and Life Science, College of Agriculture and Life Sciences, Seoul National University.

1.3. Instrumental analysis

The ^{1}H and ^{13}C nuclear magnetic resonance (NMR) spectra were recorded in CD_3CN, MeOD, or DMSO-d_6 on an AVANCE 600 spectrometer (Bruker, Rheinspettem, Germany) at 600 and 150 MHz, respectively, using tetramethylsilane as an internal standard. The chemical shifts are given in δ (ppm). Distortionless enhancement polarization transfer (DEPT) spectra were used to distinguish among ^{13}C signals for CH_3, CH_2, CH, and quaternary carbon. Ultraviolet (UV) spectra were obtained in acetonitrile or methanol on a Kontron UVICON 933/934 spectrophotometer (Milan, Italy), mass spectra on a Jeol JMS-DX 303 spectrometer (Tokyo, Japan), and the FT-IR spectra on a Nicolet Magna 550 series II spectrometer (Midac, Irvine, CA, USA). Silica gel 60 (0.063–0.2 mm) (Merck, Darmstadt, Germany) was used for column chromatography. Merck precoated silica gel plates (Kieselgel 60 F_{254}) were used for analytical thin-layer chromatography (TLC). Merck preparative TLC plates (2 mm thickness), an Isolera Isolera One medium-pressure liquid chromatograph (Biotage, Uppsala, Sweden), and an Agilent 1200 series high-performance liquid chromatograph (Agilent, Santa Clara, CA, USA) were used to isolate the active compounds.

1.4. FRET enzyme assay

Briefly, assay mixtures containing 1 μL of 0.5 μg/μL recombinant human BACE-1, 0.75 μL of a 2.5 μg/μL fluorogenic peptide substrate, 47.25 μL of 50 mM sodium acetate (pH 4.5), and the isolated compounds (1–1000 μg/mL) in 2% DMSO were preincubated for 1 h at 25°C in darkness, followed by the addition of 16.6 μL of 2.5 M sodium acetate

to terminate the reaction. Natural BACE-1 inhibitors (EGCG) and Inhibitor IV served as standard references and were similarly prepared. The fluorescence intensity was measured at room temperature using a SpectraMAX Gemini XS plate reader (Molecular Devices, Sunnyvale, CA, USA) at 320 nm excitation and 405 nm emission. The inhibition percentage was determined using the following equation: % inhibition = 100 – $[(F_S - F_{S0})/(F_C - F_{C0})] \times 100$, where F_S and F_{S0} are the fluorescence of the samples at 60 min and 0 min, and F_C and F_{C0} are the fluorescence of the control at 60 min and 0 min, respectively (Lv *et al*., 2008).

1.5. Bioassay-guided fractionation and isolation

1.5.1. *Curcuma longa* rhizomes

The dried rhizomes of *C. longa* (1.2 kg) was pulverized and extracted with methanol (3 × 5 L) at room temperature for 2 days and filtered. The combined filtrate was concentrated under vacuum at 40°C to yield ~105.4 g of a dark yellowish red tar. The extract (100 g) was sequentially partitioned into hexane- (31 g), chloroform- (6.55 g), ethyl acetate- (49 g), butanol- (3.95 g), and water-soluble (9.5 g) portions for subsequent bioassay (Fig. 12). The organic solvent-soluble portions were concentrated to dryness by rotary evaporation at 40°C and the water-soluble portion was freeze-dried. For isolation of active principles, 2 mg/mL of each *C. longa* rhizome-derived material was tested in a FRET enzyme assay, as described previously (Lv *et al*., 2008).

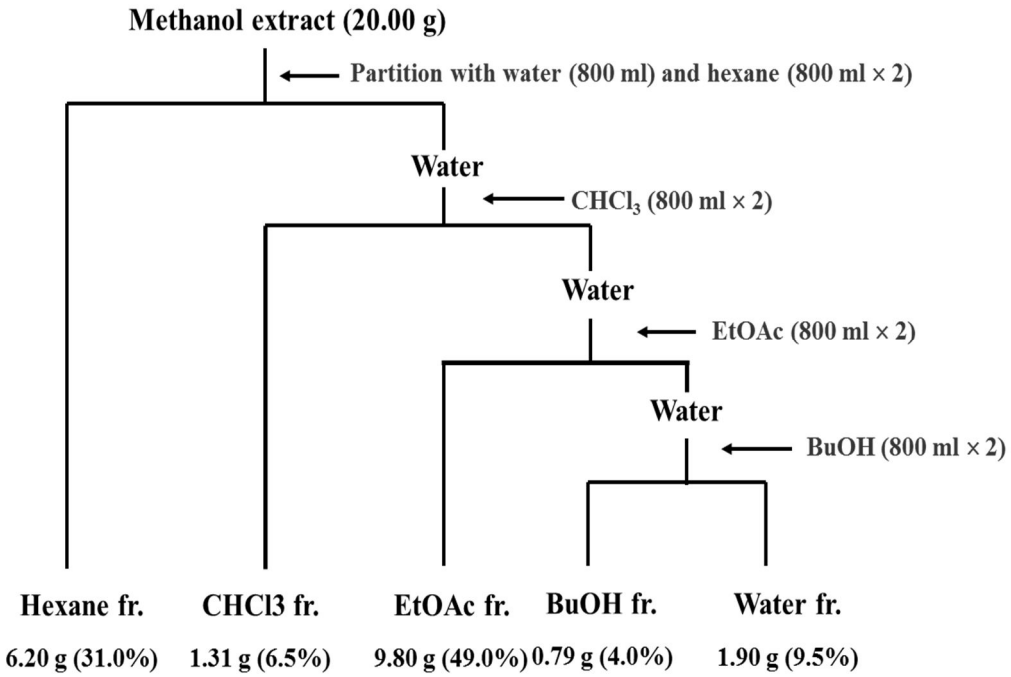

Fig. 12. Solvent partition of methanol extract of *C. longa* rhizomes.

The chloroform-soluble fraction (5 g) was most active and MPLC was performed using a Biotage Isolera apparatus equipped with a UV detector at 254 nm and a column cartridge SNAP (100 g silica gel) with column volume 132 mL. Separation was achieved with a gradient of chloroform and methanol [(100:0 (500 mL), 96:4 (1800 mL), 90:10 (400 mL), 80:20 (400 mL), and 0:100 (500 mL) by volume] at a flow rate 50 mL/min to provide 17 fractions (each about 180 mL). Column fractions were monitored by TLC on silica gel plates developed with chloroform and methanol (95:5 by volume) mobile phase. Fractions with similar R_f values on the TLC plates were pooled. Spots were detected by spraying it with 2% H_2SO_4 and then heating on a hot plate. Fractions 8 to 11 (1.5 g) were purified by methanol recrystallization to get solid fraction C41 and liquid fraction C42. The active fraction C41 (139 mg) was purified by preparative TLC with chloroform and methanol (95:5 by volume) to yield two active compounds 1 (41.7 mg, R_f = 0.47) and 2

(27.2 mg, R_f = 0.42) (Fig. 13). The purity of the compound **A1** and **A2** was monitored using high-pressure liquid chromatography (HPLC) with a UV detector at 425 nm with a mobile phase of acetonitrile and water (7:3 by volume) in flow rate of 1 mL/min. The retention time of the compound **A1** (Fig. 14) and **A2** (Fig. 15) was 2.325 min and 2.183 min, with the purity of 98.2% and 97.3%, respectively.

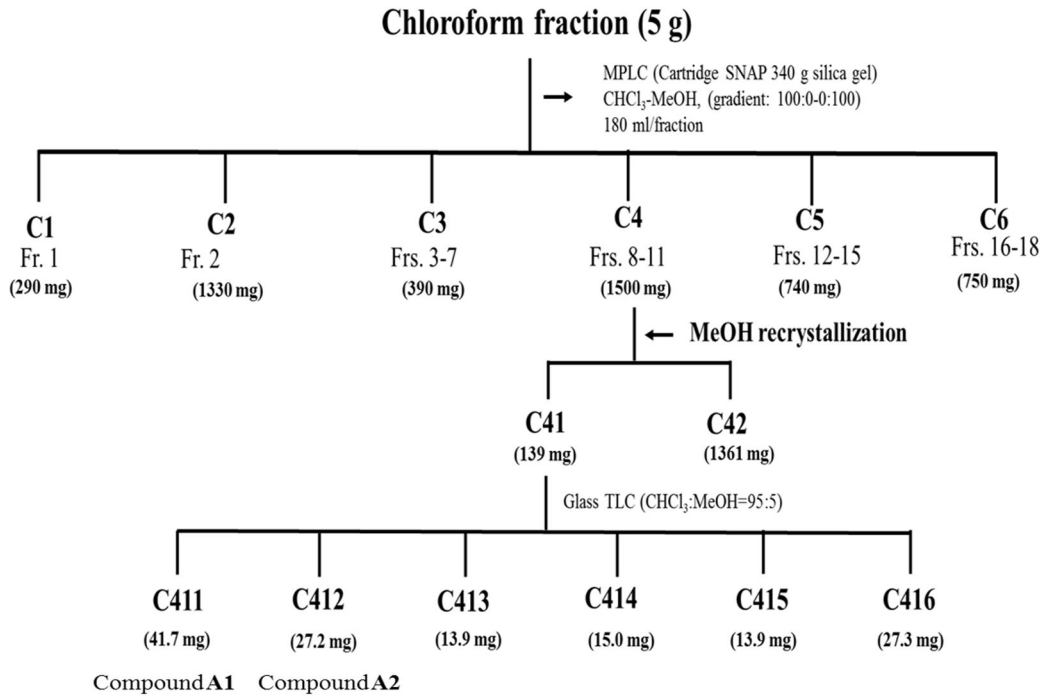

Fig. 13. Procedures to isolate BACE-1 inhibitory compounds A1 and A2 from the chloroform-soluble fraction of *C. longa* rhizomes methanol extract.

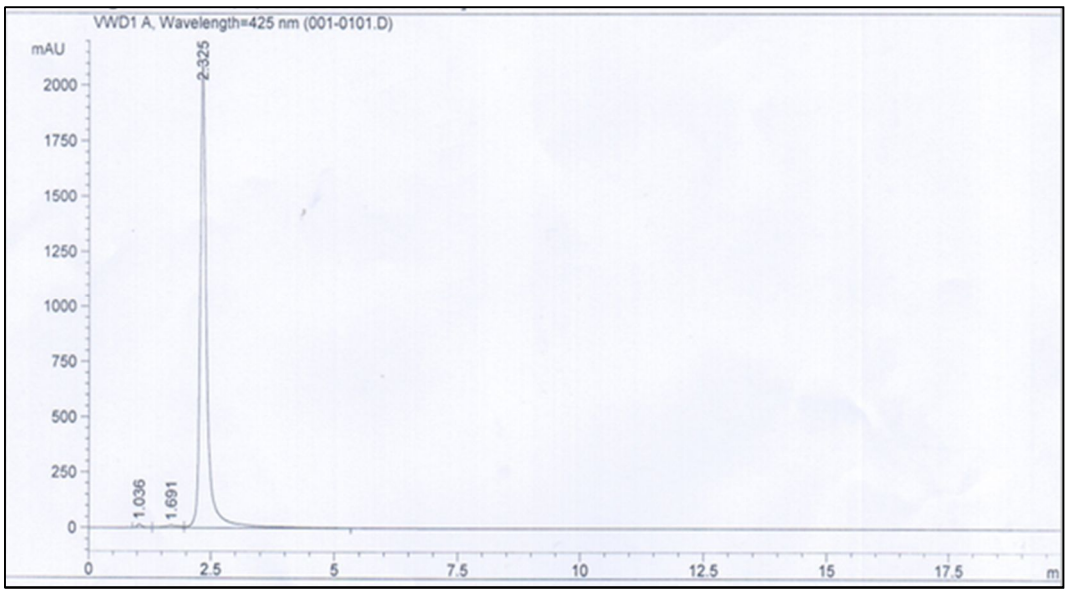

Fig. 14. HPLC chromatogram of compound A1.

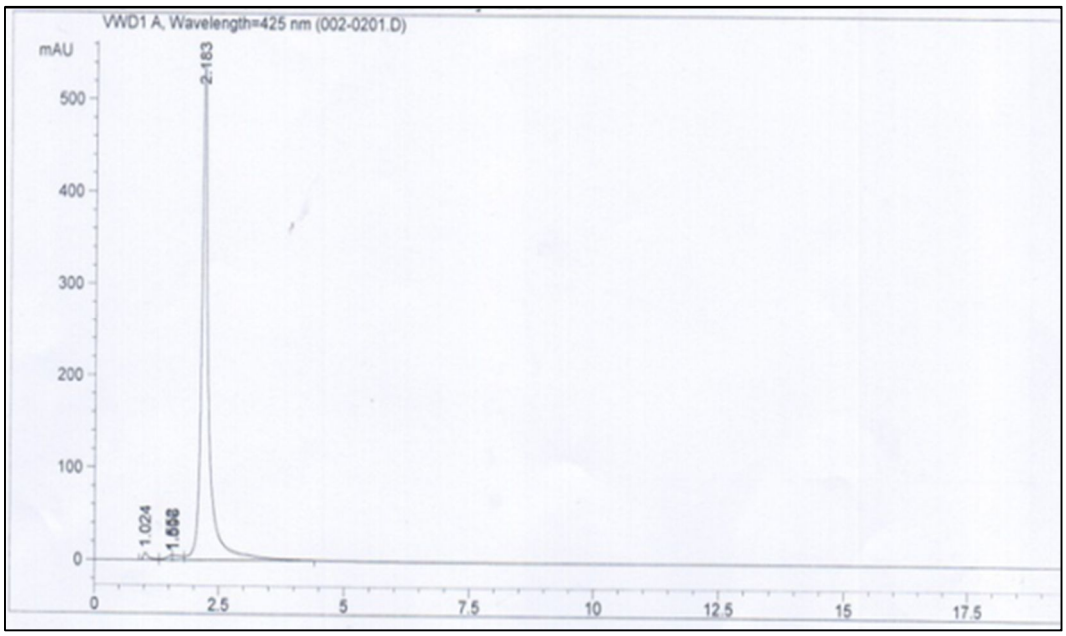

Fig. 15. HPLC chromatogram of compound A2.

The active ethyl acetate-soluble fraction (500 mg) was chromatographed on a 70 × 1.5 cm silica gel (70 g) column by elution with a gradient of chloroform and methanol [(100:0 (250 mL), 99:1 (550 mL), 98:2 (300 mL), 97:3 (300 mL), 96:4 (200 mL), 90:10 (100 mL), and 0:100 (800 mL) by volume] to afford eight fractions (each about 300 mL). The active fractions 23 to 24 (34.3 mg) were pooled and recrystallized in acetone at –20 °C to afford an active compound **A3** (13.2 mg) (Fig. 16). The purity of the compound **A3** was monitored using HPLC with a UV detector at 425 nm with a mobile phase of acetonitrile and water (7:3 by volume) in flow rate of 1 mL/min. The retention time of compound **A3** was 16.17 min with the purity of 99.2% (Fig. 17).

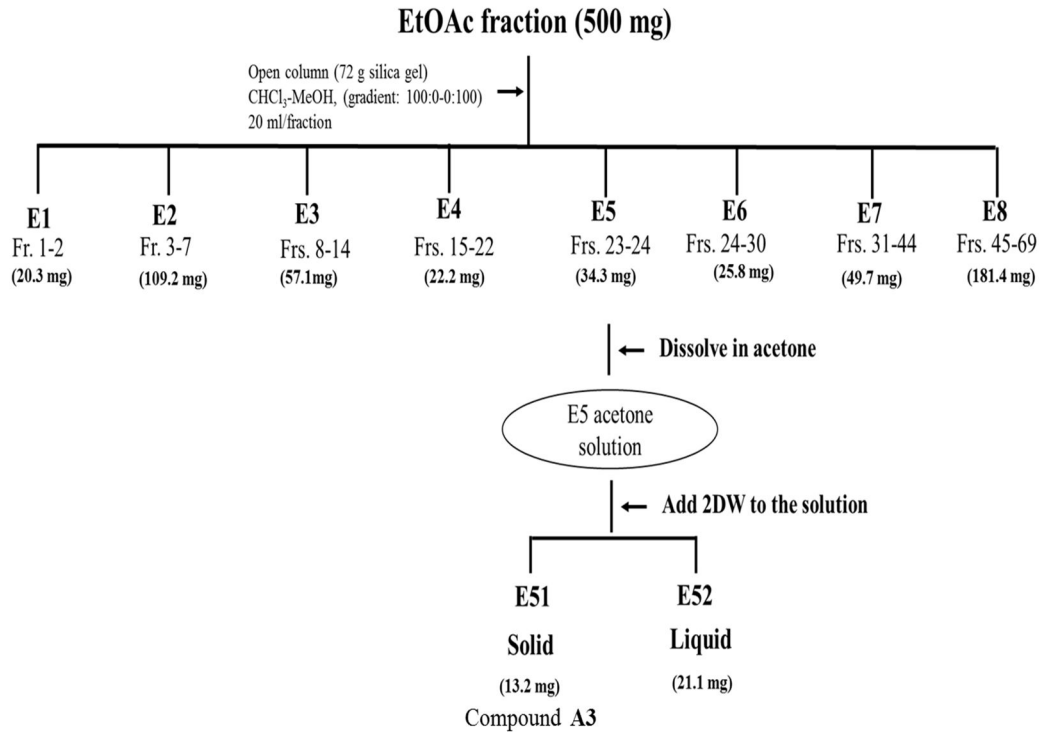

Fig. 16. Procedures to isolate BACE-1 inhibitory compound A3 from ethyl acetate-soluble fraction of *C. longa* rhizomes methanol extract.

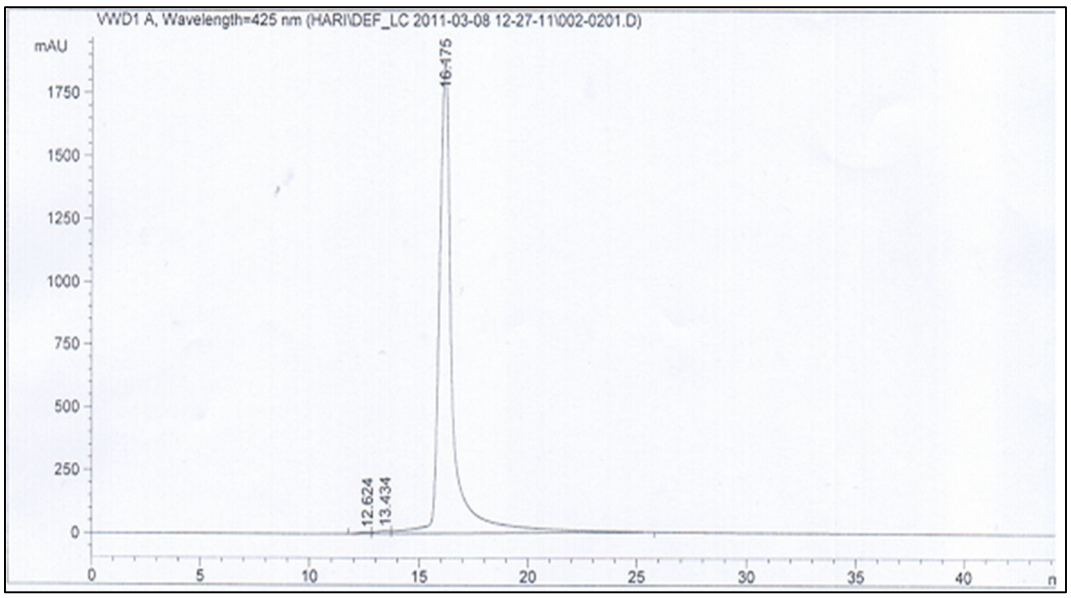

Fig. 17. HPLC chromatogram of compound A3.

1.5.2. Whole *Agastache rugosa* plants

Air-dried whole *A. rugosa* plants (5 kg) were pulverized, extracted with methanol (3 ×15 L) at room temperature for 2 days, and filtered. The combined filtrate was concentrated to dryness by rotary evaporation at 40°C to yield approximately 455 g of a black tar. The extract (400 g) was sequentially partitioned into hexane- (75.4 g), chloroform- (55.1 g), ethyl acetate- (27.6 g), butanol- (54.5 g), and water-soluble (187.4 g) portions for the subsequent bioassays (Fig. 18). The organic solvent-soluble portions were concentrated under vacuum at 40°C, and the water-soluble portion was concentrated at 50°C. To isolate the active constituents, 0.1–2 mg/mL of each *A. rugosa* whole plant-derived fraction was tested in a FRET-based enzyme assay, as described by Lv *et al*. (2008) and Wang *et al*. (2014).

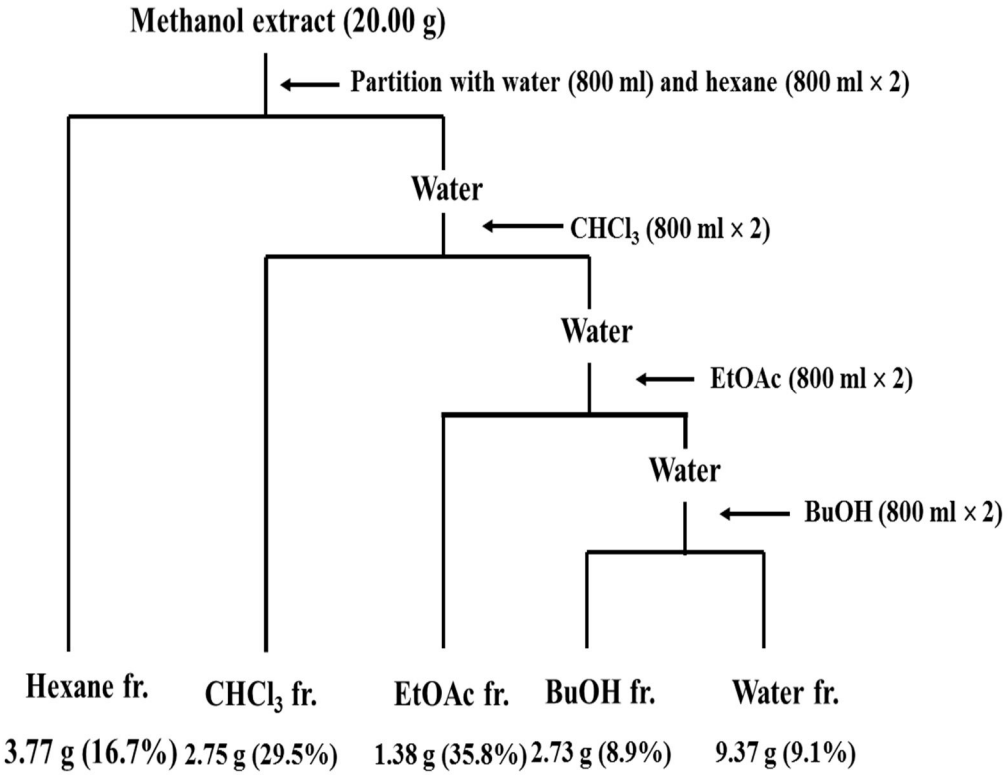

Fig. 18. Solvent partition of methanol extract of whole *A. rugosa* plants.

The hexane-soluble fraction (10 g) was the most biologically active fraction, and MPLC was performed using an Isolera apparatus equipped with a UV detector at 254 and 365 nm and a SNAP column cartridge (340 g silica gel) with a column volume of 510 mL (Fig. 19). Separation was achieved with a gradient of hexane and ethyl acetate (100:0, 90:10, 80:20, 70:30, 40:60, 50:50, 30:70, and 10:90 by volume) and finally with methanol (1 L) at a flow rate of 50 mL/min to provide 48 fractions (each approximately 180 mL). The column fractions were monitored by TLC on silica gel plates developed with a hexane and ethyl acetate (6:4 by volume) mobile phase. Fractions with similar R_f values on the TLC plates were pooled and the spots were detected by spraying the plate with 2% sulfuric acid. This separation procedure was repeated seven times. Active fractions 17–20 (H2) and 28–33 (H4) were obtained. Fraction H2 was separated by MPLC with a UV

detector and a column cartridge (100 g silica gel) with a column volume of 132 mL by elution with a gradient of hexane and ethyl acetate (100:0, 90:10, 80:20, 70:30, 60:40, 50:50, and 30:70 by volume) and finally with 500 mL methanol at a flow rate of 30 mL/min to provide 235 fractions (each approximately 22 mL). The column fractions were monitored by TLC on silica gel plates, as stated previously. Active fractions 1–34 (H21) and 35–120 (H22) were obtained. Fraction H21 was separated by MPLC with a UV detector and a column cartridge (25 g silica gel) with a column volume of 33 mL by elution with a gradient of chloroform and ethyl acetate (100:0, 95:5, 90:10, 85:15, 80:20, 70:30, and 50:50 by volume) and finally with 300 mL methanol at a flow rate of 25 mL/min to provide 79 fractions (each approximately 22 mL). Fraction H22 was separated by MPLC with a UV detector and a column cartridge (25 g silica gel) with a column volume of 33 mL by elution with a gradient of hexane and ethyl acetate (100:0, 95:5, 90:10, 85:15, 80:20, 70:30, 60: 40, 40:60, and 30:70 by volume) and finally with 300 mL methanol at a flow rate of 25 mL/min to give 116 fractions (each approximately 22 mL). A preparative high-performance liquid chromatograph was used to separate the constituents from active fractions 37–65 (H213) from H21 and fractions 33–48 (H222) from H22. The column was a 7.8 mm i.d. × 300 mm μBondapak C18 (Waters, Milford, MA, USA) with a mobile phase of methanol and water (80:20 and 95:5 by volume) at a flow rate of 1 mL/min. Chromatographic separation was monitored using a UV detector at 217 and 216 nm, respectively. Finally, two active compounds **B1** (7.26 mg) from H213 and **B2** (12.52 mg) from H222 were isolated at retention times of 13.15 (Fig. 20) and 16.86 min (Fig. 21), with the purity of 95% and 98%, respectively. Fraction H4 was recrystallized in methanol at –20°C to afford active compound **B3** (81.4 mg). The purity of the compound **B3** was monitored using HPLC with a UV detector at 425 nm with a mobile phase of methanol and water (9:1 by volume) in flow rate of 1 mL/min. The retention time of the compound **B3** was 11.31 min with the purity of 99% (Fig. 22).

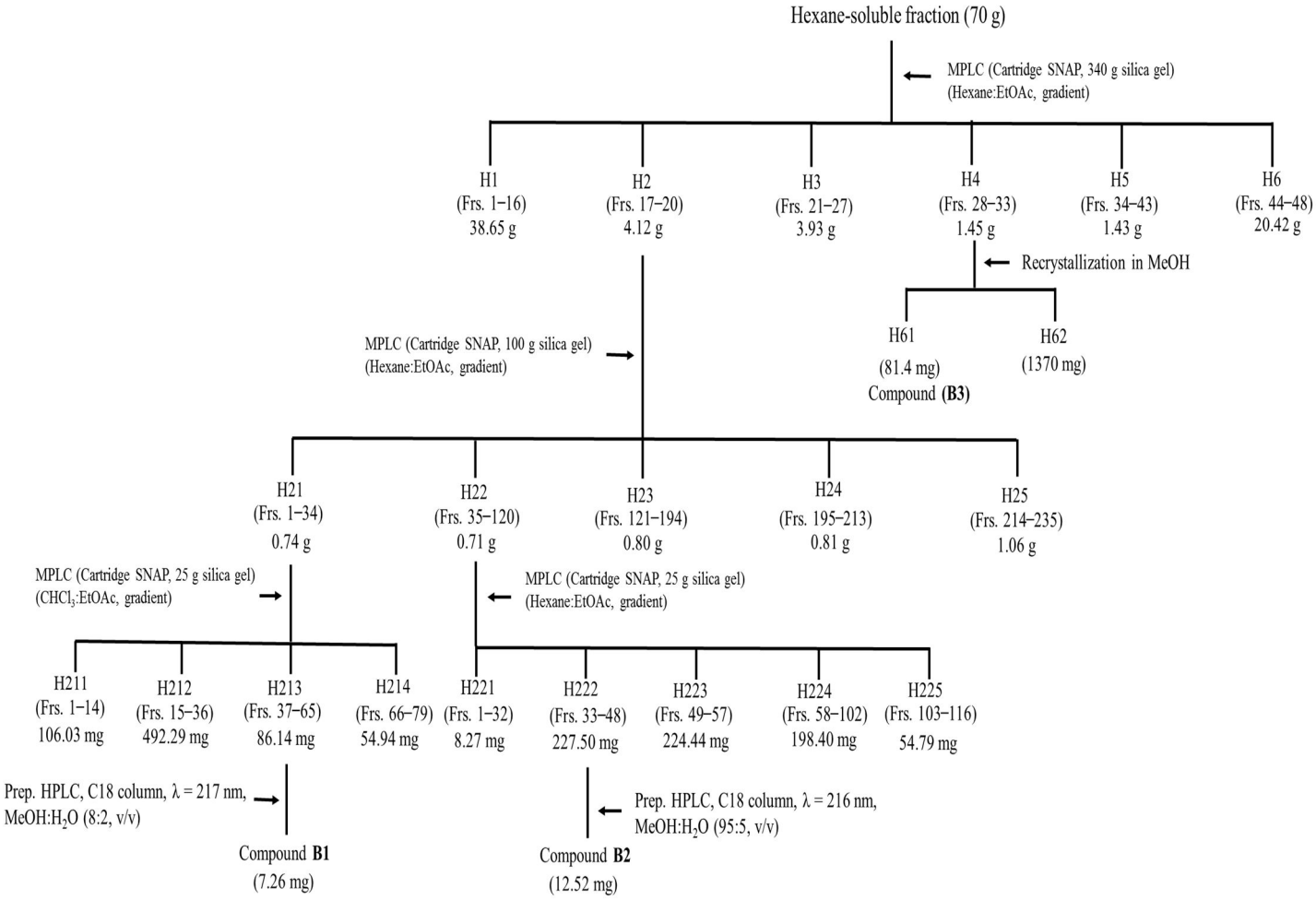
Hexane-soluble fraction (70 g)
MPLC (Cartridge SNAP, 340 g silica gel)
(Hexane:EtOAc, gradient)
H1
(Frs. 1–16)
38.65 g
H2
(Frs. 17–20)
4.12 g
H3
(Frs. 21–27)
3.93 g
H4
(Frs. 28–33)
1.45 g
H5
(Frs. 34–43)
1.43 g
H6
(Frs. 44–48)
20.42 g
Recrystallization in MeOH
H61
(81.4 mg)
Compound (B3)
H62
(1370 mg)
MPLC (Cartridge SNAP, 100 g silica gel)
(Hexane:EtOAc, gradient)
H21
(Frs. 1–34)
0.74 g
H22
(Frs. 35–120)
0.71 g
H23
(Frs. 121–194)
0.80 g
H24
(Frs. 195–213)
0.81 g
H25
(Frs. 214–235)
1.06 g
MPLC (Cartridge SNAP, 25 g silica gel)
(CHCl3:EtOAc, gradient)
MPLC (Cartridge SNAP, 25 g silica gel)
(Hexane:EtOAc, gradient)
H211
(Frs. 1–14)
106.03 mg
H212
(Frs. 15–36)
492.29 mg
H213
(Frs. 37–65)
86.14 mg
H214
(Frs. 66–79)
54.94 mg
H221
(Frs. 1–32)
8.27 mg
H222
(Frs. 33–48)
227.50 mg
H223
(Frs. 49–57)
224.44 mg
H224
(Frs. 58–102)
198.40 mg
H225
(Frs. 103–116)
54.79 mg
Prep. HPLC, C18 column, λ = 217 nm,
MeOH:H2O (8:2, v/v)
Compound B1
(7.26 mg)
Prep. HPLC, C18 column, λ = 216 nm,
MeOH:H2O (95:5, v/v)
Compound B2
(12.52 mg)

Fig. 19. Procedures to isolate BACE-1 inhibitory compounds from hexane-soluble fraction of whole *A. rugosa* plants methanol extract. Whole *A. rugosa* plants methanol extract was sequentially partitioned into hexane-, chloroform-, ethyl acetate-, butanol-, and water-soluble portions. The hexane-soluble fraction was most biologically active and MPLC was performed. To isolate active compounds from the fraction, 0.1–2 mg/L of each fraction was tested in a FRET enzyme assay.

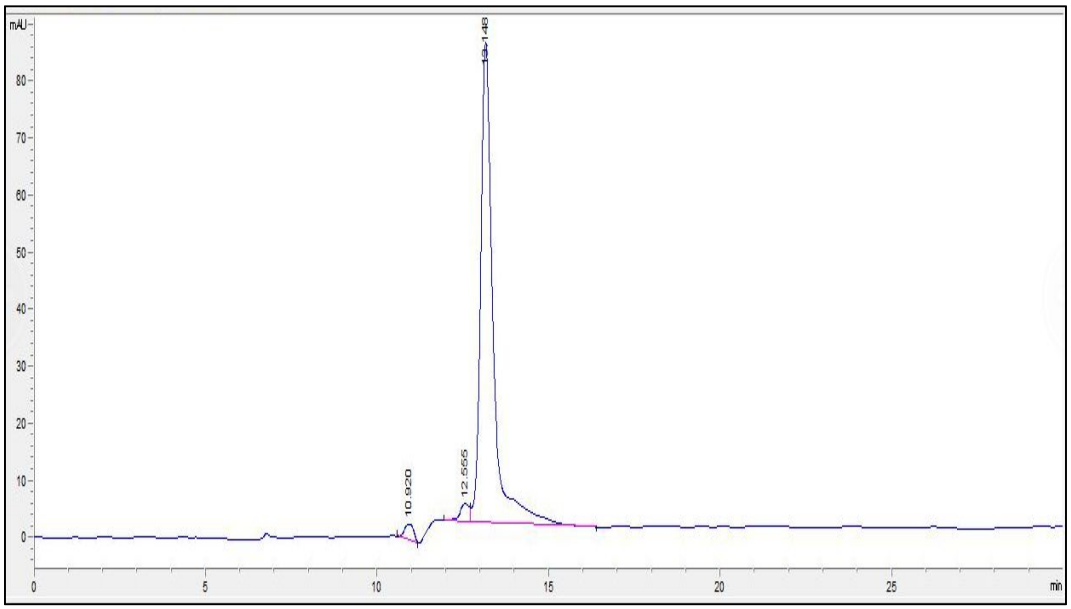

Fig. 20. HPLC chromatogram of compound B1.

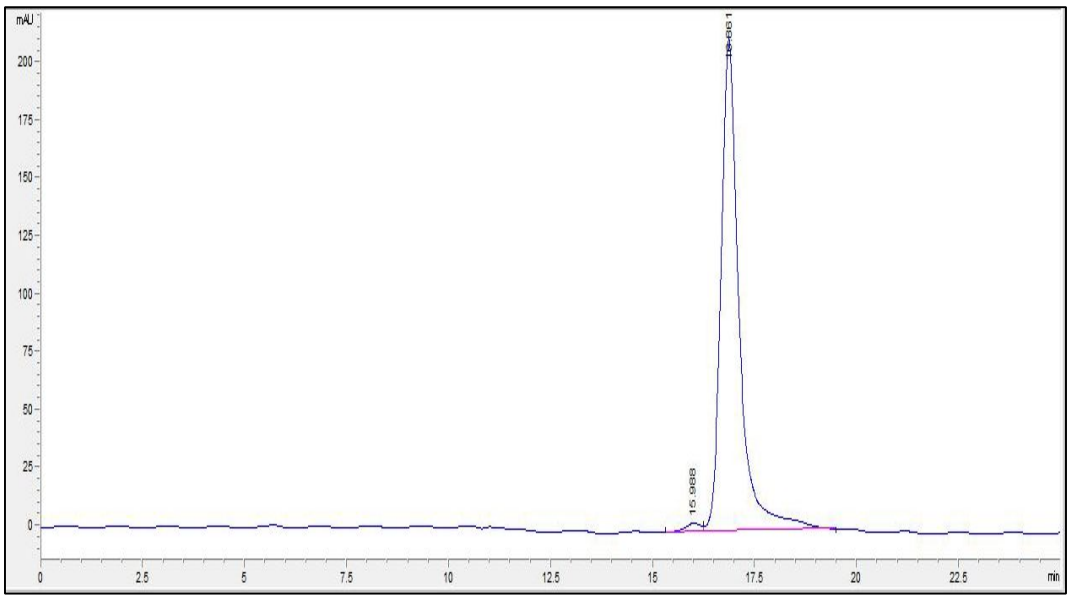

Fig. 21. HPLC chromatogram of compound B2.

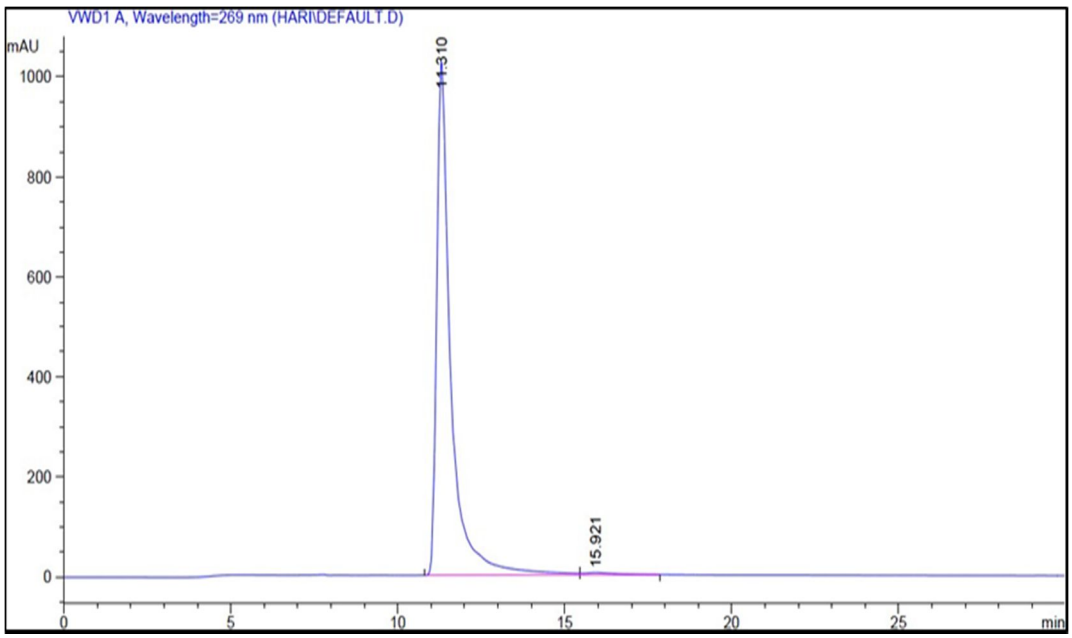

Fig. 22. HPLC chromatogram of compound B3.

1.6. Data analysis

The fifty percent inhibitory concentration (IC_{50}) was defined as the concentration of the compound that resulted in a 50% loss of BACE-1 activity. The IC_{50} values were determined using GraphPad Prism 5.1 software (GraphPad Software, La Jolla, CA, USA). The IC_{50} values for the treatments were considered significantly different from one another when their 95% confidence limits (CLs) did not overlap. The results are expressed as the means ± standard errors (SEs) of triplicate samples from three independent experiments.

RESULTS

1.1. FRET bioassay-guided fractionation and isolation

1.1.1. *Curcuma longa* rhizomes

Fractions obtained from the solvent hydrolyzable of the methanol extract of *C. longa* rhizomes were examined for inhibitory activity against human BACE-1 using a FRET-based enzyme assay (Table 7). Significant differences in inhibitory activity were observed among the fractions and were used to identify the peak activity fractions for the next step of purification. At a concentration of 2 mg/mL, both the methanol extract and chloroform-soluble fractions suppressed completely activity of BACE-1. At 1 mg/mL, the chloroform-soluble fraction was the most potent inhibitory material, followed by the ethyl acetate-soluble fraction. Low and no inhibition were produced by the butanol- and water-soluble fractions, respectively. Therefore, the chloroform- and ethyl acetate-soluble fractions were subjected to further purification steps to identify inhibitory constituents for BACE-1.

Table 7. I*n vitro* BACE-1 inhibitory activity of each fraction obtained from the solvent partitioning of the methanol extract of the *C. longa* rhizomes using a FRET-based enzyme assay

Material	**% inhibition at test concentration (mg/mL)**		
	2.0	**1.0**	**0.5**
Methanol extract	100	65	57
Hexane-soluble fraction	85	48	43
Chloroform-soluble fraction	100	81	71
Ethyl acetate-soluble fraction	84	76	70
Butanol-soluble fraction	82	26	3
Water-soluble fraction	0	0	0

FRET assay-guided fractionation of *C. longa* rhizomes extract afforded three active compounds identified by spectroscopic analyses, including MS and NMR. The three active compounds were curcumin (**A1**), demethoxycurcumin (**A2**), and

bisdemethoxycurcumin (**A3**) (Fig. 23).

The compound **A1** was obtained as a brightly yellow colored powder and identified as curcumin (**A1**) by spectroscopic analysis, including EI-MS (Fig. 24), ^{1}H NMR (Fig 25), and ^{13}C NMR (Fig. 26). The ^{13}C NMR spectra showed 21 carbons in the molecule and including two methoxyphenyl groups and double bonds suggesting the molecular formula $C_{21}H_{20}O_6$. The interpretation of proton and carbon signals was largely consistent with previously described (Jayaprakasha *et al*., 2002).

Curcumin (**A1**): a brightly yellow colored powder; UV (MeCN): λ_{max} nm = 430. EI-MS (70 eV), *m/z* (% relative intensity): 368 [M^+] (100), 350 (67), 272 (23), 231 (24), 217 (25), 191 (48), 190 (60), 177 (93), 145 (26), 137 (44). ^{1}H NMR (CD_3CN, 600 MHz) and ^{13}C NMR (CD_3CN, 600 MHz) are given in Table 8.

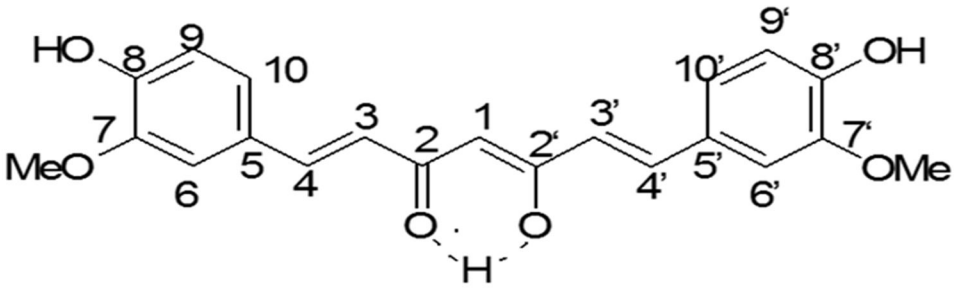

Compound **A1**

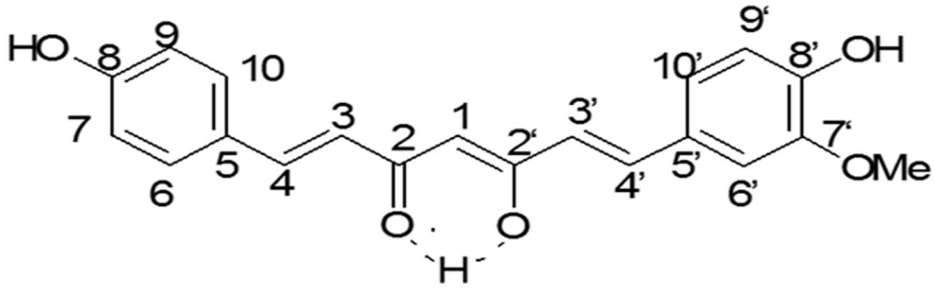

Compound **A2**

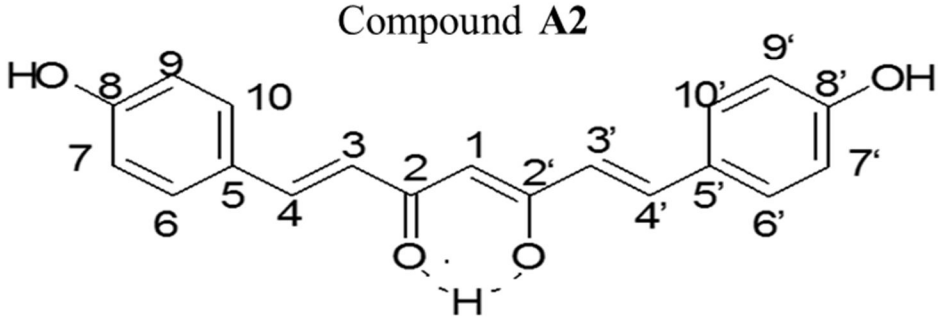

Compound **A3**

Fig. 23. Structures of the curcuminoids. These compounds were identified in the rhizomes of *C. long* in this study. The chemical formula of curcumin (**A1**) is $C_{21}H_{20}O_6$, with a molar mass of 368.39 g/mol; the chemical formula of demethoxycurcumin (**A2**) is $C_{20}H_{18}O_5$, with a molar mass of 338.36 g/mol; and the chemical formula of bisdemethoxycurcumin (**A3**) is $C_{19}H_{16}O_4$, with a molar mass of 308.33 g/mol.

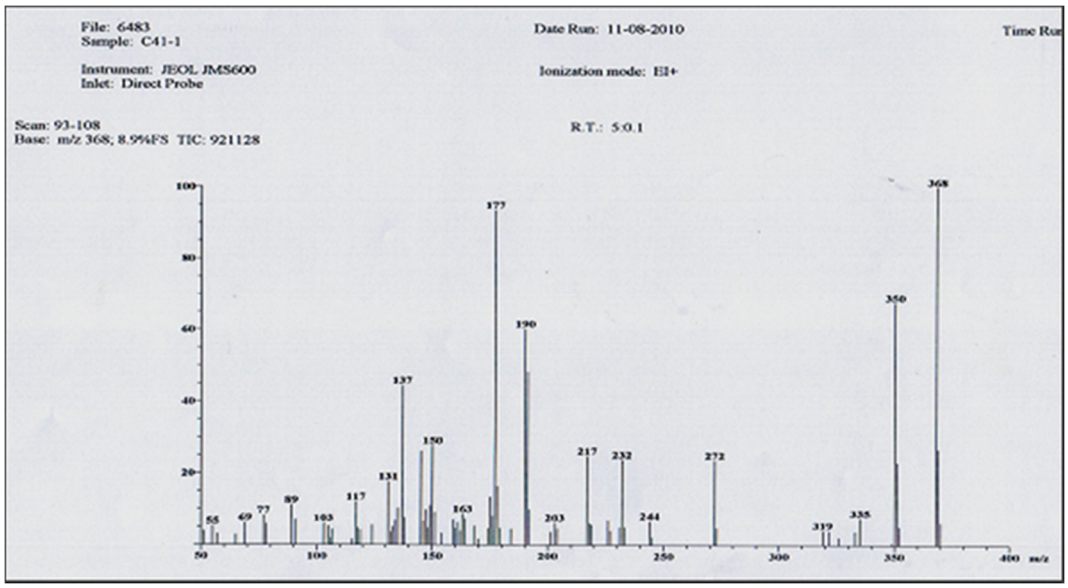

Fig. 24. EI-MS spectrum of compound A1.

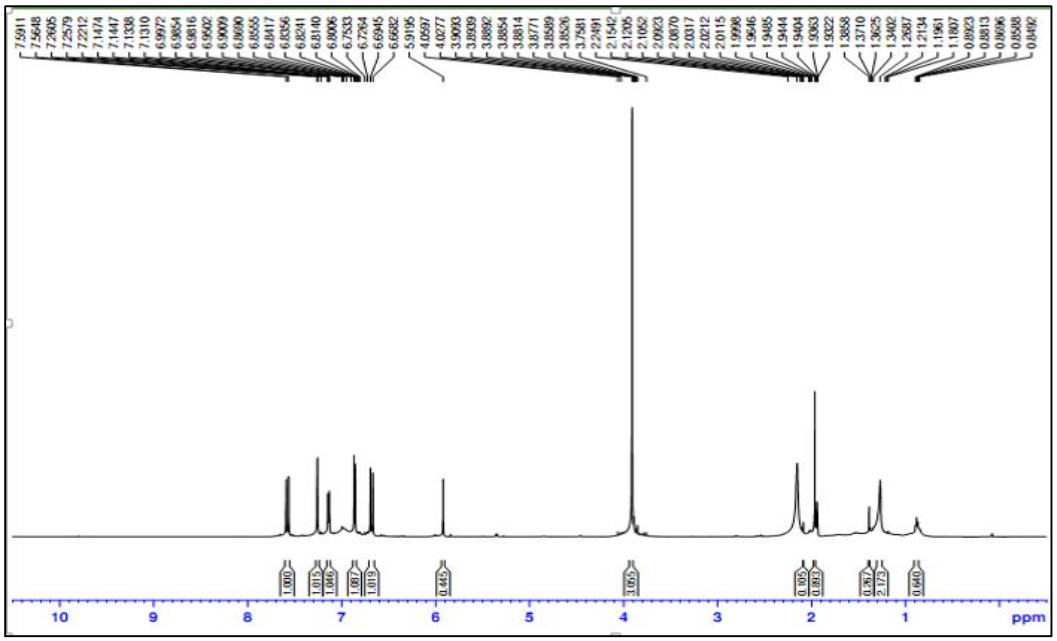

Fig. 25. ^{1}H NMR spectrum of compound A1.

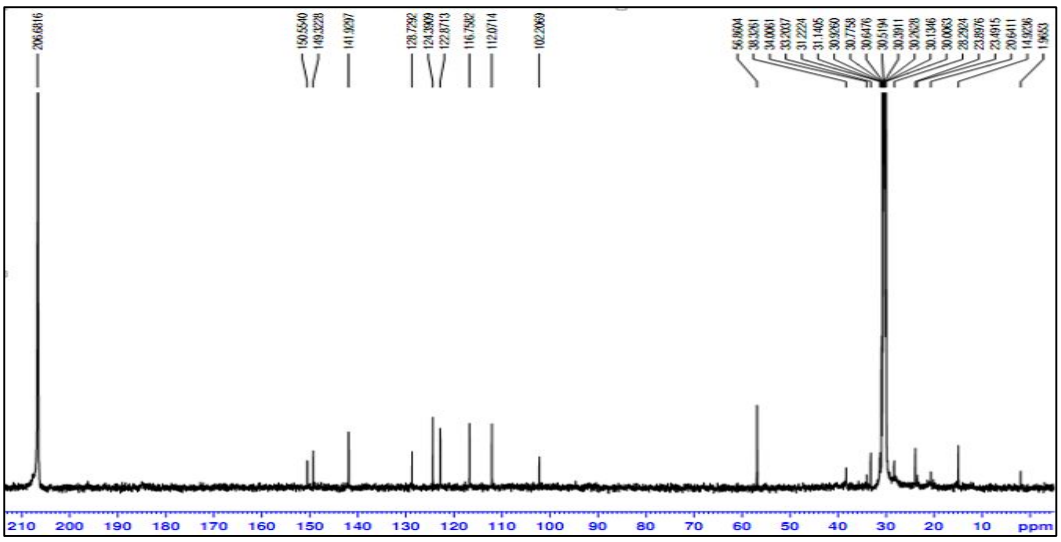

Fig. 26. ^{13}C NMR spectrum of compound A1.

Table 8. ^{1}H NMR (600 MHz) and ^{13}C NMR (150 MHz) spectral data of compound A1

Position	Partial structure	δ_C (ppm)	δ_H (ppm)	δ_C (ppm) Jayaprakasha *et al*. (2002)	δ_H (ppm) Jayaprakasha *et al*. (2002)
1	CH	102.21	5.91 s	100.8	6.06 s
2,2'	OH	206.68	16.41 bs	183.2	16.41bs
3,3'	CH	122.87	7.58 d (*J*=15.78)	121.1	7.57 d (*J*=16)
4,4'	CH	141.93	6.70 d (*J*=15.78)	140.7	6.75 d (*J*=16)
5,5’	C	128.73		126.4	
6,6'	CH	112.07	7.26 d (*J*=1.56)	111.5	7.32 d (*J*=2)
7,7'	C	149.32		148.0	
8,8'	OH	150.55	9.79 s	149.4	9.64 s
9,9'	CH	116.76	6.86 d (*J*=8.1)	115.8	6.85 d (*J*=8.1)
10,10'	CH	124.39	7.14 d (*J*=8.19)	123.0	7.16 dd (*J*=2, 8.1)
OMe	CH_3	56.86	3.31 s	55.7	3.85 s

The compound (**A2**) was obtained as a yellow-orange amorphous powder and identified as demethoxycurcumin (**A2**) by spectroscopic analysis, including EI-MS (Fig. 27), ^{1}H NMR (Fig. 28), and ^{13}C NMR (Fig. 29). The ^{13}C NMR showed 20 carbons in the molecular and including double bonds, methoxyphenyl, and hydroxyphenyl group suggesting the molecular formula $C_{20}H_{18}O_5$. The interpretation of proton and carbon signals was largely consistent with previously described (Jayaprakasha *et al*., 2002).

Demethoxycurcumin (**A2**): a yellow-orange amorphous powder. UV (MeCN): λ_{max} nm = 430. EI-MS (70 eV), *m/z* (relative intensity): 338 [M^+] (100), 320 (83), 191 (60), 190 (55), 177 (63), 150 (32), 147 (98), 140 (46), 57 (33). ^{1}H NMR (CD_3CN, 600 MHz) and ^{13}C NMR (CD_3CN, 600 MHz) are given in Table 9.

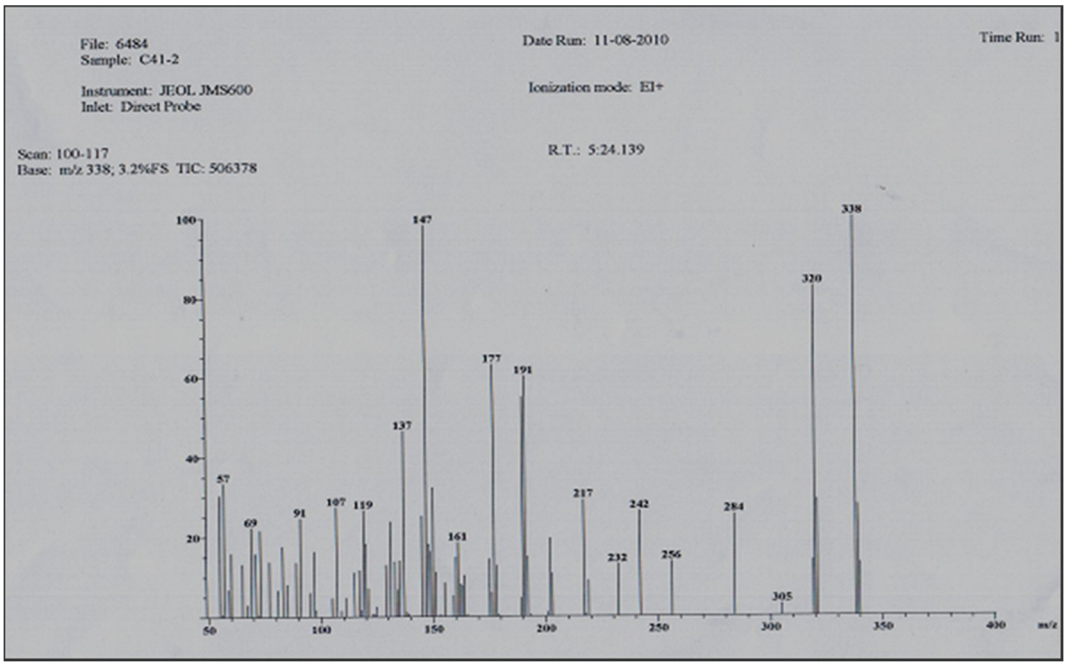

Fig. 27. EI-MS spectrum of compound A2.

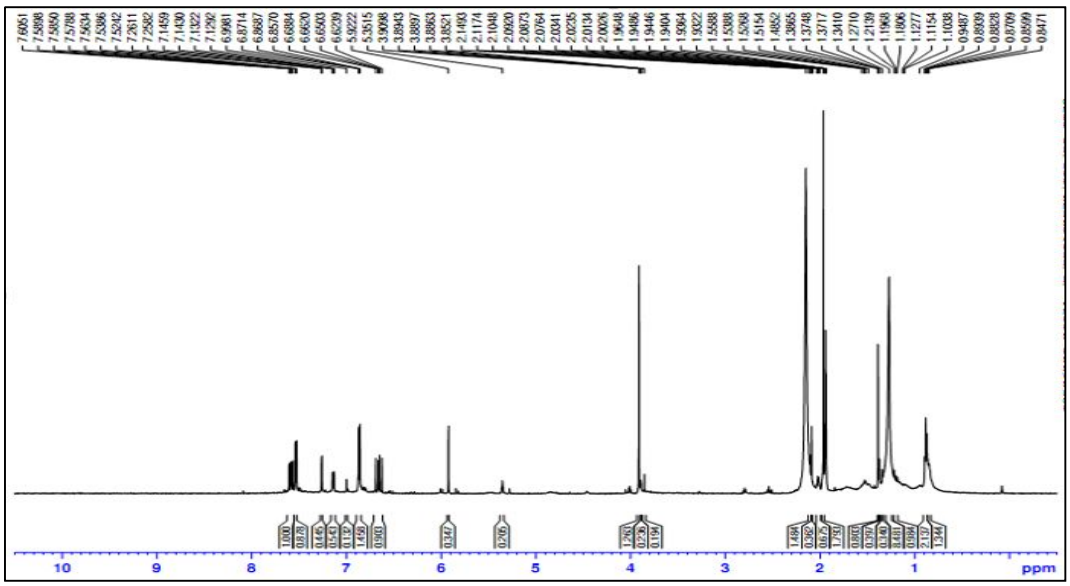

Fig. 28. ^{1}H NMR spectrum of compound A2.

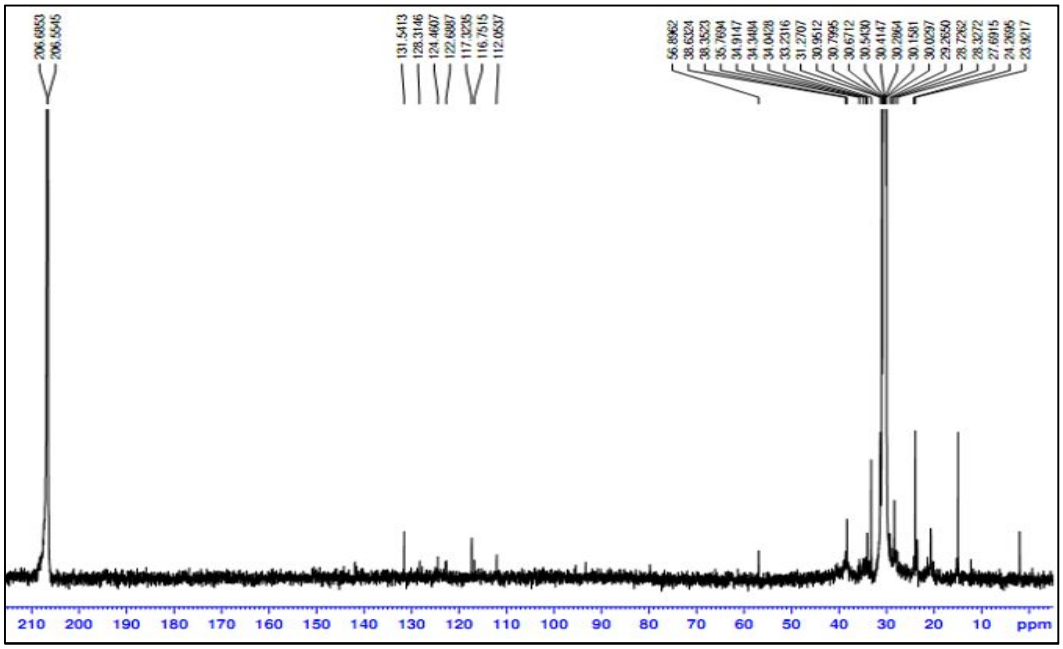

Fig. 29. ^{13}C NMR spectrum of compound A2.

Table 9. ^{1}H NMR (600 MHz) and ^{13}C NMR (150 MHz) spectral data of compound A2

Position	Partial structure	δ_C (ppm)	δ_H (ppm)	δ_C (ppm) Jayaprakasha *et al*. (2002)	δ_H (ppm) Jayaprakasha *et al*. (2002)
1	CH	101.8	5.92 (1H,S)	101.6	5.97 s
2,2'	OH	206.3, 206.3		184.4, 184.5	
3,3'	CH	122.2, 122.4	7.58 d (*J*=15.84)	122.1, 122.3	7.60 d (*J*=16)
4,4'	CH	141.5, 141.2	6.67 d (*J*=15.84), 6.64 d (*J*=15.84)	141.4, 141.0	6.69 d (*J*=16), 6.64 d (*J*=15.78)
5,5’	C	128.3, 127.7		128.2, 127.7	
6,6'	CH	111.6, 130.6	7.26 d (*J*=1.7), 6.87 d (*J*=1.6)	111.5, 130.9	7.34 d (*J*=1.7), 6.9 d (*J*=8)
7,7'	CH	147.1, 117.3	7.53 d (*J*=8.64)	148.8, 116.8	7.56 d (*J*=8)
8,8'	C	148.9, 158.4		150.0, 160.5	
9,9'	CH	116.7, 117.3	7.53 d (J=8.64), 6.85 d (J=8.4)	116.2, 116.8	7.56 d (*J*=8), 6.88 d (*J*=8)
10,10'	CH	124.5, 131.1	7.14 d (J=6.48), 6.87 d (*J*=8.64)	123.8, 130.9	7.27 dd (*J*=1.7), 6.9 d (*J*=8)
OMe	CH_3	56.89	3.31 s	56.3	3.92 s

The compound (**A3**) was obtained as a yellow-orange amorphous powder and identified as bisdemethoxycurcumin (**A3**) by spectroscopic analysis, including EI-MS (Fig. 30), ^{1}H NMR (Fig. 31), ^{13}C NMR (Fig. 32), and DEPT (Fig.33). The ^{13}C NMR showed 19 carbons in the molecular and including double bonds and two hydroxyphenyl group suggesting the molecular formula $C_{19}H_{16}O_4$. The interpretations of proton and carbon signals was largely consistent with previously described (Jayaprakasha *et al*., 2002).

Bisdemethoxycurcumin (**A3**): a yellow crystal. UV (MeCN) λ_{max} nm = 412. EI-MS (70 eV), *m/z* (relative intensity): 308 [M^+] (52), 290 (33), 202 (20), 161 (30), 160 (44),

147 (100), 120 (23), 119 (25), 107 (31). ^{1}H NMR (CD_3CN, 600 MHz) and ^{13}C NMR (CD_3CN, 600 MHz) are given in Table 10.

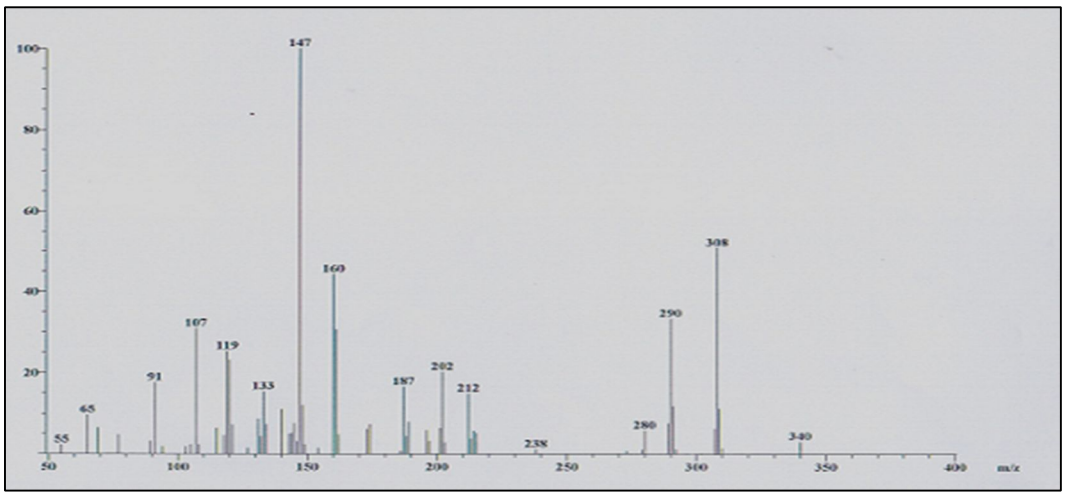

Fig. 30. EI-MS spectrum of compound A3.

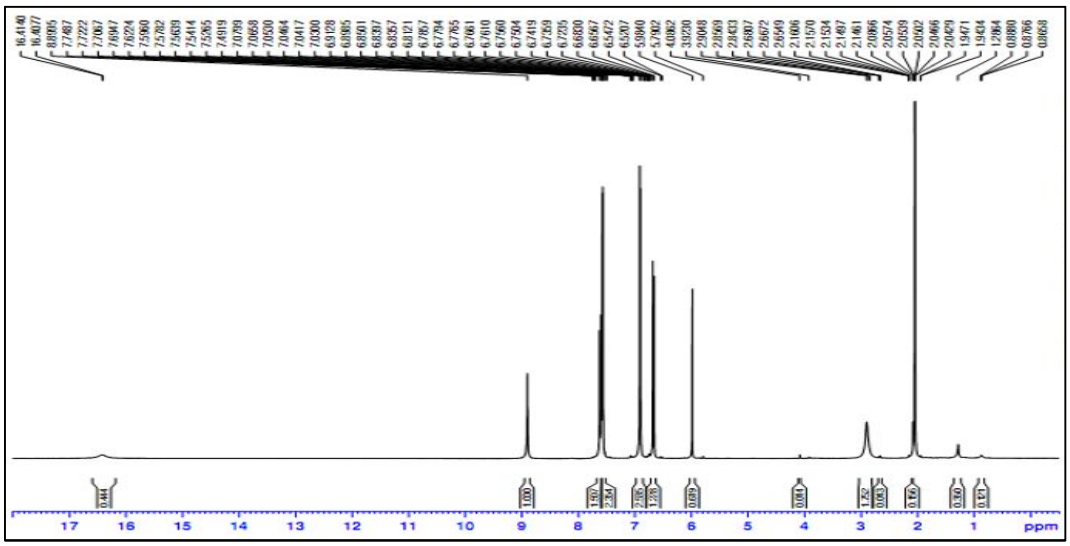

Fig. 31. ^{1}H NMR spectrum of compound A3.

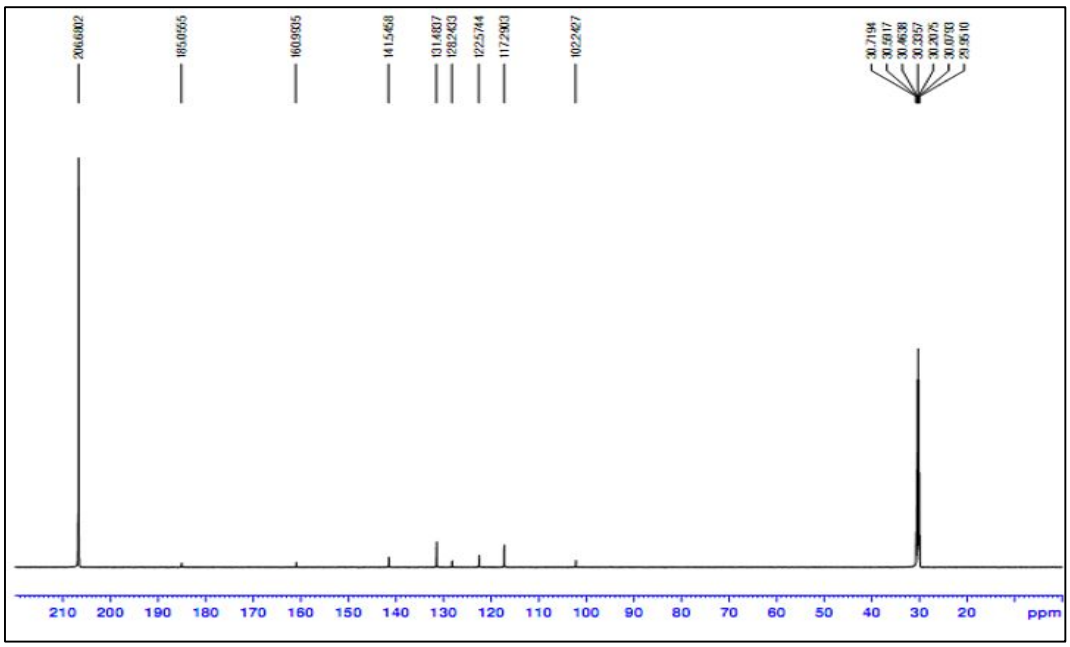

Fig. 32. ^{13}C NMR spectrum of compound A3.

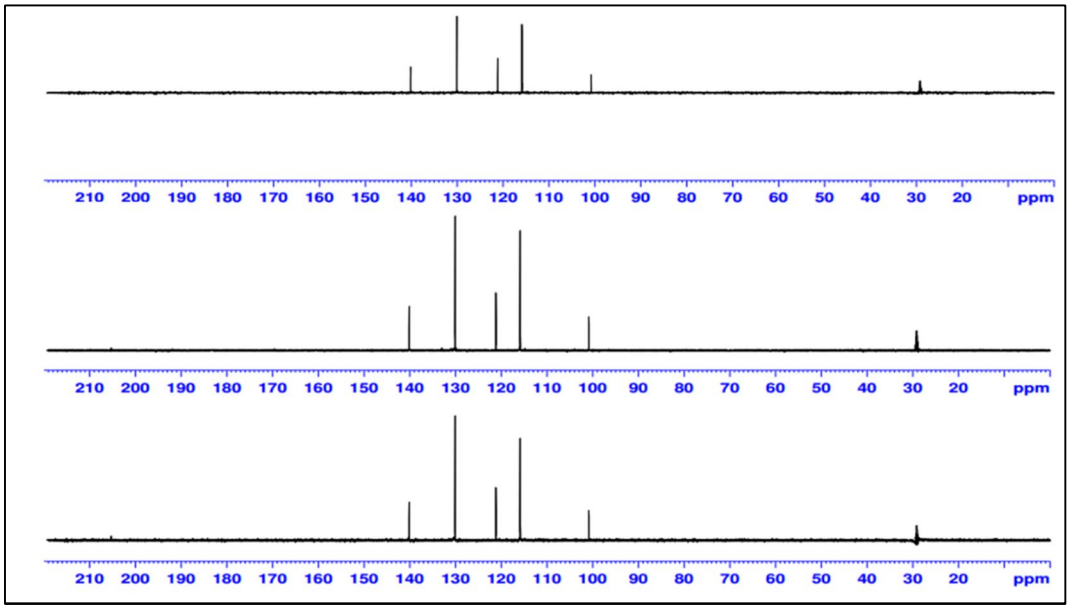

Fig. 33. DEPT spectrum of compound A3.

Table 10. ^{1}H NMR (600 MHz) and ^{13}C NMR (150 MHz) spectral data of compound A3

Position	Partial structure	δ_C (ppm)	δ_H (ppm)	δ_C (ppm) Jayaprakasha *et al* (2002)	δ_H (ppm) Jayaprakasha *et al* (2002)
1	CH	102.2	5.93 s	100.9	6.03 s
2,2'	OH	185.1	16.40 s	183.2	16.4 bs
3,3'	CH	122.6	7.48 d (J=8.58)	120.8	7.56 d (*J*=15.9)
4,4'	CH	142.0	7.56 d (J=15.78)	140.3	7.56 d (*J*=15.9)
5,5	C	128.2		125.8	
6,6'	CH	131.5	6.81 d (J=8.64)	130.3	6.84 d (*J*=8.2)
7,7'	CH	117.3	7.56 d (J=15.78)	115.9	7.56 d (*J*=15.9)
8,8'	C	161.0	8.90 s	159.8	10.03 s
9,9'	CH	117.3	7.48 d (J=8.58)	115.9	7.56 d (*J*=15.9)
10,10'	CH	131.5	6.81 d (J=8.64)	130.3	6.84 d (J=8.2)

1.1.2. Whole *Agastache rugosa* plants

Fractions obtained from the solvent hydrolyzable of the methanol extract of the whole *A. rugosa* plants were examined for inhibitory activity against human BACE-1 using a FRET-based enzyme assay (Table 11). Significant differences in inhibitory activity were observed among the fractions and were used to identify the peak activity fractions for the next step of purification. At a concentration of 1 mg/mL, the hexane-soluble fraction was the most potent inhibitor, while no inhibition was obtained using the chloroform-, ethyl acetate-, butanol-, or water-soluble fractions. Therefore, the hexane-soluble fractions was subjected to further purification steps to identify inhibitory constituents for BACE-1.

Table 11. *In vitro* human BACE-1 inhibitory activity of each fraction obtained from the solvent partitioning of the methanol extract of the whole *A. rugosa* plants using a FRET-based enzyme assay

Material	**% inhibition at test concentration (mg/mL)**		
	2.0	**1.0**	**0.1**
Methanol extract	75 ± 1.1	50 ± 1.4	24 ± 1.1
Hexane-soluble fraction	100	97 ± 1.3	47 ± 1.6
Chloroform-soluble fraction	0	0	0
Ethyl acetate-soluble fraction	20 ± 0.9	3±0.9	0
Butanol-soluble fraction	0	0	0
Water-soluble fraction	0	0	0

FRET-based enzyme assay-guided fractionation of the whole *A. rugosa* plants afforded three active compounds that were identified by spectroscopic analyses, including EI-MS and NMR spectroscopy. The three BACE-1 inhibitory compounds were maslinic acid (**B1**), oleanolic acid (**B2**), and acacetin (**B3**) (Fig. 34).

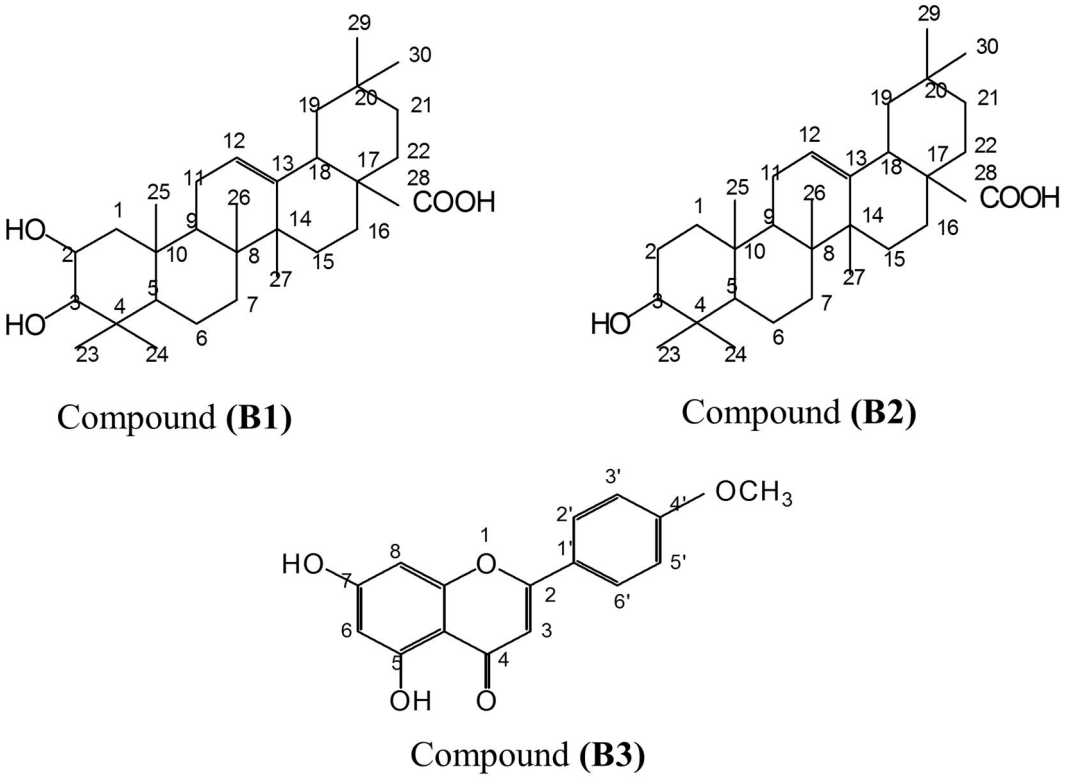

Fig. 34. Structures of maslinic acid, oleanolic acid, and acacetin. These compounds were identified in the whole *A. rugosa* plants in this study. The chemical formula of maslinic acid (**B1**) is $C_{30}H_{48}O_4$, with a molar mass of 472.70 g/mol; the chemical formula of oleanolic acid (**B2**) is $C_{30}H_{48}O_3$, with a molar mass of 456.70 g/mol; and the chemical formula of acacetin (**B3**) is $C_{16}H_{12}O_5$, with a molar mass of 284.26 g/mol.

The compound **(B1)** was obtained as a white crystal and identified as maslinic acid **(B1)** by spectroscopic analysis, including EI-MS (Fig. 35), ^{1}H NMR (Fig. 36), and ^{13}C NMR (Fig. 37). The ^{13}C NMR showed 30 carbons in the molecular including double bond, methyl, and carbonyl group suggesting the molecular formula $C_{30}H_{48}O_4$. The interpretations of proton and carbon signals were largely consistent with those of previous studies (Tanaka *et al*., 2003; Dam *et al*., 2010).

Maslinic acid **(B1)**: a white crystal; UV (MeOH): λ_{max} nm = 217; EI-MS (70 eV), *m*/*z* (% relative intensity): 472 $[M]^+$ (1.9), 284 (3.0), 256 (2.8), 248 (100), 233 (8.6), 203 (73.5), 189 (8.1), 173 (3.4), 133 (10.2), 105 (5.1), 95 (4.4), 69 (6.2), 55 (5.3). ^{1}H NMR (MeOD, 600 MHz) and ^{13}C NMR (MeOD, 150 MHz) are given in Table 12.

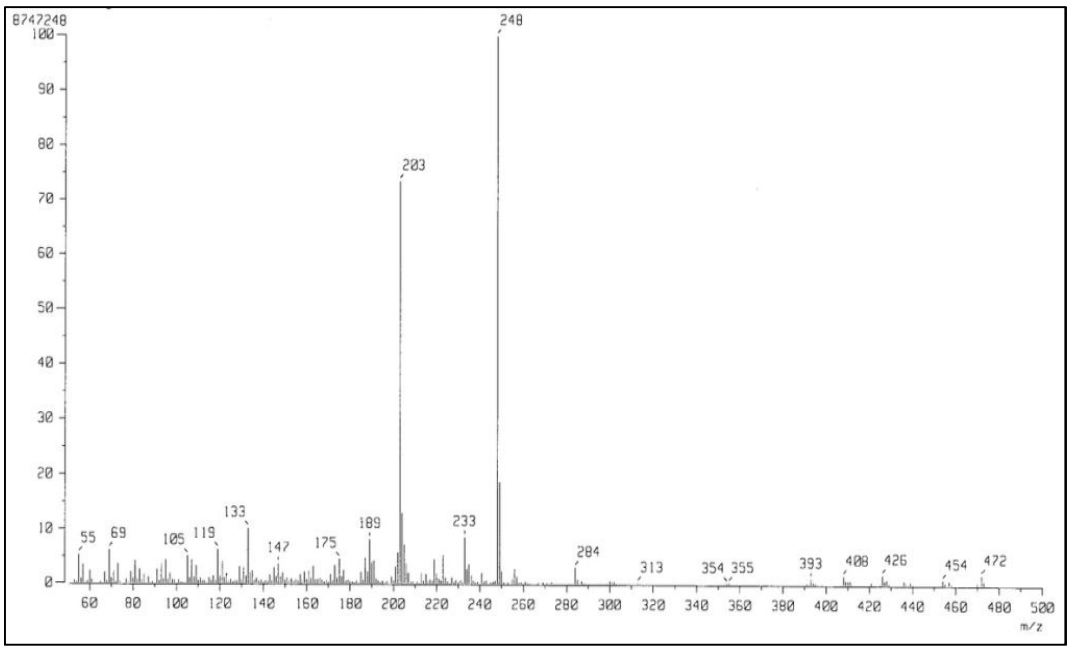

Fig. 35. EI-MS spectrum of compound B1.

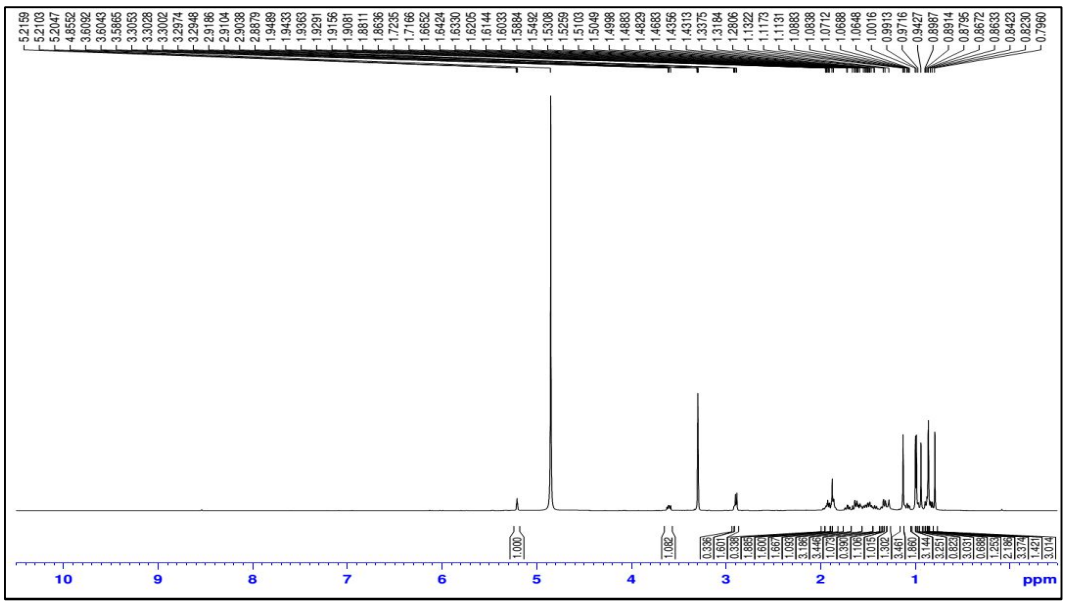

Fig. 36. ^{1}H NMR spectrum of compound B1.

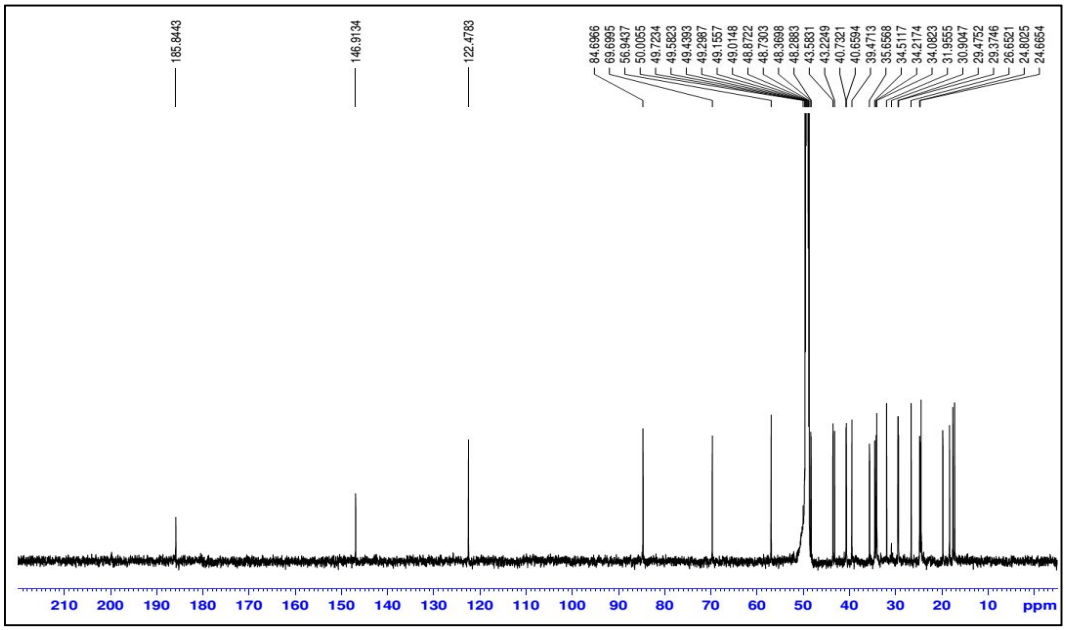

Fig. 37. ^{13}C NMR spectrum of compound B1.

Table 12. ^{1}H NMR (600 MHz) and ^{13}C NMR (150 MHz) spectral data of compound B1

Position	Partional structure	δ_C (ppm)	δ_H (ppm)	δ_C (ppm) Tanaka *et al*. 2003	δ_H (ppm) Woo *et al*. 2014
1	CH_2	48.7		48.1	
2	CH	69.7	3.61 ddd (*J*=4.5, 2.9, 3.9)	69.5	3.62 m
3	CH	84.7	2.98 d (*J*=9.5)	84.5	2.91 d (*J*=10.0)
4	C	40.7		40.5	
5	CH	56.9		56.7	
6	CH_2	19.8		19.5	
7	CH_2	34.2		33.9	
8	C	39.5		39.2	
9	CH	49.0		49.0	
10	C	40.6		39.2	
11	CH_2	26.6		24.0	
12	CH	122.5	5.21 t (*J*=6.7)	123.6	5.27 t (*J*=3.5)
13	C	146.9		145.5	
14	C	43.2		42.6	
15	CH_2	29.4		28.8	
16	CH_2	24.8		24.0	
17	C	48.4		47.7	
18	CH	43.8		42.7	
19	CH_2	48.3		47.2	
20	C	30.9		31.6	
21	CH_2	34.5		34.9	
22	CH_2	34.1		33.8	
23	CH_3	29.5	1.13 s	29.3	1.17 s

24	CH_3	17.2	0.99 s	17.0	1.01 s
25	CH_3	17.6	0.87 s	17.1	0.91 s
26	CH_3	18.3	0.86 s	17.4	0.82 s
27	CH_3	24.5	1.10 s	23.9	1.02 s
28	COOH	185.8		180.0	
29	CH_3	31.9	0.79 s	33.5	0.81 s
30	CH_3	24.7	0.94 s	23.9	0.95 s

The compound **(B2)** was obtained as a white amorphous powder and identified as oleanolic acid **(B2)** by spectroscopic analysis, including EI-MS (Fig. 38), ^{1}H NMR (Fig. 39), and ^{13}C NMR (Fig. 40). The ^{13}C NMR showed 30 carbons in the molecular including double bond, methyl, and carbonyl group suggesting the molecular formula $C_{30}H_{48}O_3$. The interpretations of proton and carbon signals were largely consistent with those of previous studies (Hossain and Ismail, 2013; Gangwal *et al*., 2010).

Oleanolic acid **(B2)**: a white amorphous powder; UV (MeOH): λ_{max} nm = 216; EI-MS (70 eV), *m/z* (% relative intensity): 456 $[M]^+$ (4.3), 249 (18.8), 248 (100), 233 (6.0), 207 (17.3), 204 (11.3), 203 (59.7), 190 (10.0), 189 (10.6), 175 (7.4), 133 (15.0), 105 (6.7), 81 (6.1), 69 (8.0), 55 (7.6). ^{1}H NMR (MeOD, 600 MHz) and ^{13}C NMR (MeOD, 150 MHz) are given in Table 13.

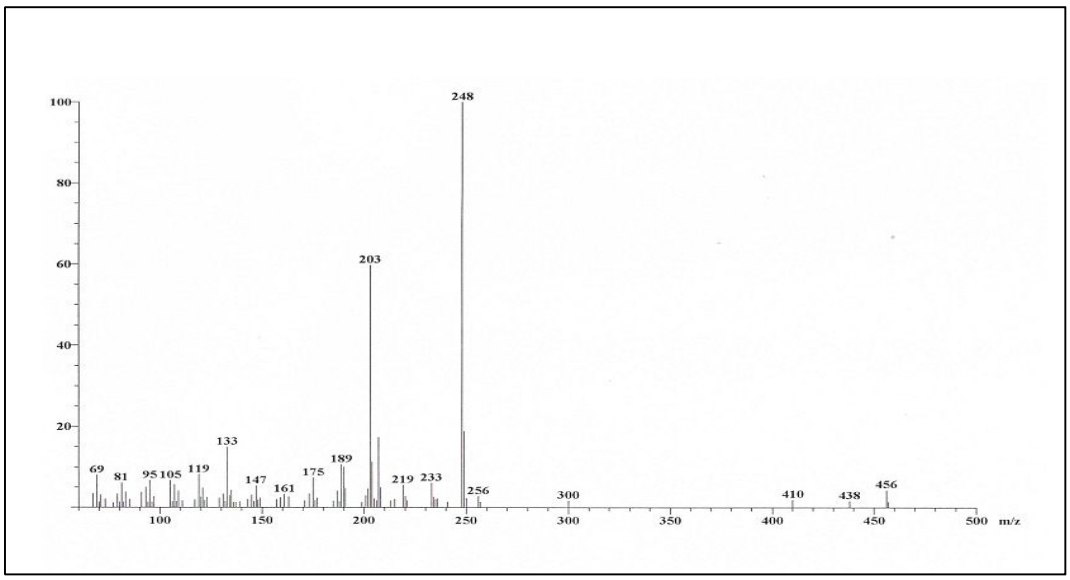

Fig. 38. EI-MS spectrum of compound B2.

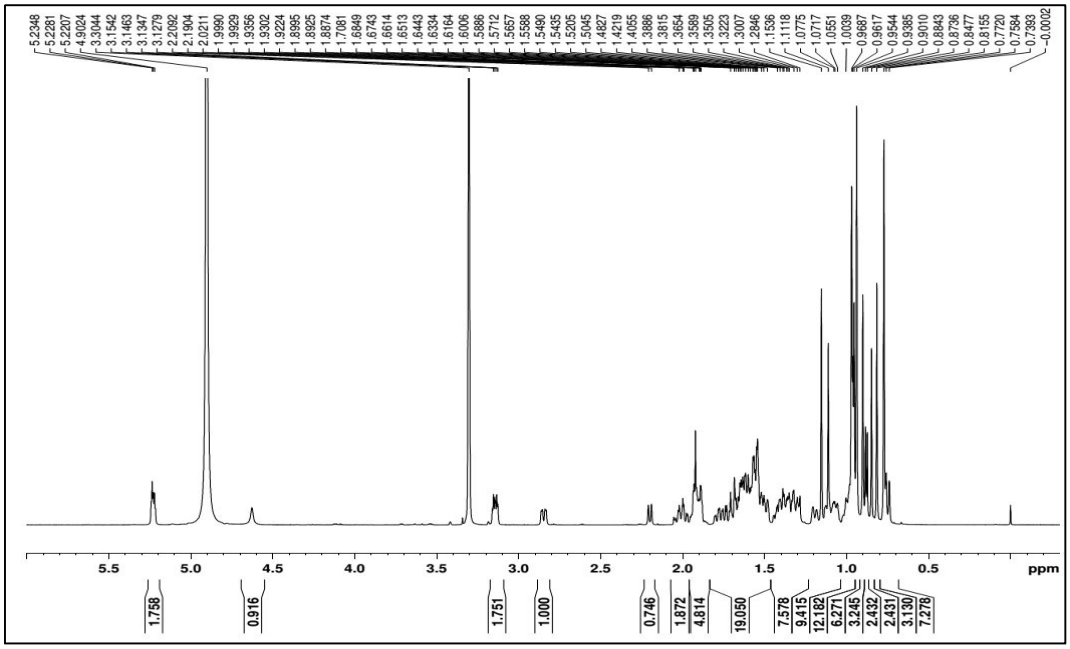

Fig. 39. ^{1}H NMR spectrum of compound B2.

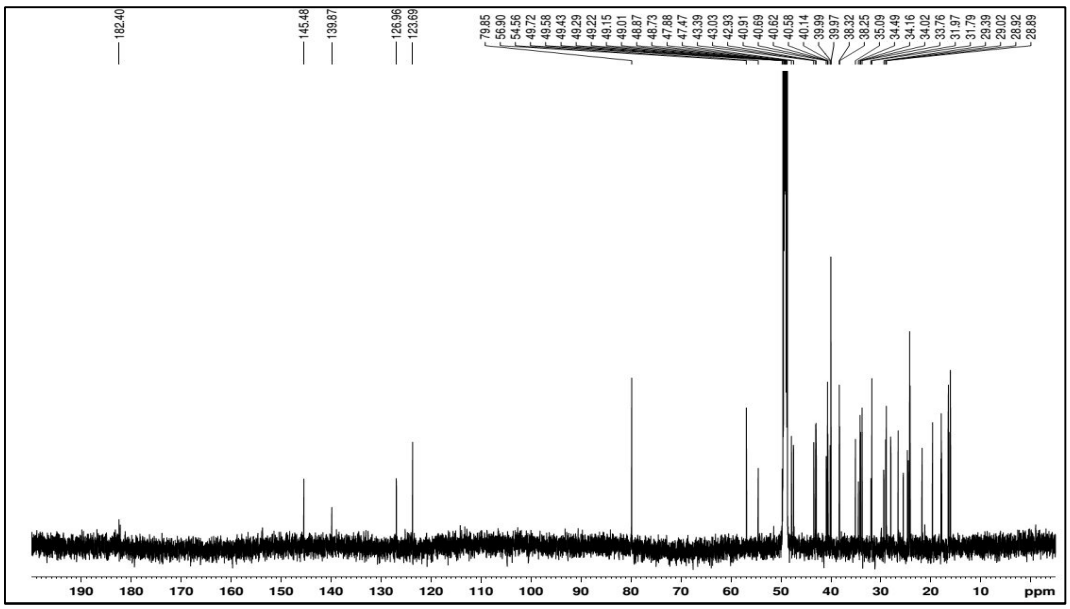

Fig. 40. ^{13}C NMR spectrum of compound B2.

Table 13. ^{1}H NMR (600 MHz) and ^{13}C NMR (150 MHz) spectral data of compound B2

Position	Partional structure	δ_C (ppm)	δ_H (ppm)	δ_C (ppm) Gangwal, 2010	δ_H (ppm) Hossain and Ismail, 2013
1	CH_2	38.2	2.20 m	38.27	2.09 m
2	CH_2	26.5	3.15 dd (J=15.8, 4.4)	26.97	3.17 t (J=7)
3	CH	79.8		78.42	
4	C	38.3		38.56	
5	CH	56.9		55.05	
6	CH_2	17.9		18.15	
7	CH_2	34.0	3.34 s	32.53	3.38 s
8	C	40.0		39.13	
9	CH	47.9	2.20 m	47.42	2.09 m

10	C	35.1		36.84	
11	CH_2	21.7	4.62 s	22.84	4.56 s
12	CH	123.7	5.23 s	121.93	4.59 s
13	C	145.5		144.5	
14	C	42.9		41.52	
15	CH_2	28.0	1.56 m	27.52	1.51 m
16	CH_2	24.3	1.41 m	23.43	1.38 m
17	C	43.0		45.87	
18	CH	40.7	2.85 dd (J=9.9, 4.5)	40.94	1.51 m
19	CH_2	47.5	1.56 m	46.01	1.51 m
20	C	31.8		30.50	
21	CH_2	34.5	1.38 m	33.73	1.37 m
22	CH_2	33.8		32.29	
23	CH_3	28.9	1.12 s	27.98	1.08 s
24	CH_3	16.5	0.90 s	15.52	0.91 s
25	CH_3	16.0	0.79 s	15.13	0.79 s
26	CH_3	16.5	0.97 s	16.88	0.97 s
27	CH_3	25.5	1.15 s	25.71	1.34 s
28	COOH	182.4		180.29	
29	CH_3	34.2	0.85 s	32.94	0.89 s
30	CH_3	24.2	0.95 s	23.17	0.92 s

The compound **(B3)** was obtained as yellow needles and identified as acacetin **(B3)** by spectroscopic analysis, including EI-MS (Fig. 41), FT-IR (Fig. 42), ^{1}H NMR (Fig. 43), and ^{13}C NMR (Fig. 44). The ^{13}C NMR showed 16 carbons in the molecular including dihydroxy and methoxyphenyl group suggesting the molecular formula $C_{16}H_{12}O_5$.; FT-IR ν_{max} cm^{-1}: 3147 (-OH), 1651 (-C=O), 1605, 1560, 1503, 1428 (-C=C)。 The interpretations of proton and carbon signals was largely consistent with those of previous studies (Wawer and Zielinska, 2001; Miyazawa and Hisama, 2003).

Acacetin **(B3)**: yellow needles; UV (MeOH): λ_{max} nm = 269, 315; EI-MS (70 eV), *m/z* (% relative intensity): 284 $[M]^+$ (100), 283 (12.5), 241 (11.4), 152 (6.9), 132 (18). ^{1}H NMR (DMSO-d_6, 600 MHz) and ^{13}C NMR (DMSO-d_6, 150 MHz) are given in Table 14.

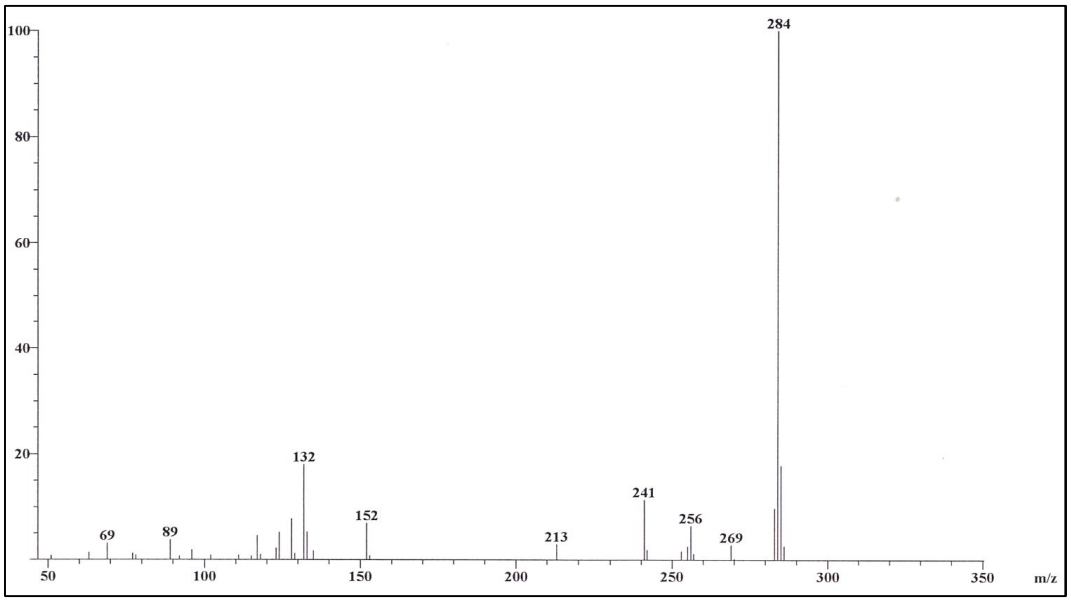

Fig. 41. EI-MS spectrum of compound B3.

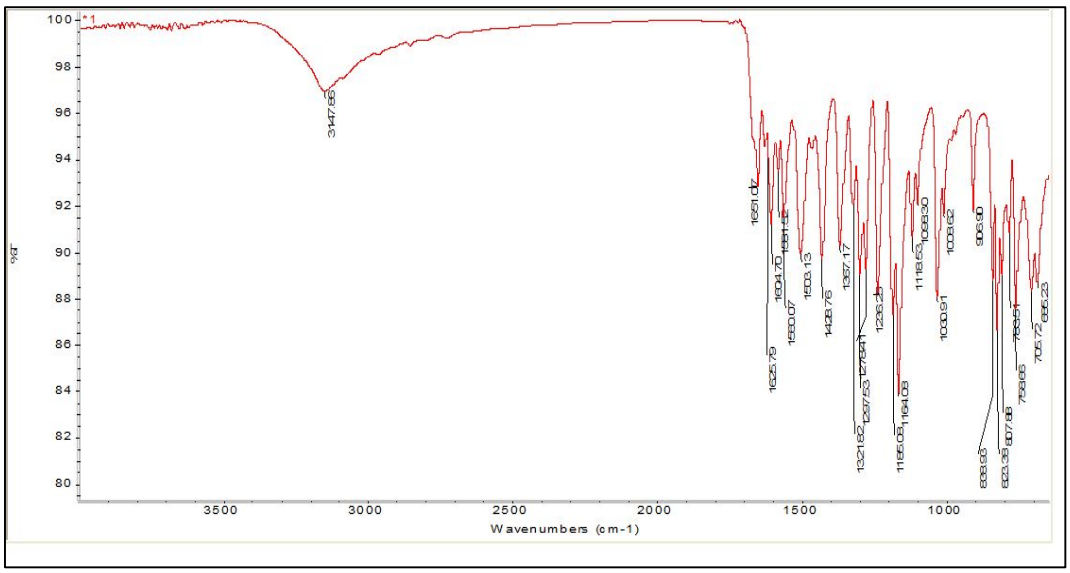

Fig. 42. FT-IR spectrum of compound B3.

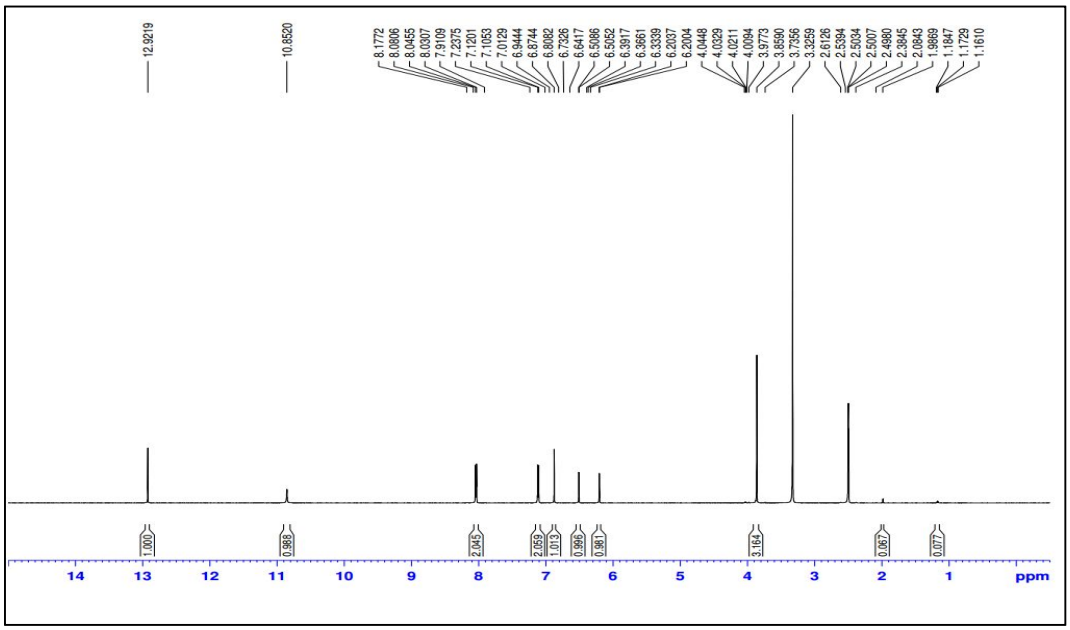

Fig. 43. ^{1}H NMR spectrum of compound B3.

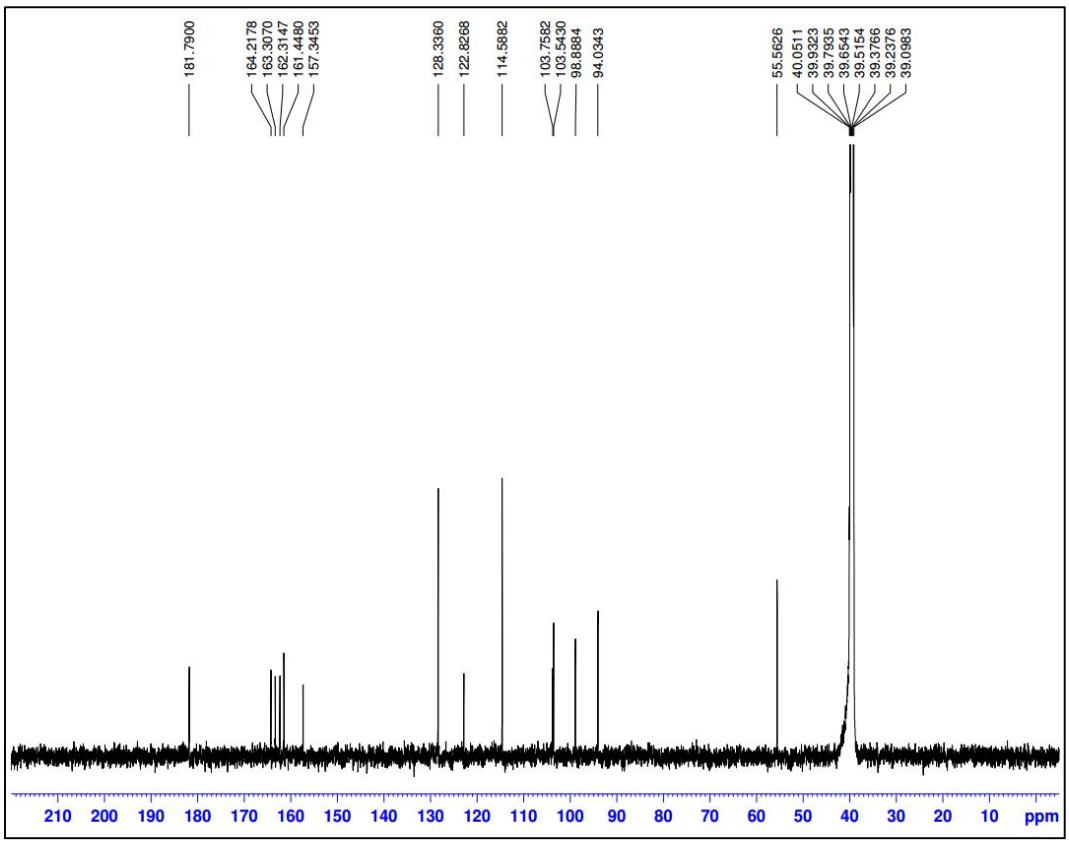

Fig. 44. ^{13}C NMR spectrum of compound B3.

Table 14. ^{1}H NMR (600 MHz) and ^{13}C NMR (150 MHz) spectral data of compound B3

Position	Partional structure	δ_C (ppm)	δ_H (ppm)	δ_C (ppm) Wawer and Zielinska, 2001	δ_H (ppm) Miyazawa and Hisama, 2003
2	C	164.2	-	164.8	
3	CH	103.5	6.87	103.9	6.74 s
4	C	181.8	-	182.3	
5	OH	161.4	12.92	162.2	12.83 s
6	CH	98.9	6.51 d (*J*=2.04)	99.4	6.85 d (*J*=2.5)
7	C	163.3	10.85	163.9	
8	CH	94.0	6.20 d (*J*=1.98)	94.3	6.45 d (*J*=2.5)
9	C	157.3	-	157.9	
10	C	103.8	-	104.4	
-1’	C	122.8		123.5	
-2’	CH	128.3	8.04 d (*J*=8.88)	128.4	8.03 d (*J*=9.0)
-3’	CH	114.6	7.11 d (*J*=8.88)	114.8	7.11 d (*J*=9.0)
-4’	C	162.3		162.8	
-5’	CH	114.6	7.11 d (*J*=8.88	114.8	7.11 d (*J*=9.0)
-6’	CH	128.3	8.04 d (*J*=8.88)	128.4	8.03 d (*J*=9.0)
OCH_3		55.6	3.16 s	56.1	3.90 s

1.2. *In vitro* BACE-1 inhibitory activity of isolated compounds

1.2.1. BACE-1 inhibitory activity of compounds from *Curcuma longa* rhizomes

The BACE-1 inhibitory activity of three curcuminoids (CCN, DMCCN, and BDMCCN) isolated from *C. longa*, commercial tetrahydrocurcumin, and human BACE-1 inhibitor IV and EGCG, which were used as positive controls, were elucidated (Table 15). Based on IC_{50} values, BDMCCN was 20 and 13 times more potent at inhibiting BACE-1 than CCN and DMCCN. The inhibitory activity of DMCCN was significantly different from that of CCN. THCCN was ineffective. BDMCCN was significantly more active than EGCG. Overall, these compounds were significantly less potent inhibitors of BACE-1 than BACE-1 inhibitor IV.

Table 15. *In vitro* human BACE-1 inhibitory activity of three isolated curcuminoids, commercial tetrahydrocurcumin, two BACE-1 inhibitors BACE-1 inhibitor IV and EGCG using a FRET-based enzyme assay

Compound	IC_{50}, µM (95% CL)	Slope ± SE	χ^2	*P*-value
CCN	340 (296–391)	0.7 ± 0.03	8.96	0.917
DMCCN	217 (197–240)	1.0 ± 0.05	7.67	0.951
BDMCCN	17 (14–20)	1.9 ± 0.21	8.65	0.958
Tetrahydrocurcumin	> 2000			
EGCG	82.0 (72.6–92.7)	0.8 ± 0.04	3.45	0.976
BACE-1 inhibitor IV	0.085 (0.075–0.095)	1.1 ± 0.05	3.15	0.991

1.2.2. BACE-1 inhibitory activity of compounds from whole *Agastache rugosa* plants

The BACE-1 inhibitory activity of three isolated compounds (acacetin, maslinic acid, and oleanolic acid) isolated from *A. rugosa*, organic pure acacetin, and human BACE-1 inhibitor IV and EGCG, which were used as positive controls, were elucidated (Table 16). Based on IC_{50} values, natural and pure organic acacetin had similar inhibitory activity, indicating that the activity of the methanol-extracted acacetin was purely due to acacetin. Natural acacetin was a 4.0-fold and 5.5-fold more potent inhibitor of BACE-1 than oleanolic acid and maslinic acid, respectively. The BACE-1 inhibitory activity of acacetin and EGCG did not differ significantly. Overall, these compounds were significantly less potent inhibitors of BACE-1 than BACE-1 inhibitor IV.

Table 16. *In vitro* human BACE-1 inhibitory activity of isolated acacetin, maslinic acid, oleanolic acid, pure organic acacetin, and two BACE-1 inhibitors BACE-1 inhibitor IV and EGCG using a FRET-based enzyme assay

Compound	IC_{50}, μM (95% CL)	Slope ± SE	χ^2	*P*-value
Natural acacetin	88.5 (60.1–130.5)	0.4 ± 0.04	5.64	0.940
Pure acacetin	81.2 (59.4–111.0)	0.4 ± 0.03	5.41	0.936
Oleanolic acid	355.1 (327.3–385.4)	1.9 ± 0.12	4.07	0.989
Maslinic acid	487.6 (439.3–542.4)	1.4 ± 0.09	4.35	0.984
EGCG	96.2 (72.1–128.2)	0.4 ± 0.02	3.48	0.965
BACE-1 inhibitor IV	0.079 (0.073–0.085)	1.2 ± 0.07	3.25	0.993

DISCUSSION

The amyloid cascade hypothesis, which presumes that the deposition of amyloid plaques in the brain is the reason for the AD pathology, has promoted the development of drugs to treat AD (Hardy and Selkoe, 2002; Karran *et al*., 2011). There are three proteases involved in APP processing to produce amyloid plaques –α-secretase, β-secretase, and γ-secretase. The β-secretase is a major therapeutic target in AD (De Strooper *et al*., 2010). Selective phytochemicals may be used to treat AD, and are of great interest because they may biodegrade to nontoxic products (Fabry *et al*., 1996). These anti-AD products can be applied to humans in the same manner as conventional drugs. Plants contain various compounds, such as alkaloids, phenols, and terpenoids, and these compounds, alone or in combination, contribute to BACE-1 inhibition (Ghosh *et al*., 2008; Mancini *et al*., 2011). The phytochemicals that inhibit human BACE-1 include alkaloids (e.g., epiberberi and groenlandicine, IC_{50} 8.55 and 19.68 μM, respectively (Jung *et al*., 2009a)); terpenoids (e.g., 16α-hydroxy-17-isovaleroyloxy-*ent*-kauran-19-oic acid and 10 other diterpenoids, IC_{50} 18.58–92.20 μM (Jung *et al*., 2009b); bakuchiol, IC_{50} 21.38 μM (Choi *et al*., 2008), (+)-vitisinol E, (+)-ampelopsin A, and (+)-vitisin (Choi *et al*., 2009); flavonoids (e.g., EGCG and other two catechins, IC_{50} 1.6–4.5 μM (Jeon *et al*., 2003); neocorylin and other five flavonoids, IC_{50} 0.7–10.2 μM (Choi *et al*., 2008); kuraridin and other two chalcones, IC_{50} 6.03–7.19 (Jung *et al*., 2010); leachianone G and six other flavonones, IC_{50} 8.56–60.88 μM (Marumoto and Miyazawa, 2010), benzopyranoids (e.g., aloeresin D and C-2′-decoumaroyl-aloeresin G, IC_{50} 39.0 and 20.5 μM, respectively (Wawer and Zielinska, 2001); imperatorin and its four derivatives, IC_{50} 91.8–359.2 μM (Marumoto and Miyazawa, 2010), phenylpropanoids (e.g., *p*-coumaric acid, IC_{50} 90 μM (Youn and Jun, 2012), amentoflavone-type biflavonoids (e.g. 2,3-dihydroamentoflavone, 2,3-dihydro-6-methylginkgetin) (Sasaki *et al*., 2010), stilbenoids (e.g., resveratrol and its eight derivatives, IC_{50} 0.34–19.80 μM (Choi *et al*., 2011), and tannins (e.g., geraniin and corilagin, IC_{50} 4 and 34 μM, respectively (Youn and Jun, 2013)).

QSAR of BACE-1 inhibitors have been well documented by John *et al*. (2003) and

Thompson *et al*. (2005). BACE-1 inhibitory activity of 10 catechins and reported that the inhibitory activity seemed to be related to the pyrogallol moiety on C-2 and/or C-3 catechin skeleton, whereas the stereochemistry of C-2 and C-3 did not have the inhibitory activity (Liu *et al*., 2010). In the current study, based on the BACE-1 inhibitory activity of curcuminoids, absence of methoxy groups in the phenyl rings of CCN increased the BACE-1 inhibitory activity. In particular, absence of two methoxy groups (BDMCCN) significantly increased BACE-1 inhibitory activity. However, THCCN was less potent at inhibiting BACE-1 inhibitory activity than CCN, indicating that the double bonds appear to be essential for the enzyme inhibitory activity. This current finding indicates that structural characteristics, such as degrees of saturation, carbon skeleton, types of functional group, and hydrophobicity rather than MW appear to play a role in determining the BACE-1 inhibitory activity. Previous study (Liu *et al*., 2010) also reported that BDMCCN exhibited the most potent inhibitory action on BACE-1 mRNA level, followed by DMCCN and CCN. The active constituents were determined to be the *O*-methylated flavone acacetin, and the oleanane triterpenoids maslinic acid and oleanolic acid assessed by FRET-based enzyme assay from *A. rugosa* whole plant extracts. The chemical structure of oleanolic acid differs from that of maslinic acid by the lack of a hydroxyl group at the 2-carbon position. The IC_{50} values of these constituents were between 17 and 487.6 μM, while the IC_{50} values of the natural compounds described above are between 0.34 and 359.2 μM.

CHAPTER II

Effects of Phytochemicals on Behavior, Eye Morphology, and Lifespan of *Drosophila* Models of Alzheimer's Disease

INTRODUCTION

Drosophila has been widely used as a human disease model organism such as neurological and neurodegenerative disorders including AD, Huntington's disease, Parkinson's disease, amyotrophic lateral sclerosis (ALS), and other polyglutamine disease (Iijima-Ando and Iijima, 2010). *Drosophila* models of amyloid toxicity and tau have been developed to simulate the underlying pathogenesis of AD (Prüßing *et al*., 2013). Several researchers have evaluated whether phytochemicals have therapeutic effects in *Drosophila* AD models. Caesar *et al*. (2012) studied the behavior of CCN as a drug candidate to alleviate Aβ toxicity in five different transgenic *Drosophila* AD models. They reported that CCN treatment resulted in an improved lifespan (up to 75%) and climbing activity in transgenic flies; Aβ deposition was not decreased following treatment.

In this study, *Drosophila* models of AD based on UAS-Gal4 system, which was used widely for target genes expression in *Drosophila* specific tissue (Duffy, 2002), were constructed. The drive line Gal4 binds to upstream activating sequence (UAS) to activate expression of target gene downstream. It can induce target gene expressed in specific tissue. *GMR* and *elav* driver to drive human APP and BACE-1 expressed in retinal and pan-neuronal system, respectively, was used. The effects of the two curcuminoids (CCN and BDMCCN) and acacetin on feeding, climbing, eclosion, and life span of a *Drosophila* mutant that co-expresses human *APP* and *BACE-1* within the developing nervous system were evaluated. The morphological changes (ommatidia atrophy at the edges of the compound eye, absence of ommatidial bristles, and ommatidial fusion) in the compound eyes of the transgenic flies that co-expressed human APP and BACE-1 in photoreceptor were also examined using light microscopy and scanning electron microscopy (SEM).

MATERIALS AND METHODS

2.1. Materials and reagents

Acid red was purchased from Amresco (Cochran Road Solon, OH, USA). *Drosophila* vials and bottles were purchased from Hansol Tech (Seoul, ROK). All of the other chemicals and reagents used in this study were of analytical grade quality and available commercially.

2.2. *Drosophila* stocks and rearing conditions

The flies were cultured on standard cornmeal agar medium (Ren *et al*., 2009) at 25°C and 70% relative humidity (RH) under a 12:12 h light:dark cycle. Following fly stocks were obtained from Bloomington Stock Center at Indiana University: *w1118* (stock number, 3605), *UAS-BACE-1, UAS-APP* (33797), *UAS-BACE-1* (29877), *elav-GAL4* (8760), and *GMR-GAL4* (1104). The GAL4/UAS system was employed for the overexpression of desired genes in a specific tissue of the fly. The transgenic fly stock *UAS-BACE-1* (29877) in this study was also used in previous study (Chakraborty *et al*., 2011). The characterizations of trans-human genes *APP* and *BACE-1* flies as a reliable AD model were presented in results section. Curcumnoid supplementary flies were cultured at 25°C (Wang *et al*., 2014), and acacetin supplementary flies were cultured on 29°C (Wang *et al*., 2015).

2.3. Experimental groups

2.3.1. Curcuminoid supplementation

In this experiment, three curcuminoids isolated from *C. longa* and one commercial curcuminoid were tested *in vitro*. Among these compounds, only two curcuminoids, CCN and BDMCCN, were tested to flies, because the BACE-1 inhibitory activity of DMCCN *in vitro* lied between CCN and BDMCCN. With this issue, DMCCN was removed from the *in vivo* study. The experimental groups tested of *in vivo* study were illustrated in Fig. 45. *GMR-Gal4* drove target human *APP* and *BACE-1* genes expressed in flies' compound

eyes, and morphological changes of these compound eyes with the supplementation of compounds with different concentration were observed, while *GMR-Gal4/+* flies were used as the control group (Fig. 45A). The *elav-Gal4*-drove co-expression of target genes in flies' nervous system. The behaviors (climbing and feeding) and lifespan with the supplementation of compounds with different concentrations were tested, while *elav-Gla4/+* and *elav<BACE-1* were used as control groups (Fig. 45B).

2.3.2. Acacetin supplementation

Acacetin, maslinic acid, and oleanolic acid were tested *in vitro* using a FRET-based enzyme assay. Among these constituents, acacetin was tested in flies because it was a more potent inhibitor of BACE-1 than either oleanolic acid or maslinic acid. The experimental groups examined for the *in vivo* study are given in Fig. 46. The flies used in this study were cultured from the egg stage in 94 × 25 mm polystyrene *Drosophila* vials containing standard media supplemented with acacetin in 0.1% dimethyl sulfoxide (DMSO), with the exception of the feeding assay. Based on the preliminary test results, the behavior and eye morphology of *Drosophila* models were determined with three concentrations (100, 300, and 500 μM) of acacetin. Newly emerged male flies were cultured on standard media supplemented with acacetin for the feeding assays. *GMR-Gal4* drove the co-expression of human *APP* and *BACE-1* in the compound eyes of the flies, while *GMR-Gal/+* flies were used as the control group. The age-dependent morphological changes in the flies' compound eyes were observed using light microscopy and SEM. The compound eyes' phenotypes were also observed by histologic analysis; Carson's trichrome staining was used to distinguish the histologic changes, while Congo red staining was used to detect the amyloid plaques in the compound eyes (Fig. 46A). The *elav-Gal4* promoter drove the co-expression of the targeted transgenes in the nervous system; *elav-Gal4/+* was used as the control group. The behavior (climbing and feeding), eclosion (pupation and emergence) rate, and lifespan of the flies were also tested (Fig. 46B).

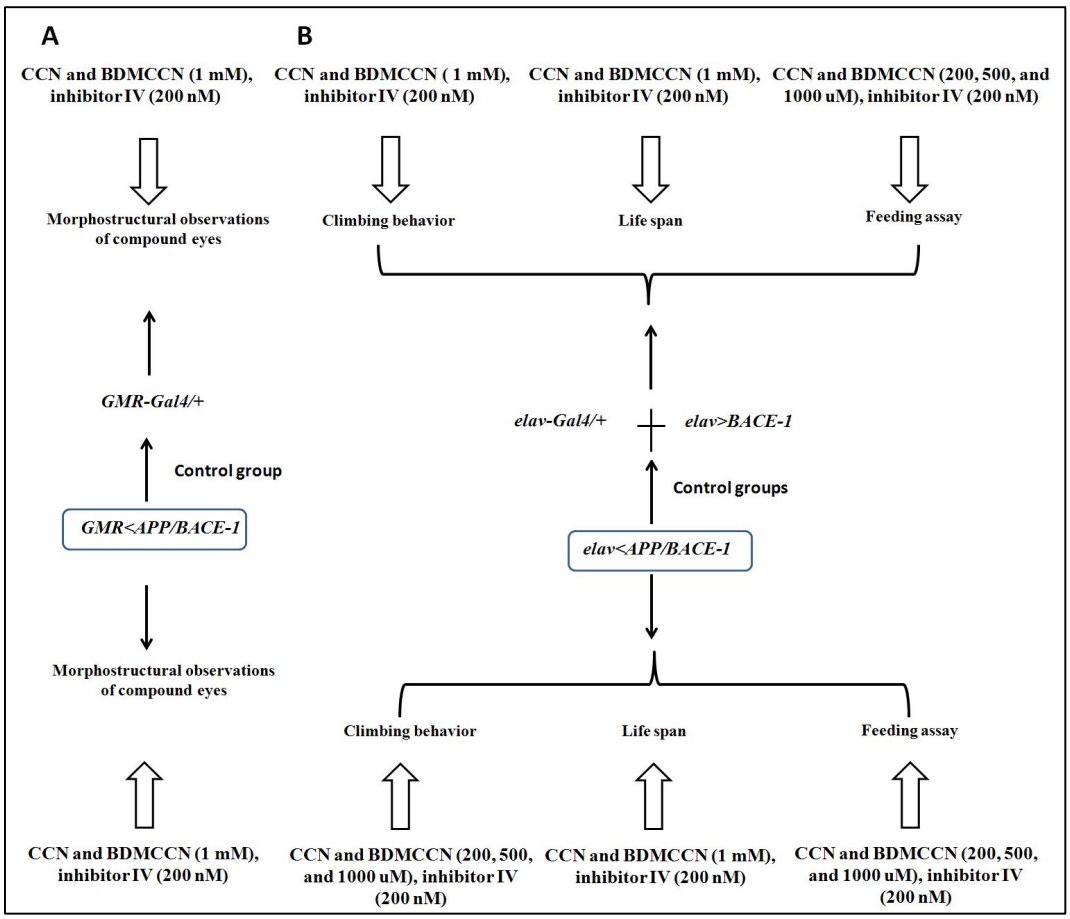

Fig. 45. Schematic of the curcuminoids supplementation experimental fly groups included in this study. The flies used in this study were cultured from the egg stage in 94 × 25 mm polystyrene vials containing standard media supplemented with curcumin (CCN), and bisdemethoxycurcumin (BDMCCN) (200, 500, and 1000 μM), as well as BACE-1 inhibitor IV (200 nM) in dimethyl sulfoxide, with the exception of the feeding assay. Newly emerged male flies were cultured on standard media supplemented with curcuminoids and inhibitor IV for the feeding assay. (**A**) *GMR-Gal4* drives the co-expression of the human *BACE-1* and *APP* genes in the flies' compound eyes, and the morphological changes in the compound eyes of these flies were tested. The *GMR-Gal4/+* flies were used as the control group. (**B**) The *elav-Gal4* promotor drives the

co-expression of the targeted transgenes in the flies' nervous system, and the behavior (climbing and feeding), and lifespan of the *elav<APP/BACE-1*, *elav<BACE-1*, and *elav-Gla4/+* flies were tested. The *elav-Gla4/+* and *elav-Gla4/+* flies were used as the control groups.

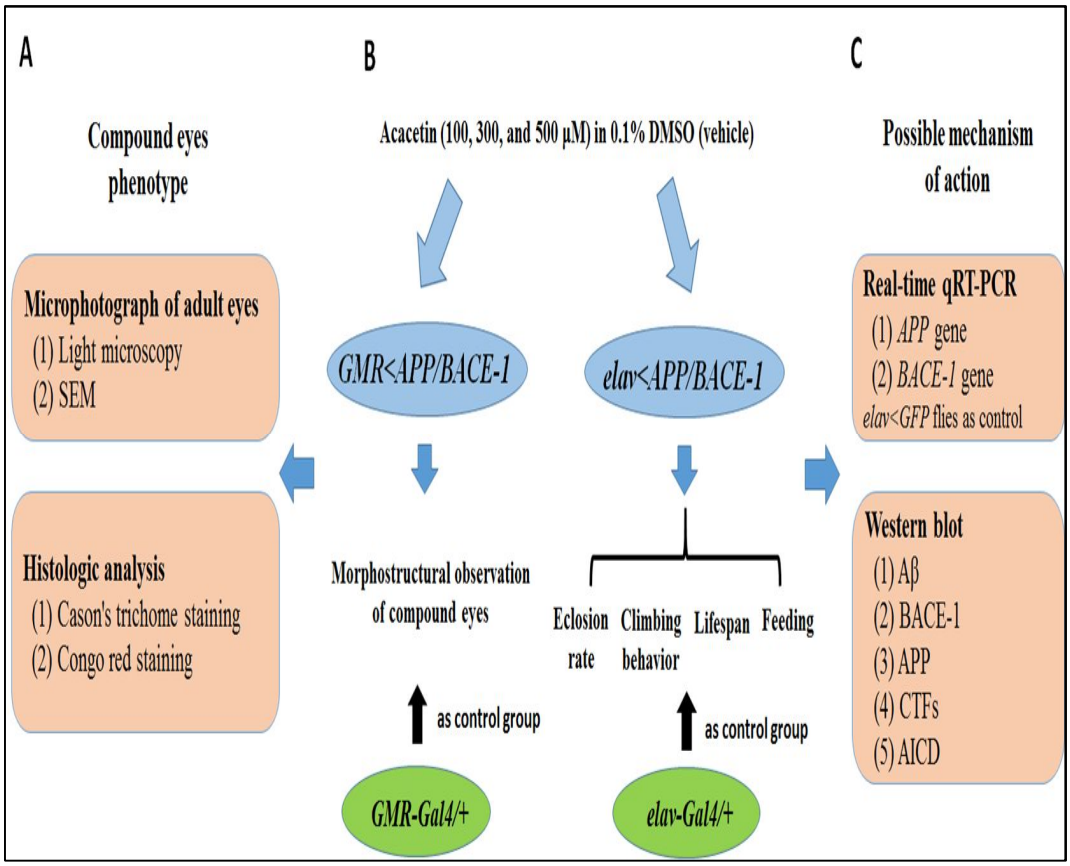

Fig. 46. Schematic of the acacetin supplementation experimental fly groups used in this study. The flies used in this study were cultured from the egg stage in 94 × 25 mm polystyrene vials containing standard media supplemented with acacetin (100, 300, and 500 μM) in dimethyl sulfoxide, with the exception of the feeding assay. Newly emerged male flies were cultured on standard media supplemented with acacetin for the feeding assay. (**A**) *GMR-Gal4* drives the co-expression of the human *BACE-1* and *APP* genes in

the flies' compound eyes, and the morphological changes in the compound eyes of these flies were tested. The *GMR-Gal4/+* flies were used as the control group. (**B**) The *elav-Gal4* promotor drives the co-expression of the targeted transgenes in the flies' nervous system, and the behavior (climbing and feeding), eclosion rate, and lifespan of the *elav<APP/BACE-1* flies were tested. The *elav-Gla4/+* flies were used as the control group. (**C**) The possible mechanism of the anti-Alzheimer's disease action of acacetin was elucidated using real-time quantitative reverse transcription polymerase chain reaction (qRT-PCR) and western blot analyses.

2.4. Light and scanning electron microscopy of the adult eyes

GMR<APP/BACE-1 flies were cultured from the egg stage in polystyrene vials containing standard media supplemented with CCN, BDMCCN, and acacetin in 0.1% DMSO, based on the preliminary test results. The controls received 0.1% DMSO only. The male flies were anesthetized on ice and placed on a microscope slide at room temperature for light microscopy. The morphology of the compound eyes was observed using an EZ4 HD stereo microscope (×35) equipped with an Integrated 3.0 Mega-Pixel CMOS camera (Leica, Hicksville, NY, USA). The flies with aberrant eye phenotypes were collected, and the number of the flies with dark deposits in the eye was counted.

For SEM, the anesthetized male flies were attached to a copper mount using silver paint as a conducting adhesive, as described previously (Greeve *et al*., 2004). They were then put directly into the viewing chamber of an SEM without prior coating, as described by Hartman and Hayes (1971). The external surface morphology of the compound eye was visualized using a Supra 55VP field-emission scanning electron microscope (Carl Zeiss, Jena, Germany) operated at 15 kV.

2.5. Histological analysis

Carson's trichome staining was performed, as described previously (Perumalsamy *et al*., 2013). In brief, the heads of male *GMR<APP/BACE-1* flies, cultured in vials as stated previously, were fixed in a 4% paraformaldehyde buffer solution (pH 7.4) overnight at

4°C, and paraffin-embedded preparations of the fly heads were then sectioned at 10 μm thickness using a HM 340E rotary microtome (Thermo Scientific Microm, Walldorf, Germany). The sections were dried at 40°C overnight, subsequently deparaffinized with CitriSolv (Fisher Scientific, Fair Lawn, NJ, USA), and rehydrated using a series of ethanol solutions in phosphate-buffered saline (PBS). The rehydrated paraffin sections were soaked in Carson's trichrome solution for 15 min, and the slides were gently swashed in tap water and subsequently rinsed three times in distilled water. The excess water was removed with tissue paper, and the samples were mounted using Vectashield H-1000 mounting medium (Vector Laboratories, Burlingame, CA, USA).

Congo red staining was performed to detect the amyloid plaques in the *Drosophila* AD model. The paraffin-embedded sections described above were deparaffinized and then stained using NovaUltra Special Stain Kits (IHC World, Woodstock, MD, USA) according to the manufacturer's instructions. Finally, the sections were dehydrated and mounted with mounting medium. The images were observed and captured using an EZ4 HD stereo microscope.

2.6. RT-PCR analysis of human *APP* and *BACE-1* genes in transgenic fly

Real-time qRT-PCR was performed to assess the expression levels of human *APP* and *BACE-1* genes in transgenic fly. Total RNA was extracted from the 30–35 heads of 10-day-old male flies using Trizol (Invitrogen Corparation, Carlsbad, CA). RNA and primers were subjected to RT-PCR by using AccuPower RT-PCR Premix (Cat. no. K-2055) (Bioneer, Alameda, CA, USA). This premix contained optimal concentration of all the components necessary for cDNA synthesis and RTase inactivation, as well as amplification in a single 0.2 mL tube. The PCR amplifications were performed with specific primers in a total volume of 20 μL containing 2 μL of forward and reverse primer mixture (10 pmol of each primer), 1 μg RNA and diethylpyrocarbonate water. The mixture was used for the amplification after initial denaturation at 95°C and 32 cycles (95°C for 30 s, 60 for 30 s, and 72 for 30 s). PCR products were visualized by 2% agarose gel electrophoresis containing ethidium bromide. The primer sequence were as follows:

for human *APP*, 5'-GCCGTGGCATTCTTTTGGGGC-3'(forward) and 5'-GTGGTCAGTCCTCGGTCGGC-3' (reverse) (Pirooznia *et al.,* 2012); for human *BACE-1*, 5'-GCAGGGCTACTACGTGGAGA-3' (forward) and 5'-GTATCCACCAGGATGTTGAGC-3' (reverse) (Kwak *et al*., 2011). *rp 49*, which encodes the *Drosophila* ribosomal protein 49, was used as an internal standard and reference gene using forward and reverse primer pairs 5'-CTGCTCATGCAGAACCGCGT-3' and 5'-GGACCGACAGCTGCTTGGCG-3' (Pirooznia *et al*., 2012), respectively. The ethidium bromide stained gel image was digitalized using the Molecular Imager Gel Doc XR System (Bio-Rad, Hercules, CA, USA), and calculated by densitometry (Park *et al*., 2013). Results are presented as relative mRNA expression of each gene to that of *rp 49* mRNA.

2.7. Measurement of the fly eclosion rate

The pupation and emergence rates were determined according to the previous method (Tamura *et al*., 2011). The *elav<APP/BACE-1* flies were cultured from the egg stage in vials, as stated previously. Groups of 50 third instar larvae climbing on the wall were transferred into vials containing fresh media. The treated and control (0.1% DMSO only) flies were grown under the same conditions as those used for fly maintenance. The numbers of pupae and adults were determined. All treatments were repeated four times using 50 larvae per replicate.

2.8. Lifespan assay

Groups of 200 newly eclosed male flies equally distributed in 10 vials were incubated in media supplemented with 1 mM CCN, 1 mM BDMCCN, or 200 nM inhibitor IV, or acacetin (100, 300, and 500 μM) in 0.1% DMSO. Controls received 0.1% DMSO only. Survivors were transferred to fresh media vials every 4 days. The median life time ($T_{1/2}$) was defined as the time when the survivor function equaled 50%, because median survivorship is a more reliable index than mean survival time, as described previously (Chakraborty *et al*., 2011). All treatments were repeated 10 times using 20 males per

replicate.

2.9. Climbing assay

The climbing activity was tested following procedure described previously (Crowther *et al*., 2005; Park *et al*., 2012). Flies were collected at eclosion and cultured in groups of 20 flies in media supplemented with 1 mM CCN, 1 mM BDMCCN, or 200 nM inhibitor IV, or acacetin (100, 300, and 500 μM) in 0.1% DMSO. Flies over-expression APP/BACE-1 were treated with different concentrations (200, 500, and 1000 μM) of curcuminoids, and (100, 300, and 500 μM) of acacetin, as described previously (Mahoney *et al*., 2009; Lee *et al*., 2010). Control flies received media with 0.1% DMSO. Groups of 20 male *elav<APP/BACE-1* flies, cultured in vials as stated previously, were separately placed in an empty vial conjoined with another vial on top, and manually tapped twice. After 20 s, the flies that climbed from the bottom and crossed the 9.5 cm line were counted, and the climbing index was determined as the number of flies that climbed to the top vial relative to the total number of test flies and expressed as a percentage (Fig. 47). The controls received 0.1% DMSO. All trials were repeated five times using 20 males per replicate.

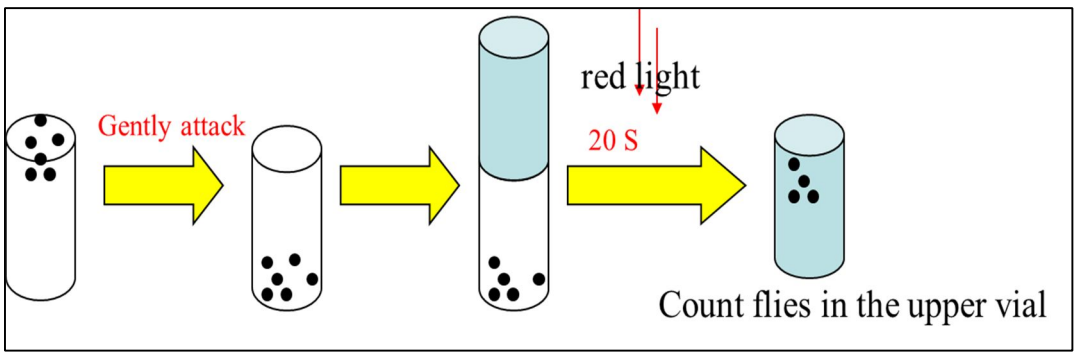

Fig. 47. Schematic of flies climbing behavior assay.

2.10. Feeding assay

The adult feeding assay was performed according to the method of Bahadorani *et al*.

(2008) with minor modifications. Groups of 15 newly emerged male *elav<APP/BACE-1* flies were cultured on standard media for 3 days and then starved for 20 h in vials containing three layers of Whatman no. 2 filter paper (Whatman, Maidstone, UK) soaked in distilled water. The flies were then transferred into vials containing media (with 0.2% Acid red) supplemented with CCN (200, 500, or 1000 μM), BDMCCN (200, 500, or 1000 μM), or inhibitor IV (200 nM), or acacetin (100, 300, and 500 μM) in 0.1% DMSO. The controls were fed with media supplemented with 0.2% Acid red and 0.1% DMSO. After 2 h of feeding, the abdomens became red (Fig. 48), and then isolated and homogenized in 1 mL DW. After centrifugation (5000 rpm, 25°C, 5 min), the optical density (OD) of the supernatant was measured at 505 nm, because this OD value is considered to index the amount of food intake by flies, as described previously (Min and Tatar, 2006). All treatments were replicated three times using 15 males per replicate.

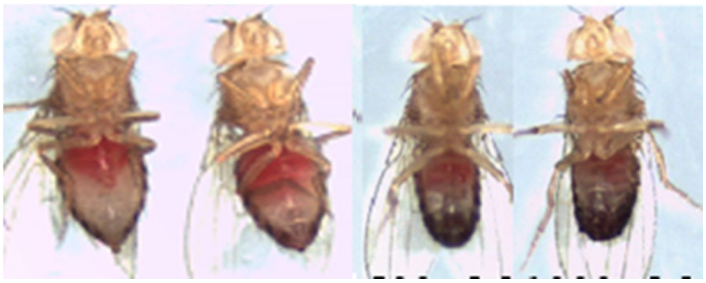

Fig. 48. Flies with red abdomen after feeding assay.

2.11. Data analysis

The IC_{50} values for each *Drosophila* line and their treatments were considered to be significantly different from one another when their 95% confidence limits (CL) did not overlap. All data are presented as means ± SEs, and the significance between means was determined using one-way or two-way analysis of variance (ANOVA) statistical test (GraphPad Prism 5.1 software, La Jolla, CA, USA). Statistical analysis for survival data were carried out using the Bonferroni post tests (GraphPad Prism 5.1 software).

RESULTS

2.1. Characterization of trans-human *APP* and *BACE-1* genes fly as reliable models of Alzheimer's disease

The GAL4/UAS system was employed for the overexpression of desired genes in a specific tissue of the fly. In this experiment, human *APP* and *BACE-1* genes induced eye degeneration of transgenic fly under *GMR-Gal4* driver strain. Control *GMR-Gal4/+* flies showed a normal, well-organized, and smooth external eye surface (Fig. 49A), well-organized photoreceptor and normal retina were stained by Carson's trichome staining (Fig. 49B) and Congo red staining (Fig. 49C and D). However, rough and irregular external eye surface was observed in fly co-expression human APP and BACE-1 (Fig. 49E), damages of photoreceptor were observed in transgenic *GMR<APP/BACE-1* flies stained by Carson's trichome staining (Fig. 49F), and amyloid depositions were observed by Congo red staining marked by arrows (Fig. 49G and H). APP and BACE-1 were co-expressed in the nervous system of flies under *elav-GAL4* driver strain. The expression of *APP* and *BACE-1* genes was reconfirmed in the transgenic flies using qRT-PCR analysis (Fig. 50). Target genes electrophoresis results were observed (Fig. 50A). The *rp 49* gene was used as the reference gene to normalize mRNA amount and human *APP* and *BACE-1* genes showed high expression amount in transgenic fly, without expression in *elav-GAL4* control fly (Fig. 50B). Accordingly, trans-human *APP* and *BACE-1* fly can be used as a reliable AD model.

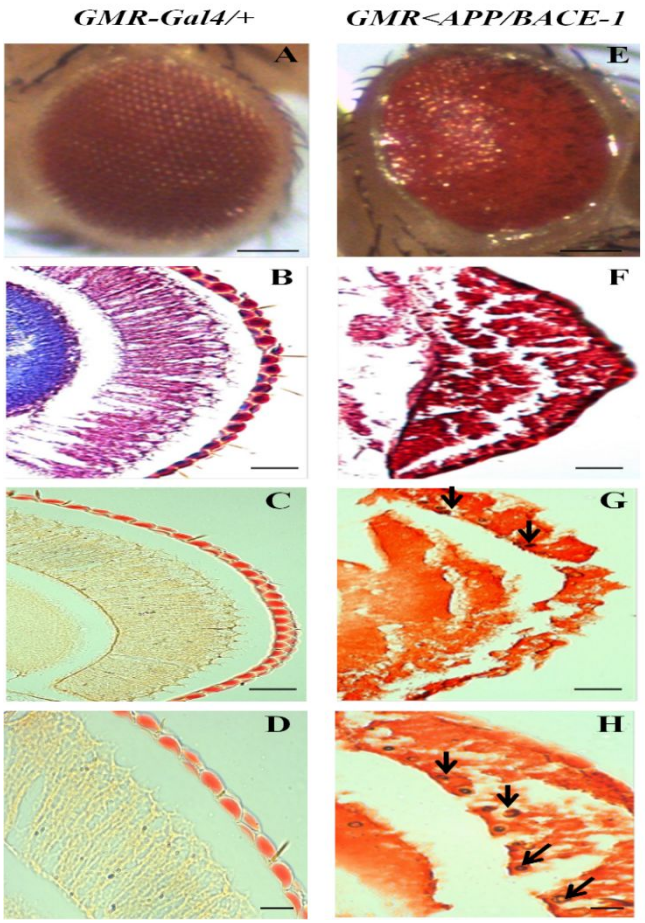

Fig. 49. Human *APP* and *BACE-1* genes induced eye degeneration of transgenic fly under *GMR-Gal4* driver strain. (**A**) Control *GMR-Gal4*/+ flies showed normal and well-organized compound eyes. Carson's trichome staining. (**B**) Well-organized photoreceptors structure was observed in control male *GMR-Gal4*/+ flies. Congo red staining. (**C, D**) Amyloid plaques were not observed in the control male *GMR-Gal4*/+ flies. (**E**) *GMR<APP/BACE-1* flies exhibited rough and irregular external eye surface. Cason's trichome staining. (**F**) Damages of photoreceptor were detected in transgenic *GMR<APP/BACE-1* flies. Congo red staining. (**G, H**) Scattered amyloid plaque deposits were observed in transgenic *GMR<APP/BACE-1* flies marked by arrows. Scale bar, 50 μm.

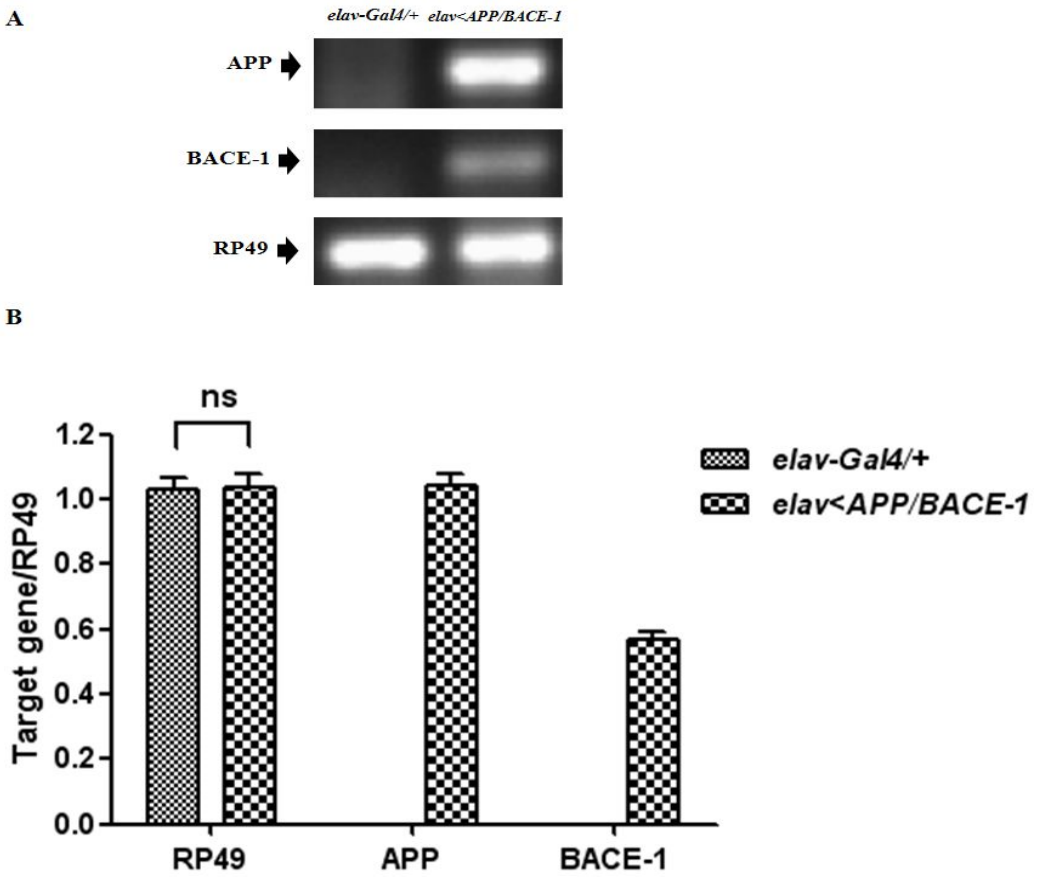

Fig. 50. The expression of human *APP* and *BACE-1* mRNAs. (**A**) Target genes human *APP* and *BACE-1* electrophoresis results. (**B**) qRT-PCR analysis of human *APP* and *BACE-1* genes mRNA expression level. Gene *rp 49* was used as the reference gene to normalize mRNA amount. The *elav-Gal4/+* fly was used as a control group. For *rp 49* mRNA expression amount, there was no significant difference between control flies and transgenic flies. However, mRNA of target genes human *APP* and *BACE-1* were not expressed in control flies. ns: no significant difference. Each bar represents standard error.

2.2. Effects of curcuminoids on behavior, eye morphology and lifespan of *Drosophila* models of AD

2.2.1. Effects on the eye morphology

Morphological defects in flies expressing APP/BACE-1 in compound eye (*GMR<Gal4, UAS-APP, UAS-BACE-1 or GMR<APP/BACE-1*) were first examined. Control carrying *GMR-GAL4* alone showed wild-type eye morphology (Fig. 51A). In contrast, *GMR<APP/BACE-1* developed ommatidia atrophia at the edge of compound eye (marked with star in Fig. 51B). Next, we cultured *GMR<APP/BACE-1* flies in media supplemented with 1 mM CCN, 1 mM BDMCCN or 200 nM Inhibitor in 0.1% DMSO during entire developmental stages. Even on 1 day post-eclosion, the edge atrophia was already ameliorated in the flies cultured in CCN- (Fig. 51C1) or BDMCCN-media (Fi. 51D1), compared with the vehicle (0.1% DMSO) control (Fig. 51B1). The manifestation of ommatidia atrophia was also considerably reduced in Inhibitor IV-fed flies (Fig. 51E1). However, any of tested curcuminoids and Inhibitor IV failed to suppress completely the eye degeneration phenotype observed in *GMR<APP/BACE-1*. Nevertheless, protective effects of CCN, BDMCCN and Inhibitor IV remained evident in 24 day- and 36-day old flies (Fig. 51).

To compare the protective activities of curcuminoids in high resolution, compound eyes of *GMR<APP/BACE-1* treated with each compound were examined using a scanning electron microscope (SEM). Control flies (*GMR-GAL4*/+) flies showed smooth appearance of the eye without any defects of ommatidia size and bristles (Fig. 51A4). In contrast, *GMR<APP/BACE-1* flies showed varying degrees of eye disorganization. The eye of flies treated with the vehicle showed the strongest phenotypes characterized by absence of ommatidial bristles and fusion of ommatidia (marked with arrows) (Fig. 51B4). The rough eye phenotype was suppressed partially in 1 mM CCN-fed flies, but most ommatidial bristles were still absent and the size of some ommatidia reduced (arrows in Fig. 51C4). Remarkably, protective potency of 1 mM BDMCCN (Fig. 51D4) was comparable to that of 200 nM inhibitor IV (Fig. 51E4).

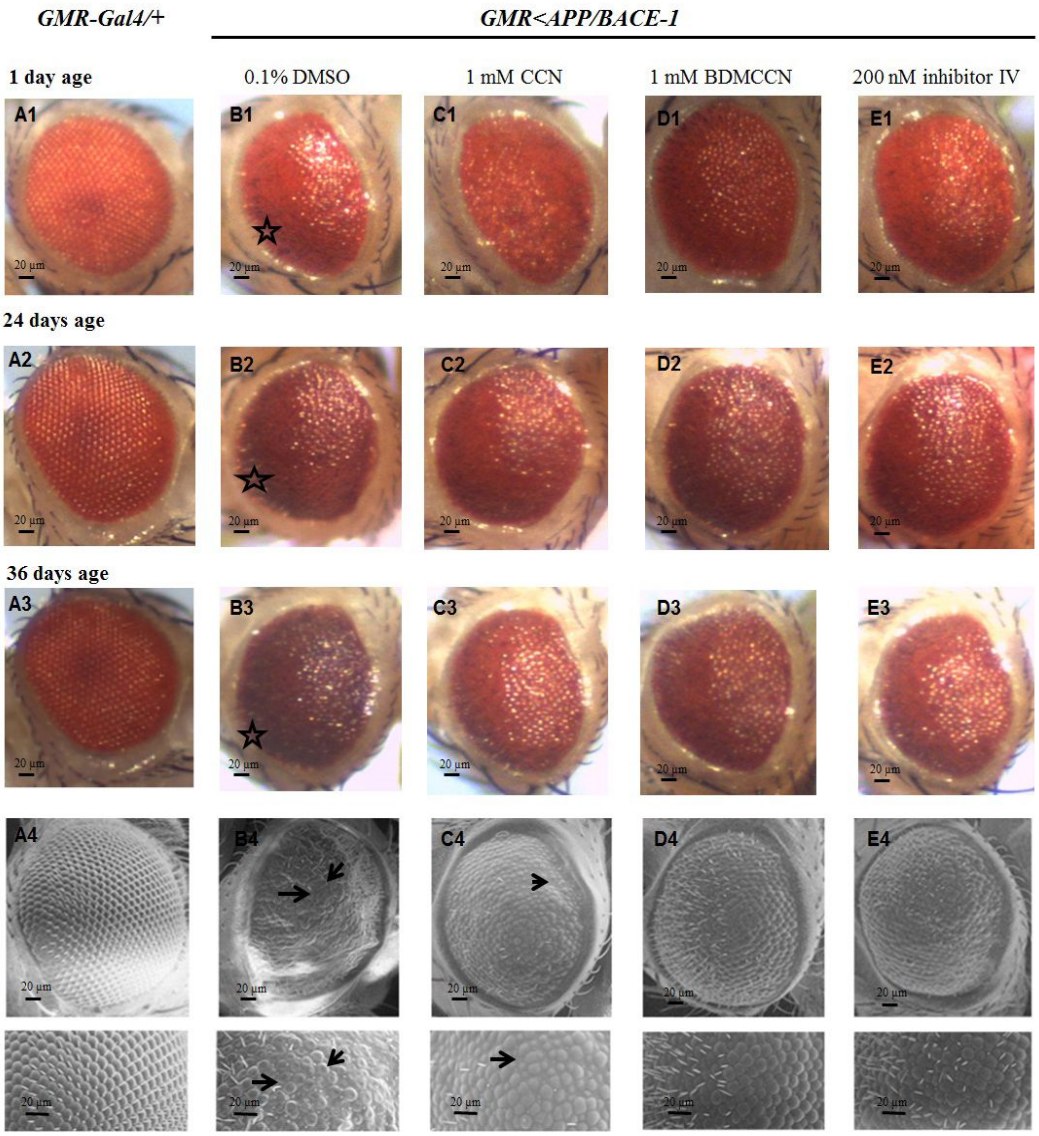

Fig. 51. Rough eye phenotype associated with *GMR<APP/BACE-1 Drosophila* eye development observed by light microscope and scanning electron microscope. Light micrographs of *GMR<GAL4* flies (**A1-A3**), *GMR<APP/BACE-1* cultured on 0.1% dimethyl sulfoxide (**B1-B3**), 1 mM curcumin (CCN) (**C1-C3**), 1 mM demethoxycurcumin (DMCCN) (**D1-D3**), and 200 nM BACE-1 Inhibitor IV (**E1-E3**). Scanning electron micrographs of day 36 *GMR<GAL4* flies (**A4**) and *GMR<APP/BACE-1* cultured on different media (**B4-E4**). Stars indicate ommatidia

atrophia.

2.2.2. Effects on climbing behaviors

Most of neurodegenerative diseases including AD are characterized by age-dependent deterioration in locomotory coordination. In *Drosophila* model, the locomotory coordination can be quantified by the negative geotaxis assay, which takes advantage of fly's innate tendency to climb against gravity after gentle tapping. In the assay, control flies cultured on standard media (*elav-Gal4/+*) showed a clear age-dependent reduction in the climbing indices, for example measured in females as 98%, 93%, 89% and 66% in 1, 10, 20 and 30 days after eclosion, respectively (Fig. 52A). Further, expression of BACE-1 with or without its substrate APP in the nervous system resulted in even stronger age-dependent locomotory deterioration in both genders (Fig. 52). The climbing defect was slightly more pronounced in males than in females, there was virtually no climbing activity scored in *elav<APP/BACE-1* males from 20 days after eclosion (Fig. 52B).

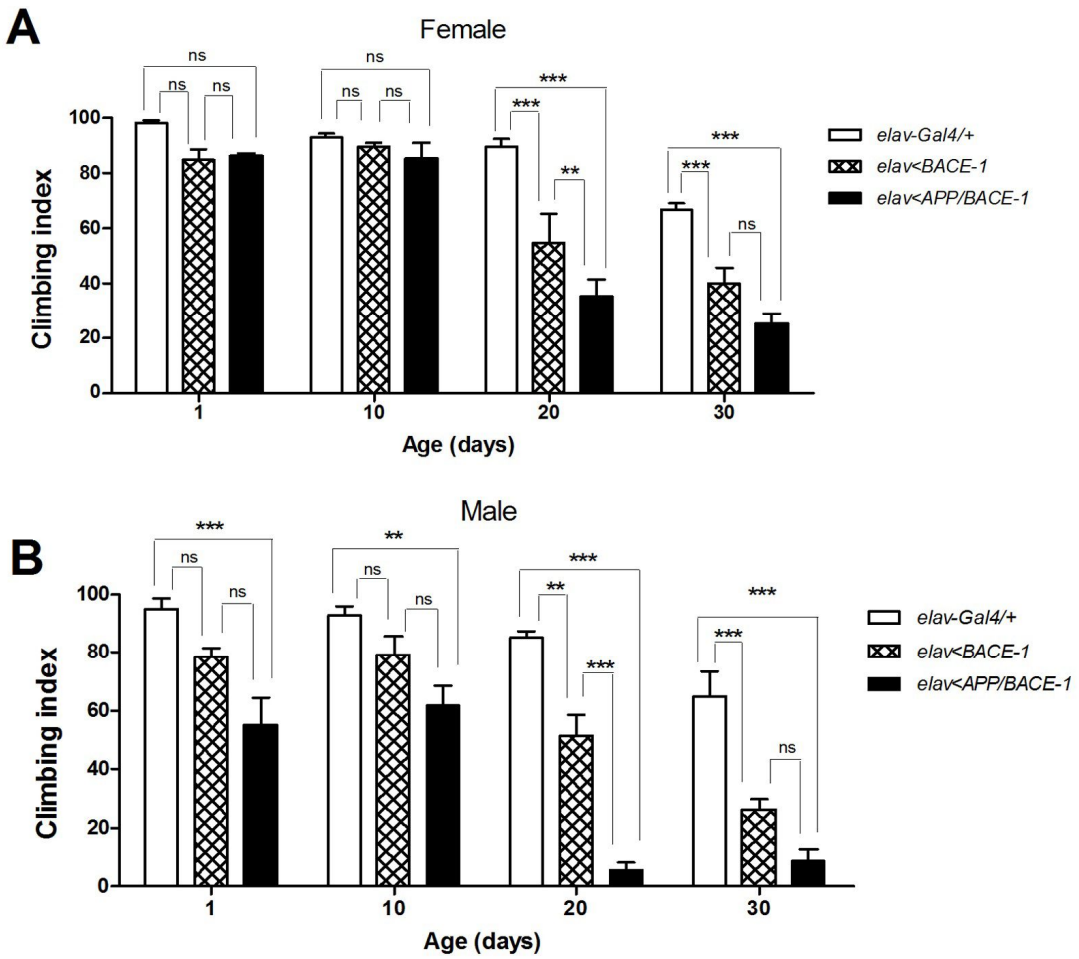

Fig. 52. Climbing behavior of females (A) and males (B) from *elav-Gal4/+*, *elav<BACE-1*, and *elav<APP/BACE-1* fed on standard media (n = 50–100 flies. ***: $p < 0.001$; **: $p < 0.01$; ns, no significant difference, using Bonferroni's multiple comparison test). Each bar represents standard error.

Then, it was determined whether two curcuminoids and Inhibitor IV BACE-1 blockers could rescue climbing defects in males expressing BACE-1 alone (*elav<BACE-1*) of three different age groups (10, 20 and 30 days post-eclosion). In 10 days after eclosion, all tested compounds except 1 mM CCN did not significantly improve climbing ability, probably because overall behavioral defect was not pronounced in this age group. In contrast, at 20 and 30 days after eclosion, *elav<BACE-1* males cultured in media containing 1 mM CCN, 1 mM BDMCCN, or 200 nM Inhibitor IV showed significantly improved climbing indices, compared with those cultured in vehicle control (0.1% DMSO) media (Fig. 53B1-B3).

Subsequently, analogous experiments with *elav<APP/BACE-1* males, which show much severe age-dependent progression of locomotory defects, were carried out. In 10 days post-eclosion, males cultured with CCN (1 mM only), BDMCCN (200 μM, 500 μM, and 1 mM), or inhibitor IV (200 nM) showed less severe impairments in the climbing ability compared with flies cultured in vehicle control (Fig. 53C1). In 20 days post-eclosion, virtually no *elav<APP/BACE-1* males can climb against gravity, due to poor movement coordination. However, dietary supplement of 1 mM CCN, 1 mM BDMCCN, or 200 nM Inhibitor IV delayed age-dependent progression of locomotory defects, and improved climbing ability compared with vehicle control (Fig. 53C2). The climbing ability was also partially rescued with 1 mM CCN- and 200 nM Inhibitor IV in 30 days post-eclosion males (Fig. 53C3).

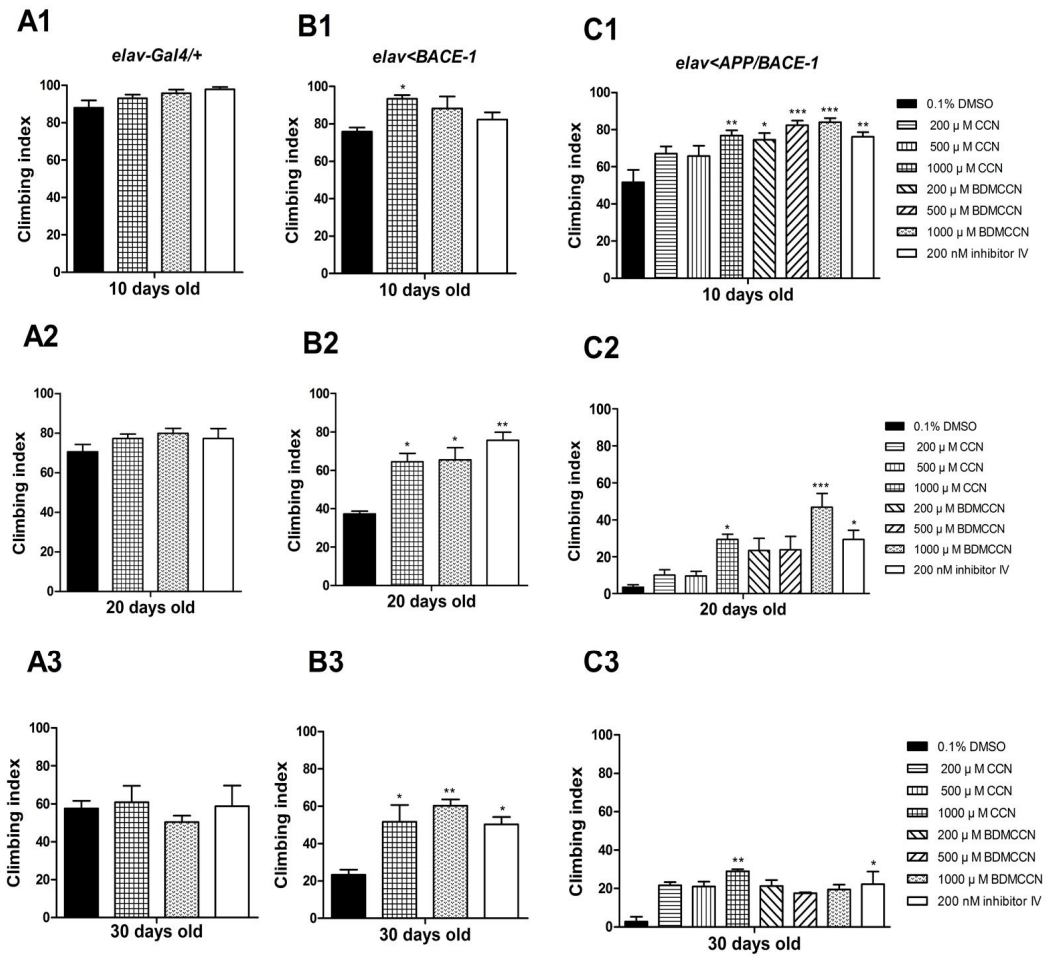

Fig. 53. Effect of CCN, BDMCCN, and BACE-1 Inhibitor IV on climbing behavior of the transgenic flies. Climbing behavior of 10-, 20-, and 30-day-old *elav-Gal4/+* male flies (**A1, A2, and A3**), *elav<BACE-1* flies (**B1, B2, and B3**), and *elav<APP/BACE-1* flies (**C1, C2, and C3**). Each bar represents the mean ± SE from three independent experiments. (n = 50–100 flies. (***: $p < 0.001$; **: $p < 0.01$; *: $p < 0.05$, using Bonferroni's multiple comparison test).

2.2.3. Effects on lifespan and feeding

Previously, it was reported that expression of BACE-1 with APP reduced life span of

adult flies (Chakraborty *et al*., 2011). Thus, it was determined whether prolonged exposure of *elav<BACE-1* or *elav<APP/BACE-1* to curcuminoids increases life span. The life span of the male flies fed on standard media did not differ significantly from each other (Fig. 54A). Supplementation of 1 mM CCN, 1 mM BDMCCN, and 200 nM BACE-1 inhibitor IV did not affect longevity of *elav-Gal4/+* flies (Fig. 54B), *elav<BACE-1* flies (Fig. 54C), and *elav<APP/BACE-1* flies (Fig. 54D). Interestingly, *elav<BACE-1* males cultured in vehicle control showed significantly shorter $T_{1/2}$ (33 days) than control ($T_{1/2}$, 37 days in *elav-Gal4/+*). Expression of APP together with BACE-1 (*elav<APP/BACE-1*) reduced $T_{1/2}$ even further to 30 days (Fig. 54E). Flies supplemented with curcuminoids or BACE-1 Inhibitor IV increased $T_{1/2}$ in *elav<BACE-1* and *elav<APP/BACE-1*, but not in control lacking *UAS-BACE-1* (*elav-Gal4/+*). 1 mM BDMCCN increased $T_{1/2}$ as much as 200 nM Inhibitor IV did in *elav<BACE-1* flies (42 vs. 41 days). 1 mM BDMCCN also significantly rescue $T_{1/2}$ in *elav<APP/BACE-1* flies ($T_{1/2}$, 36 days), but 1 mM CCN did not (Fig. 54F).

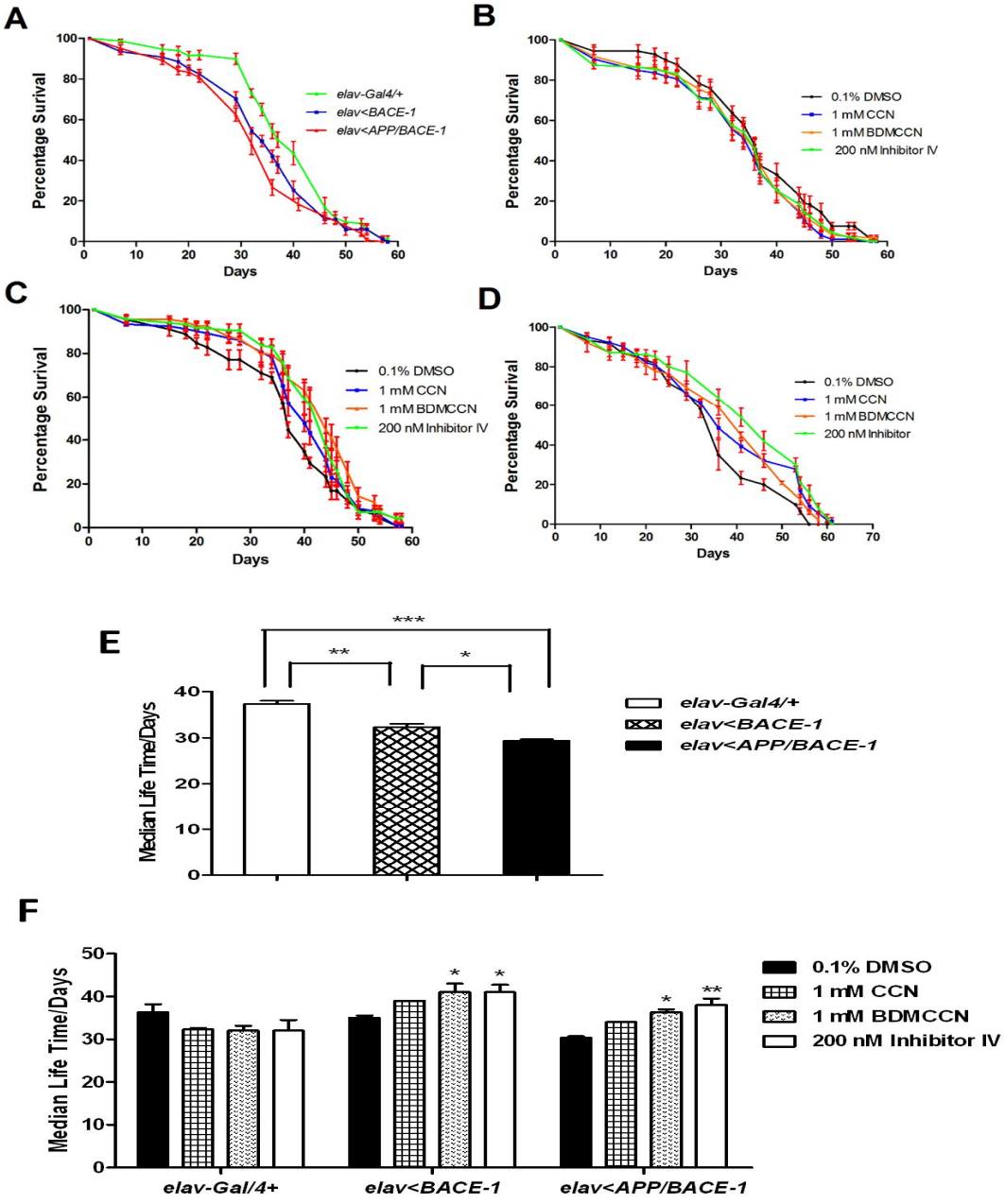

Fig. 54. Effect of CCN, BDMCCN, and BACE-1 Inhibitor IV supplementation on longevity of *elav-Gal4/+*, *elav<BACE-1*, and *elav<APP/BACE-1* flies. (**A**) There was no significant difference in the longevity among three different genotype flies. Compound

supplementation did not affect longevity of flies *elav-Gal4/+* (**B**), *elav<BACE-1* (**C**), and *elav<APP/BACE-1* (**D**). (**E**) Median life time of three genotype flies cultured on standard medium. (**F**) Median life time of three genotype flies fed on curcuminoids and BACE-1 Inhibitor IV supplementation media. Each bar represents the mean ± SE from five independent experiments ($^{***}P<0.001$; $^{**}P<0.01$; $^{*}P<0.05$, using Bonferroni's multiple comparison test).

Because feeding behavior is one of the essential factors determining longevity of flies and other animals (Carvalho *et al.*, 2005), the effects of compounds on amount of food intake in adults expressing APP/BACE-1 in the nervous system (*elav<APP/BACE-1*) were examined. Irrespective of compounds and concentrations examined, CCN, BDMCCN, and Inhibitor IV did not affect amount of feeding in any of tested genotypes (Fig. 55). This finding indicates that protective effects of BDMCCN and Inhibitor IV on longevity are not attributed to their possible anorectic effects.

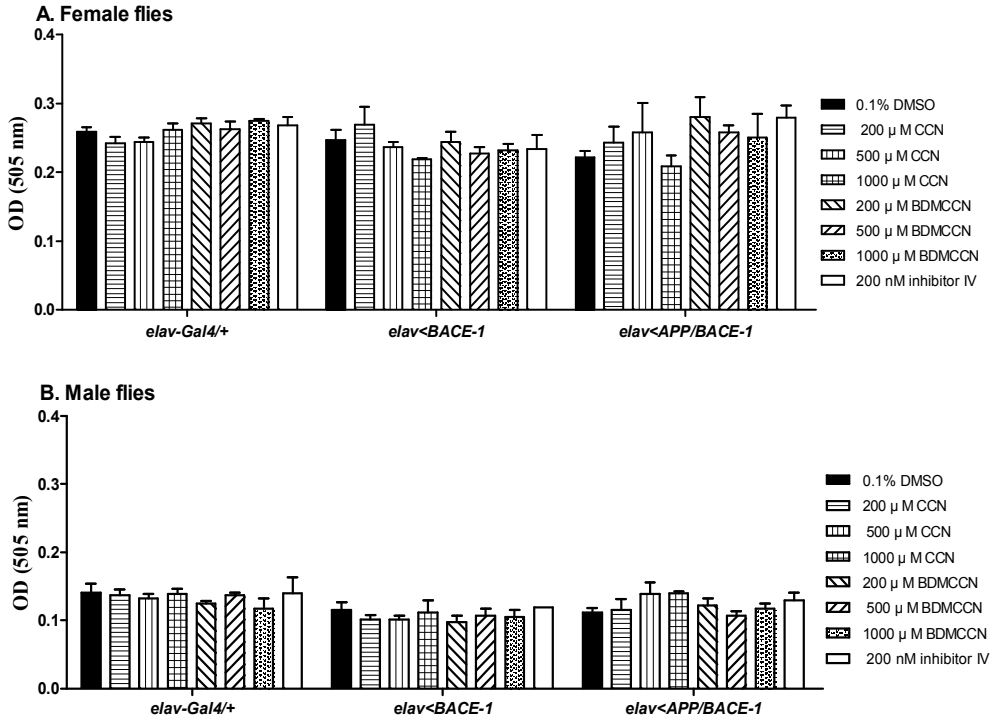

Fig. 55. Effect of test compounds on feeding of three genotypes adult flies. To determine feeding behavior, newly emerged transgenic male flies were cultured on standard media for 3 days, and then starved for 20 h. The flies were transferred into vials containing media (with 0.2% Acid red) supplemented with compounds. The control flies were fed with media containing 0.2% Acid red and vehicle. The abdomens of flies fed with Acid red were cut and homogenized in distilled water, and the optical density (OD) of the supernatant was measured at 505 nm as the index of amount of food consumed by the flies. Curcumin (CCN), bisdemethoxycurcumin (BDMCCN), and BACE-1 inhibitor did not affect the feeding behavior of female flies (**A**) and male flies (**B**). $n = 45$ flies. Each bar represents the mean ± SE from three independent experiments.

2.3. Effects of acacetin on behavior, eye morphology and lifespan of *Drosophila* models of AD

2.3.1. Effect on age-dependent neurodegeneration, as reflected by an aberrant eye phenotype

Overexpression of human *BACE-1* and *APP* during *Drosophila* eye development resulted in an aberrant rough eye phenotype in the male *GMR<APP/BACE-1* flies (1-day-old) (Figs. 56B and C), particularly those with dark deposits in the eye (marked with an arrow in Fig. 56C), compared to the control male *GMR-GAL4/+* flies with normal and well-organized compound eyes (Fig. 56A). Similar results were also observed with the transgenic female *GMR<APP/BACE-1* flies. The effects of acacetin on the morphological defects in the eyes with dark deposits were examined (Fig. 56D). Acacetin (100, 300, and 500 μM) suppressed the ratios of female flies (6.3–8.0%) and male flies (5.0–7.0%) with dark deposits in the eyes compared to the vehicle dimethyl sulfoxide-fed control females (12.0%) and males (18.7%).

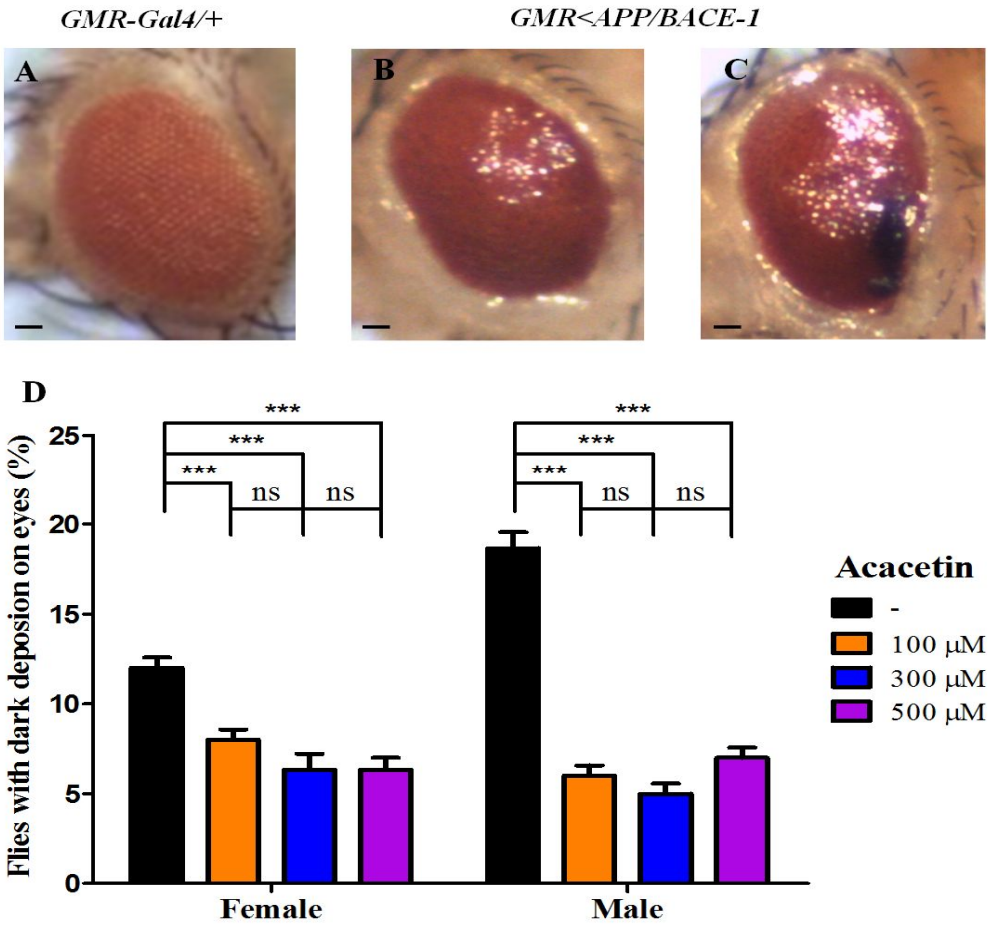

Fig. 56. Effect of acacetin on the morphological defects in the compound eyes of the transgenic flies. Human *APP* and *BACE-1* transgenic flies (*GMR<APP/BACE-1*) were cultured from the egg stage in polystyrene vials containing standard media supplemented with acacetin (100, 300, and 500 μM) in 0.1% dimethyl sulfoxide. The morphology of the compound eyes of male and female flies (1 day old) was observed with a stereo microscope (×35). The flies with aberrant eye phenotypes were collected, and the number of flies with dark deposits in the eyes was counted. (**A**) Control male *GMR-Gal4* flies with a wild-type phenotype of a smooth surface compound eye. (**B**) Transgenic male *GMR<APP/BACE-1* flies with a compound eye with an abnormal appearance. (**C**) Male *GMR<APP/BACE-1* flies with morphological defects, particularly dark deposits in the

eyes. (**D**) Quantitation of the phenotype of male and female flies showing serious morphological defects with dark deposits in the eyes. Each bar represents the mean ± SE from three independent experiments ($^{***}P<0.001$; ns, no significant difference, using Bonferroni's multiple comparison test). The scale bars represent 20 μm.

It has been reported that co-expression of the human *APP* and *BACE-1* genes induced the age-dependent neurodegeneration of the photoreceptor cells in *Drosophila* compound eyes (Greeve *et al*., 2004). To evaluate whether acacetin affected eye degeneration over time, the morphological changes in the eyes were first investigated in flies of different ages (1, 10, 20, and 30 days old). The control strain carrying *GMR-GAL4* alone showed a normal, well-organized, and smooth external eye surface, and there were no obvious morphological changes as time elapsed (Figs. 57A1-A4). In contrast, external phenotypic changes were observed in flies co-expressing human APP and BACE-1, and these changes became more severe as time elapsed (Figs. 57B-E). In vehicle-fed flies, dark deposits were observed at the edges of the compound eyes, even in 1-day-old flies (marked with an arrow in Fig. 57B1), and the size of the deposits had increased in 10-day-old flies (marked with an arrow in Fig. 57B2). As time elapsed, the flies with dark spots in their eyes died earlier than those without the dark spots. Furthermore, the number of ommatidial fusions increased in 20-day-old fly eyes compared to the 1-day-old fly eyes (marked with asterisks in Fig. 57B3) and were further exacerbated in 30-day-old fly eyes (marked with asterisks in Fig. 57B4).

Next, *GMR<APP/BACE-1* flies in the egg stage were cultured in media supplemented with acacetin (100, 300, and 500 μM) dissolved in 0.1% DMSO. Acacetin suppressed the numbers of flies with dark spots in their eyes (Fig. 56) at 1 day, although there were no obvious external structural changes in acacetin-fed fly eyes at 1 and 10 days old (Figs.57C1-E1 and C2-E2). However, the visible eye color changed from light red to dark red in 20- or 30-day-old flies (Figs. 57C3-E3 and C4-E4). Furthermore, the compound eyes in these older flies had a rougher surface and more severe ommatidial fusions than those in the younger flies; this was especially pronounced for the 30-day-old flies

(marked with asterisks in Figs. 57C4-E4). At concentrations of 100, 300, and 500 μM, acacetin significantly suppressed ommatidial fusion in the central side of the flies' eyes compared to the vehicle-fed flies (marked with an asterisk in Figs. 57B3-E3 and B4-E4). In particular, 300 and 500 μM acacetin ameliorated ommatidial fusion at the edges of the fly eyes. Although acacetin did not completely suppress the morphological changes in the eyes, it delayed this age-dependent degeneration progress.

The protective effects of acacetin on the compound eyes of the male *GMR<APP/BACE-1* flies (30 days old) were examined using SEM. The control *GMR-GAL4/+* flies had eyes with a smooth appearance, without any defects in the ommatidia size (Fig. 57F1) or ommatidial bristles (Fig. 57G1). In contrast, the transgenic *GMR<APP/BACE-1* flies showed varying degrees of eye disorganization. The eyes of the vehicle-fed flies showed the strongest phenotypes; they were characterized by ommatidial collapse (marked with arrows in Fig. 57F2), fused ommatidia (marked with arrowheads in Fig. 57G2), a reduced ommatidia size (marked with an asterisk in Fig. 57G2), and the absence of ommatidial bristles (Fig. 57G2). These eye phenotype defects were partially suppressed in male flies treated with three concentrations of acacetin (100, 300, and 500 μM) (Figs. 57F3-5 and G3-5). Remarkably, external surface collapse was not observed in flies fed 300 μM acacetin (Fig. 57F4), but there was still some collapse in flies fed 100 and 500 μM acacetin (marked with arrows in Figs. 57F3 and F5). Ommatidial external surface fusion was not observed in acacetin-fed flies, but the reduced ommatidia size (marked with asterisks in Figs. 57G3-5) was observed, irrespective of concentration.

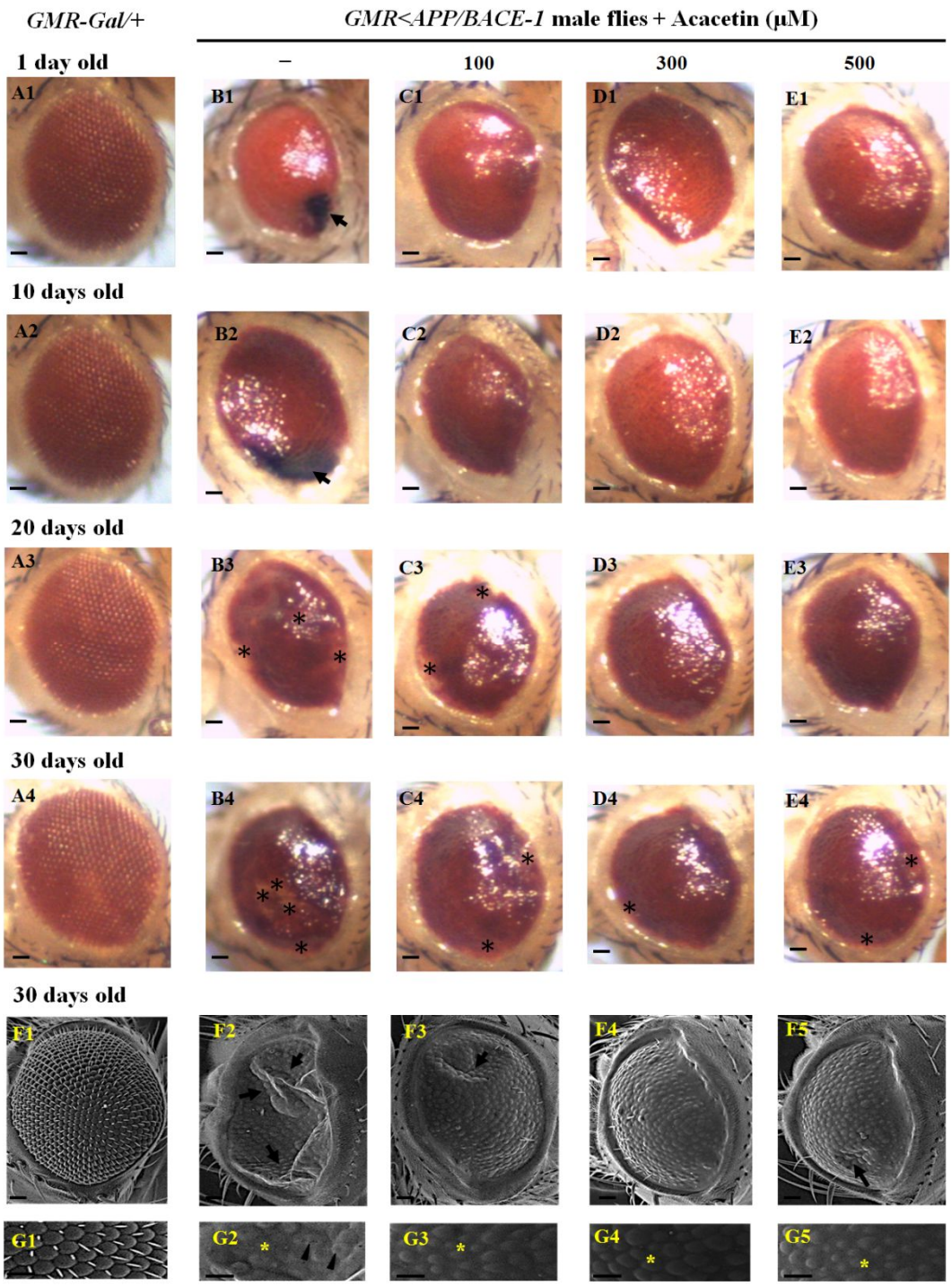
GMR-Gal/+
GMR<APP/BACE-1 male flies + Acacetin (μM)
1 day old
–
100
300
500
A1
B1
C1
D1
E1
10 days old
A2
B2
C2
D2
E2
20 days old
A3
B3
C3
D3
E3
30 days old
A4
B4
C4
D4
E4
30 days old
F1
F2
F3
F4
F5
G1
G2
G3
G4
G5

Fig. 57. Effect of acacetin on the aberrant eye phenotype associated with age-dependent eye development. Human *APP* and *BACE-1* transgenic flies (*GMR<APP/BACE-1*) were cultured from the egg stage in polystyrene vials containing standard media supplemented with acacetin (100, 300, and 500 μM) in 0.1% dimethyl sulfoxide. Light micrographs. (**A**) The control male *GMR-GAL4/+* flies (1, 10, 20, and 30 days old) had a normal and well-organized eye morphology. There were no obvious morphological changes as time elapsed. (**B**) The vehicle-fed male *GMR<APP/BACE-1* flies exhibited dark deposits at the edge of the compound eye, even at the youngest age evaluated (marked with an arrow in Fig. 3B1); the size of the deposits had increased at 10 days (marked with an arrow in Fig. 3B2). As time passed, the flies with dark spots in their eyes tended to die earlier than the control flies, and more ommatidial fusions were observed in 20-day-old fly eyes with deposits (marked with asterisks in Fig. 3B3), with further exacerbation of these fusions in 30-day-old fly eyes (marked with asterisks in Fig. 3B4). (**C-E**) Acacetin partially suppressed the morphological defects in the eyes. Scanning electron micrographs. (**F1, G1**) Thirty-day-old male *GMR-GAL4/+* flies with smooth surface compound eyes, without any defects in the ommatidia size, ommatidial bristles, or fused ommatidia. (**F2, G2**) Vehicle-fed male *GMR<APP/BACE-1* flies (30 days old) with abnormal phenotypes, characterized by the collapse (marked with arrows) and fusion of ommatidia (marked with arrowheads), and the absence of ommatidial bristles (marked with an asterisk). (**F3-5, G3-5**) Acacetin partially suppressed these eye defects. The scale bars represent 20 μm.

2.3.2. Acacetin has a protective effect on age-dependent neurodegeneration of the eye

Male compound eye sections were examined to demonstrate the protective effects of acacetin on the age-dependent neurodegeneration induced by co-expression of human *BACE-1* and *APP*. Photoreceptor degeneration in the transgenic *GMR<APP/BACE-1* flies depended on age, but this was not the case for the control *GMR-Gal4/+* flies (Fig. 58). The *GMR-Gal4/+* flies (5 and 15 days old) had well-organized photoreceptors, without age-dependent phenomena, as determined by Carson's trichrome staining (Figs. 58A1 and A2). In contrast, photoreceptor degeneration was observed in young transgenic flies (Figs. 58B1-E1) and 15-day-old flies (Figs. 58B2-E2). In the vehicle-fed transgenic flies, remarkable retinal collapse was observed, even in young flies (5 days old) (Fig. 58B1), and external surface collapse of the photoreceptors was detected in the 15-day-old flies (marked with an arrowhead in Fig. 58B2). Acacetin (100, 300, and 500 μM) partially suppressed the photoreceptor degeneration in 5- (Figs. 58C1-E1) and 15-day-old flies (Figs. 58C2-E2). In particular, acacetin significantly suppressed the photoreceptor collapse (Figs. 58C2-E2). Although acacetin did not completely suppress photoreceptor degeneration, it delayed this age-dependent process.

Congo red staining was performed to investigate whether amyloid deposition was age-dependent or due to the effects of acacetin on these deposits. Amyloid plaques were not detected in the compound eyes of the control male *GMR-Gal4/+* flies (5 and 15 days old) (Figs. 58A3 and A4). However, scattered amyloid plaque deposits (marked with arrows in Fig. 58B3) were evident in 5-day-old vehicle-fed transgenic flies, and many amyloid plaque deposits (marked with arrows in Fig. 58B4) had accumulated in the 15-day-old flies. Interestingly, Congo red staining revealed that 100 and 300 μM acacetin significantly suppressed the number of amyloid deposits in 5- (Figs. 58C3 and D3) and 15-day-old transgenic flies (Figs. 58C4 and D4); however, a few amyloid plaque deposits were also detected in 5- (marked with arrows in Fig. 58E3) and 15-day-old transgenic flies (marked with arrows in Fig. 58E4) supplemented with 500 μM acacetin. Although acacetin did not completely suppress amyloid deposition in the flies' photoreceptors, it reduced the number of amyloid deposits.

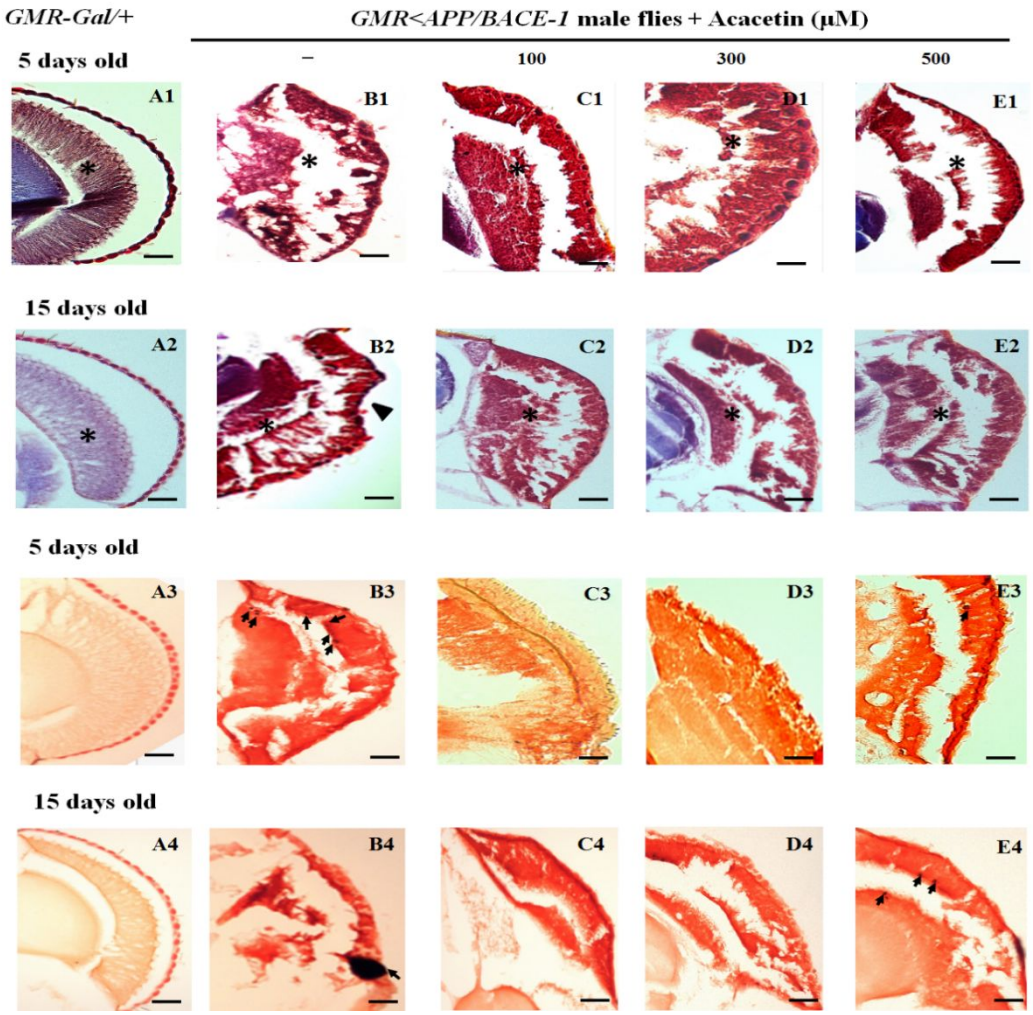

Fig. 58. Protective effect of acacetin on the age-dependent eye degeneration induced by co-expression of human *BACE-1* and *APP*. Human *APP* and *BACE-1* transgenic flies (*elav<APP/BACE-1*) were cultured from the egg stage in polystyrene vials containing standard media supplemented with acacetin (100, 300, and 500 µM) in 0.1% dimethyl sulfoxide. Carson's trichrome staining. (**A1, A2**) Staining of the photoreceptors of control male *GMR-Gal4/+* flies (5 and 15days old). (**B1, B2**) Staining of the photoreceptors of vehicle-fed transgenic male *GMR<APP/BACE-1* flies (5 and 15days old). Remarkable retinal collapse (marked with an asterisk in B1) was observed even in young flies (5 days old), and more severe external surface collapse of the photoreceptors

was detected in 15-day-old flies (marked with an arrowhead in B2) compared to 5-day-old flies. (**C1-E1**) The photoreceptor degeneration was partially suppressed in 5-day-old acacetin-fed transgenic flies. (**C2-E2**) The external surface collapse of the photoreceptors was significantly suppressed in 15-day-old acacetin-fed flies. Congo red staining. (**A3, A4**) Amyloid plaques were not observed in the control male *GMR-Gal4/+* flies (5 and 15 days old). (**B3, B4**) Scattered amyloid plaque deposits were apparent in the 5-day-old vehicle-treated transgenic flies (marked with arrows in B3). Many amyloid plaque deposits (marked with an arrowhead in B4) had accumulated in the 15-day-old flies. (**C3-E3**) Acacetin reduced the number of scattered amyloid plaque deposits in the photoreceptors of 5-day-old transgenic flies. (**C4-E4**) Acacetin reduced the number of amyloid plaque deposits in the 15-day-old transgenic flies. The images were observed and captured using a stereo-microscope. The scale bars represent 20 μm.

2.3.3. Effect on the flies' age-dependent motor abnormalities

AD is characterized by age-dependent degeneration in locomotor coordination (Ali *et al*., 2011). In *Drosophila* AD models, locomotor coordination can be quantified by the negative geotaxis assay, as described by Wang *et al*. (2014) and Crowther *et al*. (2005). The male flies were used because the climbing defects were more pronounced in males than in females (Wang *et al*., 2014). The male *elav-Gal4/+* flies showed a clear age-dependent reduction in climbing, with climbing indices of 80, 66, 53, and 34% at 1, 5, 10, and 15 days postemergence, respectively (Figs. 59A-D). In contrast, the vehicle-fed male *elav<APP/BACE-1* flies showed severe defects in performance, with climbing indices of 47, 39, 36, and 11% at 1, 5, 10, and 15 days postemergence, respectively (Figs. 59A-D). Acacetin improved the motor abnormalities to approximately 68% as early as 1 day after emergence, irrespective of the concentration (100, 300, and 500 μM) (Fig. 59A). The acacetin treatment resulted in a 60–66% climbing index at 5 days postemergence (Fig. 59B) and a 53–54% climbing index at 10 days postemergence (Fig. 59C). At 15 days postemergence, acacetin significantly ameliorated the climbing defects (climbing index, 27–30%) (Fig. 59D).

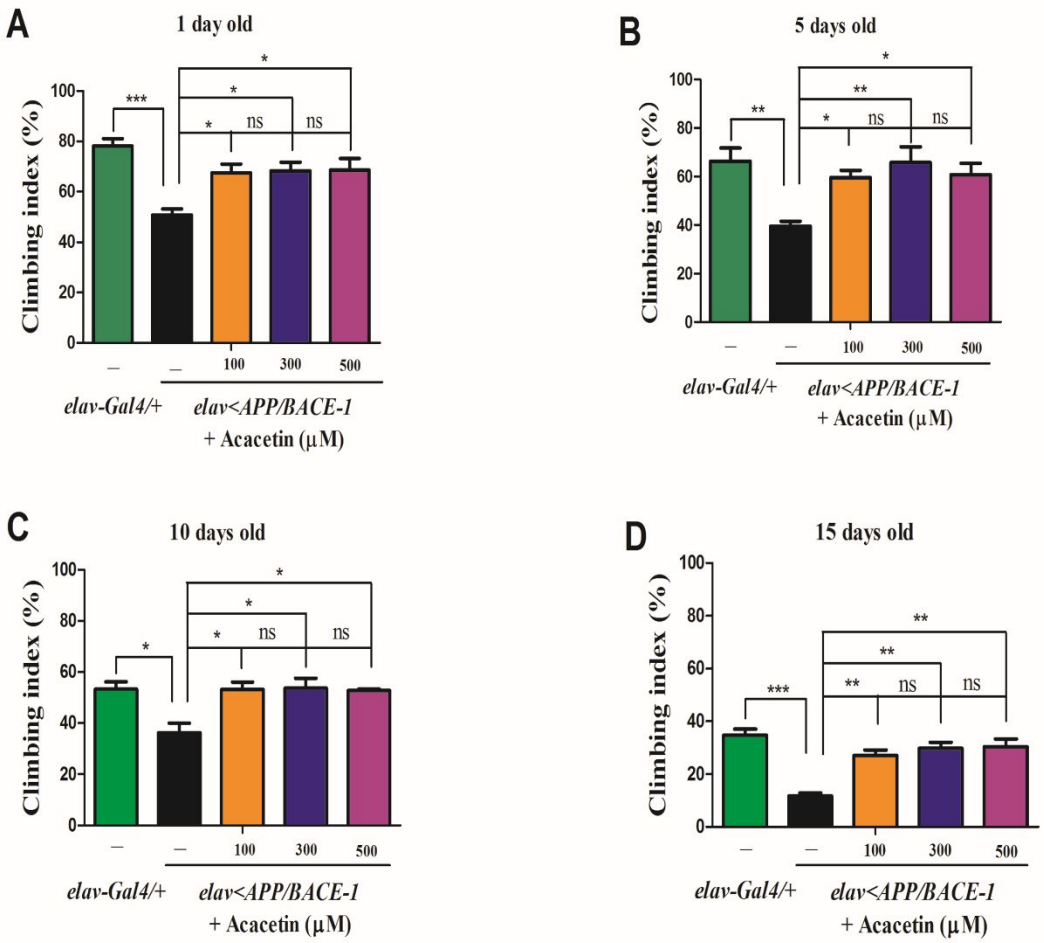

Fig. 59. Effect of acacetin on the age-dependent climbing behavior of the transgenic flies. Human *APP* and *BACE-1* transgenic flies (*elav<APP/BACE-1*) were cultured from the egg stage in polystyrene vials containing standard media supplemented with acacetin (100, 300, and 500 µM) in 0.1% dimethyl sulfoxide. Male flies (1, 5, 10, and 15 days old) were placed in empty vials conjoined with another vial on top and manually tapped twice. After 20 s, the flies that climbed from the bottom and crossed the 9.5 cm line were counted, and the climbing index was calculated as the number of flies that climbed to the top vial relative to the total number of test flies and expressed as a percentage. Climbing behavior of 1- **(A)**, 5- **(B)**, 10- **(C)**, and 15-day-old male flies **(D)**. Co-expression of

human *BACE-1* and *APP* significantly decreased the flies' climbing activities compared to the control *elav-Gal4/+* flies. Acacetin ameliorated the climbing defects of the *elav<APP/BACE-1* flies compared to the vehicle-fed flies, irrespective of concentration. Each bar represents the mean ± SE from three independent experiments ($^{***}P<0.001$; $^{**}P<0.01$; $^{*}P<0.05$; ns, no significant difference, using Bonferroni's multiple comparison test).

2.3.4. Effect on fly feeding and longevity

A feeding assay was used as an index to quantify the effect of different concentrations of the active compound on the amount of food consumed by the flies (Carvalho *et al*., 2005; Deshpande *et al*., 2014). The effects of acacetin on food intake were examined in transgenic male *elav<APP/BACE-1* flies. Acacetin did not significantly affect feeding by transgenic flies, irrespective of the concentration (100, 300, and 500 μM) (Fig. 60A), indicating that any changes in the flies' behaviors were due to the ingestion of compounds by food intake rather than the effect of acacetin on their appetite.

The $T_{1/2}$ is a more credible measurement of lifespan than the mean survival time (Chakraborty *et al*., 2011). The effects of acacetin on the lifespan and $T_{1/2}$ of the *Drosophila* AD model were investigated, because it was previously reported that co-expression of BACE-1 and APP reduced the lifespan of the adult flies (Chakraborty *et al*., 2011). Acacetin (100, 300, and 500 μM) did not significantly increase the lifespan of the male *elav<APP/BACE-1* flies compared to the vehicle-fed transgenic flies and control *elav-Gal4/+* flies (Fig. 60B). However, co-expression of human BACE-1 and APP markedly reduced the $T_{1/2}$ (26 days) of vehicle-fed flies compared to the *elav-Gal4/+* flies ($T_{1/2}$, 36 days) (Fig. 60C). Treatment of transgenic flies with 100 μM acacetin increased the $T_{1/2}$ (31 days), while 300 and 500 μM acacetin did not significantly extend the $T_{1/2}$. These findings suggest that the lowest concentration of acacetin (100 μM) has an effect on the $T_{1/2}$ of *elav<APP/BACE-1* flies; however, this is limited to young adults. Taken together, these data suggest that BACE-1 may not have a major function in the survival of *elav<APP/BACE-1* flies, which is consistent with the conclusions of a previous study

(Chakraborty *et al*., 2011).

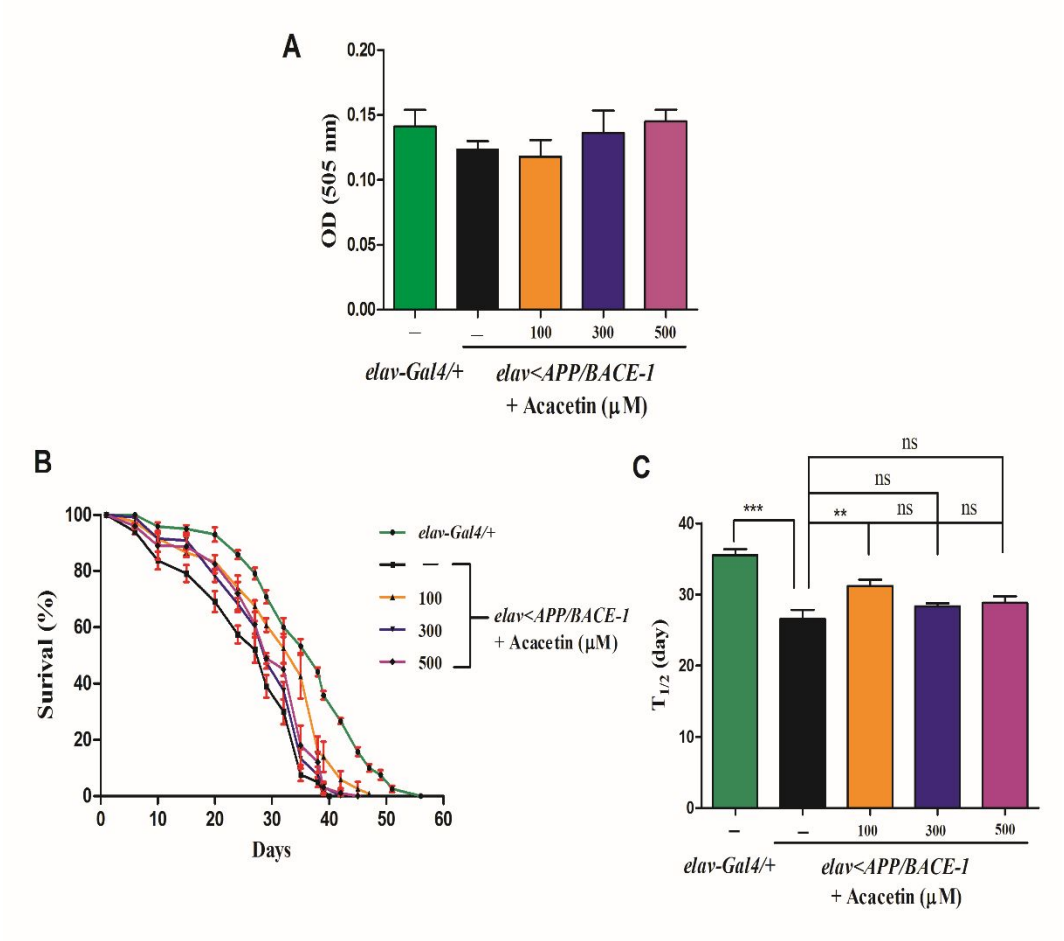

Fig. 60. Effect of acacetin on the feeding and longevity of the transgenic flies. Human *APP* and *BACE-1* transgenic flies (*elav<APP/BACE-1*) were cultured from the egg stage in polystyrene vials containing standard media supplemented with acacetin (100, 300, and 500 µM) in 0.1% dimethyl sulfoxide to determine the lifespan and median life time ($T_{1/2}$). (**A**) To determine feeding behavior, newly emerged transgenic male flies were cultured on standard media for 3 days, and then starved for 20 h. The flies were transferred into vials containing media (with 0.2% Acid red) supplemented with acacetin. The control flies were fed with media containing 0.2% Acid red and vehicle. The abdomens of flies fed with Acid red were cut and homogenized in distilled water, and the optical density (OD)

of the supernatant was measured at 505 nm as the index of amount of food consumed by the flies. Acacetin did not affect the feeding behavior of the flies. (**B**) Acacetin did not significantly prolong the transgenic flies' lifespan compared to the vehicle-fed male transgenic and *elav-Gal4/+* flies. (**C**) Co-expression of human BACE-1 and APP reduced the $T_{1/2}$ of the male flies compared to that of the control male *elav-Gal4/+* flies. Supplementing the diet with 100 μM acacetin only significantly extended the $T_{1/2}$ of the male *elav<APP/BACE-1* flies. Each bar represents the mean ± SE from 10 independent experiments for longevity and from three independent experiments for feeding ($^{***}P<0.001$; $^{**}P<0.01$; ns, no significant difference, using Bonferroni's multiple comparison test).

2.3.5. Effect on eclosion of the transgenic flies

The pupation and emergence rates were examined to determine whether acacetin affected the development of the transgenic flies. Co-expression of human *BACE-1* and *APP* in the nervous system did not affect pupation compared to the control *elav-Gal4/+* flies. The acacetin-treated flies showed nearly normal pupation rates, irrespective of the treatment concentration (100, 300, and 500 μM), and these rates were not significantly different from those of the vehicle-fed transgenic flies (Fig. 61A). This could be due to the relatively weak promoter – *elav* – used to drive human *APP* and *BACE-1* gene expression. However, the emergence rate (76%) of the vehicle-fed *elav<APP/BACE-1* flies was significantly different from that (99%) of the *elav-Gal4/+* flies (Fig. 61B). This finding indicates that co-expression of human *BACE-1* and *APP* is toxic during fly development, particularly at the emergence stage. Acacetin (100, 300, and 500 μM) did not have a significant effect on the emergence of flies (82–86%) compared to the vehicle.

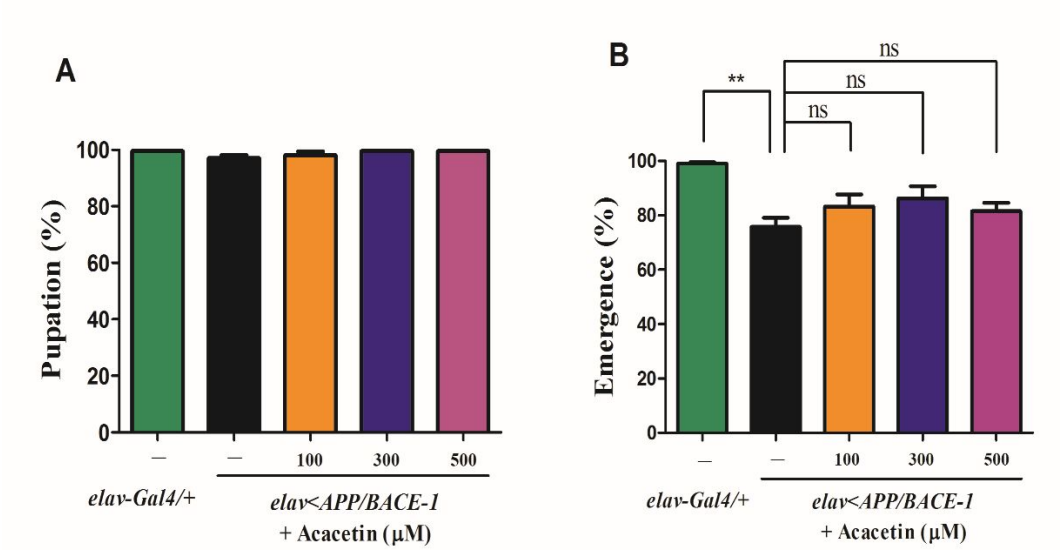

Fig. 61. Effect of acacetin on the eclosion rate of the transgenic flies. Human *APP* and *BACE-1* transgenic flies (*elav<APP/BACE-1*) were cultured from the egg stage in polystyrene vials containing standard media supplemented with acacetin (100, 300, and 500 µM) in 0.1% dimethyl sulfoxide. The third instar larvae climbing on the wall were collected in vials containing fresh media. The numbers of pupae and adults were counted. (**A**) Co-expression of human *BACE-1* and *APP* as along with acacetin supplementation did not affect the pupation of the male *elav-Gal4/+* and *elav<APP/BACE-1* flies. (**B**) Co-expression of human *BACE-1* and *APP* significantly reduced the emergence of the male transgenic flies. Acacetin had no significant effect on the emergence defect. Each bar represents the mean ± SE from four independent experiments ($^{**}P<0.01$; ns, no significant difference, using Bonferroni's multiple comparison test).

DISCUSSION

Although multiple pathogenetic factors such as Aβ and tau aggregation, excessive metal ions, oxidative stress, acetylcholine level, and increased BACE-1 activity have been suggested for AD, lifestyles and genetic factors also are associated with AD development (Ji and Zhang, 2008). Based on Gal4-UAS system, transgenic *Drosophila* models of AD can be constructed through two ways. One is by modeling amyloid toxicity, while another is by modeling tauopathies (Siddhita *et al*., 2013). Modeling amyloid toxicity can be realized by directly expression of Aβ (Finelli *et al*., 2004; Iijima *et al*., 2004; Crowther *et al*., 2005; Hong *et al*., 2011; Caesar *et al*., 2012) or through expression of APP, BACE-1, or/and presenillin (Greeve *et al*., 2004; Sarantseva *et al*, 2009; Chakraborty *et al*., 2011). In this study, as for the *elav<APP/BACE-1* flies, no effect on lifespan and pupation were observed, while decreased $T_{1/2}$, age-dependent climbing deficits, and decreased emergence were observed, compared with control *elav-Gal4/+*. BACE-1 inhibitory compounds curcuminoids and acacetin significantly prolonged $T_{1/2}$ and improved climbing deficits of transgenic flies, while acacetin did not affect the pupation and emergence of AD flies in their development. Greeve *et al.* (2004) demonstrated that APP, BACE-1, and/or DPsn co-expressed significantly suppressed eclosion rate, and BACE-1 inhibitor at concentration ranging from 1 to 50 nM increased eclosion rate. In addition, treatment of *act<APP/BACE-1/DPsn* flies with the BACE-1 inhibitor significantly prolonged lifespan (Greeve *et al.*, 2004). Chakraborty *et al.* (2011) reported that APP and BACE-1 co-expressed flies showed decreased survival and climbing ability, while only BACE-1 expression did not affect the survival time. They also compared the lifespan for *elav<APP/BACE-1* flies fed on DMSO and γ-secretase inhibitor L-685,458 and reported that there was no significant difference observed, although the inhibitor significantly rescued the climbing defects of flies. The modified SuHeXiang Wan (KSOP1009) extract was reported without effects on survival and normal development of the control flies (*elav-Gal4*), but improved the decreased lifespan and motor activity of flies with Aβ overexpressed (Hong *et al*., 2011). It has been also

reported that low (0.0001% w/w in yeast paste) and intermediate (0.001% w/w in yeast paste) concentration of curcumin showed positive effect on lifespan and $T_{1/2}$ of $A\beta_{42}$ and double $A\beta_{42}$ expressed flies, while high concentration (0.01% w/w in yeast paste) of curcumin did not affect lifespan and $T_{1/2}$ of their flies (Caesar *et al*., 2012). Besides, curcumin enhanced climbing ability of $A\beta_{42}$ and double $A\beta_{42}$ expressed flies, but the effect of curcumin decreased with the increasing age (Caesar *et al*., 2012). Ng *et al.* (2013) reported that *Gastrodia elata* (GE) extract significantly improved both lifespan and $T_{1/2}$ of Aβ expressed *Drosophila*. In this study, APP and BACE-1 co-expressed did not induced the decreased lifespan and pupation of AD flies that may be due to the weaker driver strain applied. Curcuminoids and acacetin did not significantly prolonged lifespan of AD flies but increased $T_{1/2}$, suggesting that the effect of these phytochemicals on survival was only limited to young adult flies.

As for *GMR<APP/BACE-1* flies, APP and BACE-1 co-expression induced rough phenotypes with morphological defects including dark deposition, photoreceptor collapse and fusion, and absence of ommatidial bristles. Curcuminoids and acacetin showed amyloid clearance ability and significantly rescued these defects. Greeve *et al*. (2004) studied co-expression of human APP and BACE-1 under *gmr-Gal4* driver induced age-dependent neurodegeneration in photoreceptor cells of flies and reported amyloid plaque depositions. It has been reported that Congo red decreased plaque formation in retinal tissue of flies with double expression of $A\beta_{42}$ (Crowther *et al*., 2005). Hong *et al*. (2011) reported $A\beta_{42}$ expression induced strong eye degeneration, and KSOP1009 extract treatment suppressed this defects. Ng *et al*. (2013) demonstrated that GE extract rescued the neurodegeneration in the ommatidia of Aβ expressed *Drosophila.*

The morphological eye defects became severe when raised at 29^{o}C that may be due to the higher activity of GAL4 at this temperature (Kramer and Staveley, 2003). Compared with flies cultured at 25^{o}C, some dark spots were observed in the compound eyes of the *GMR<APP/BACE-1* flies. It has been reported the presence of melanotic masses on both the ventral abdomen and proboscis of *elav<APP/BACE* flies (Chakraborty *et al*., 2011). The number of masses was significantly decreased in these flies after treatment with the

γ-secretase inhibitor L-685,458. They suggested that the masses were composed of Aβ or induced by Aβ. Greeve *et al*. (2004) reported that Aβ deposits were localized outside the retinas of the *GMR<APP/BACE-1* flies. The dark spots in the *Drosophila* eyes might be composed of Aβ due to the expression of the human *APP* and *BACE-1* genes in the photoreceptor cells and secretion of Aβ by these photoreceptor cells into the projection areas (Greeve *et al*., 2004). The Aβ could induce the immune response by activating the Toll pathway (Lemaitre *et al*., 1995; McGeer *et al*., 1998), resulting in the formation of dark spots on the surfaces of the compound eyes. In this study, prolonged exposure to either CCN, BDMCCN or acacetin could rescue morphological defects (dark deposition, photoreceptor collapse and fusion, and absence of ommatidial bristles) observed in flies expressing APP and BACE-1 in the eyes of the *GMR<APP/BACE-1* flies that co-express BACE-1 and APP in their compound eyes. In addition, dietary supplement of CCN, BDMCCN, or acacetin also improved the locomotor coordination in the *elav<APP/BACE-1* flies and prolonged the $T_{1/2}$ of the transgenic flies, without any effects on feeding behavior, but not in control. These findings, together with the elucidation of the inhibitory action of acacetin on BACE-1, indicates that materials derived from *C. longa* rhizomes or whole *A. rugosa* plants-derived materials may hold promise for the development of novel, effective naturally occurring anti-AD products.

In conclusions, *C. longa* rhizome- or whole *A. rugosa* plants-derived preparations containing curcuminoids or acacetin could be useful as sources of potential therapeutics or lead molecules for prevention or treatment of AD. For practical use of *C. longa* rhizomes or whole *A. rugosa* plants-derived materials as novel anti-AD products to proceed, further research is needed to establish their human safety and whether this activity could be exerted *in vivo* after consumption of the product by humans. Historically, the rhizome has been commonly used as a spice in curries and other South Asian and Middle Eastern cuisine, flavoring agents, and coloring agents (Itokawa *et al*., 2008). *A. rugosa* is used as a wild vegetable and herbal drug in traditional therapies (Zielinska and Matkowski, 2014). In addition, their anti-AD modes of action need to be established and formulations for improving anti-AD potency and stability need to be developed.

CHAPTER III

Possible Mechanisms of Action of Acacetin on *Drosophila* Model of Alzheimer's Disease

INTRODUCTION

An investigation of the mechanisms of action of naturally occurring anti-AD compounds may provide useful information for the development of selective anti-AD therapeutic alternatives with novel target sites (Caesar *et al*., 2012). The target sites and mechanisms underlying the anti-dementia actions of plant secondary substances have been well documented by Howes and Perry (2011). CCN has been proposed to alleviate Aβ toxicity in transgenic human Aβ and human tau flies by reducing the pre-fibrillar/oligomeric species of Aβ (Caesar *et al*., 2012). Curcuminoids were reported to be able to suppress Aβ production (Liu *et al*., 2010). CCN could reduce APP protein expression, but none of curcuminoids affected *APP* mRNA level (Liu *et al*., 2010). BDMCCN could reduce BACE-1 both mRNA and protein levels, while DMCCN only affected *BACE-1* mRNA expression (Liu *et al*., 2010). Therefore, CCN could decrease Aβ formation through modulation of APP, while BDMCCN may be mediated through modulation of BACE-1(Liu *et al*., 2010). Many *in vivo* studies have shown that flavonoids can be absorbed by oral administration, cross the blood brain barrier, and work on the central nervous system (Jäger and Saaby, 2011; Faria *et al*., 2014). Acacetin has been reported to possess antioxidant (Cholbi *et al*., 1991), anti-inflammatory (Pan *et al*., 2006), and anticarcinogenic (Shen *et al*., 2010) activities and have neuroprotective effects on the central nervous system. They also have therapeutic potential for treating neurological diseases associated with excitotoxicity (Lin *et al*., 2014). However, no previous studies have investigated the anti-amyloidogenic effect of acacetin *in vivo*. In this study, the possible mechanism underlying the anti-AD actions of acacetin was elucidated using qRT-PCR and western blot analyses.

MATERIALS AND METHODS

3.1. Materials and reagents

Commercially-available organic pure acacetin and BSA were purchased from Santa Cruz Biotechnology (Dallas, TX, USA). RIPA buffer and the mammalian cell protease inhibitor cocktail were purchased from Sigma-Aldrich (St. Louis, MO, USA). The PageRuler Prestained Protein Ladder and Spectra Multicolor Low Range Protein Ladder were purchased from Thermo Scientific (Walldorf, Germany). All of the other chemicals and reagents used in this study were of reagent-grade quality and are available commercially.

3.2. Antibodies

The primary antibodies used in this study were as follows: APP C-terminal antibody (A8717) purchased from Sigma-Aldrich; anti-BACE-1 antibody (ab2077) and anti-actin antibody (ab1801) purchased from Abcam (Cambridge, MA, USA); and Aβ, 17-24 (4G8) monoclonal antibody (SIG-39240) purchased from Covance (Princeton, NJ, USA). The secondary antibodies used in this study were goat anti-rabbit IgG H&L (HRP) (ab6721-1) purchased from Abcam and goat anti-mouse IgG-HRP (sc-2005) purchased from Santa Cruz Biotechnology.

3.3. *Drosophila* stocks and rearing conditions

The flies stocks and rearing conditions were described in 'Materials and Methods' section of Chapter 2.2. *UAS-mCD8-GFP/cyo* fly stock was obtained from Dr. Young Ho Koh, Ilsong Institute of Life Science, Hallym University (Anyang, Gyeonggi, ROK). The GAL4/UAS system was used to overexpress the target genes in specific tissues.

3.4. Experimental groups

In the Gal4 system, the promoter (or enhancer) drives the expression of the yeast transcriptional activator Gal4 in cell- and tissue-specific patterns, and Gal4, in turn, directs the transcription of Gal4-UAS target genes in an identical pattern (Phelps and Brand, 1998). To confirm that the effects of acacetin on human *APP* and *BACE-1* mRNA expression were not due to a promoter (or enhancer) effect in the Gal4 system, the levels of the *GFP* mRNA were compared in vehicle-fed and acacetin-fed male *elav<GFP* flies by qRT-PCR. The possible mechanisms of the anti-AD action of acacetin were elucidated using western blotting analyses (Fig. 46).

3.5. Real-time reverse transcription-PCR analysis

Real-time qRT-PCR with SYBR Green dye was performed to determine whether acacetin affected the expression levels of the human *APP* and *BACE-1* mRNAs in the transgenic flies. The *elav<APP/BACE-1* and *elav<GFP* flies were cultured from the egg stage in vials, as stated previously. The controls received 0.1% DMSO only. The total RNA was extracted from 30 heads (30 mg) of male *elav<APP/BACE-1* and *elav<GFP* flies (20 days old) using the RNeasy Mini Kit (Qiagen, Hilden, Germany) according to the manufacturer's instructions. The residual genomic DNA was removed using RQ1 RNase-Free DNase (Promega, Fitchburg, WI, USA), and 1 μg of the total RNA from each sample was used for complementary DNA (cDNA) synthesis with an oligo (dT) 12–18 primer (Invitrogen, Carlsbad, CA, USA) according to the protocol of the SuperScript III Reverse Transcriptase Kit. Real-time qRT-PCR was performed in 96-well plates using the StepOne Plus Real-Time PCR System (Applied Biosystems, Darmstadt, Germany). Each reaction mixture consisted of 10 μL of the SYBR Green PCR Master Mix Kit (Applied Biosystems), 2 μL of the forward and reverse primers (5 pmol each) (Table 17), 25 ng of the cDNA, and diethylpyrocarbonate water for a final volume of 20 μL. The oligonucleotide PCR primer pairs are listed in Table 3 and were purchased from Bioneer (Daejeon, ROK). The cycling program was an initial hold at 95°C for 5 min, followed by 40 cycles of denaturation at 95°C for 30 s, annealing at 62°C for 30 s, and extension at

72°C for 30 s. The mRNA expression levels of the target genes were normalized to the mRNA expression level of the housekeeping gene *rp 49* that encodes the *Drosophila* ribosomal protein 49, and analyzed by the $2^{-\Delta\Delta CT}$ method using the StepOne Software v2.3 and DataAssist Software (Applied Biosystems).

Table 17. Primers used for real-time quantitative reverse transcription polymerase chain reaction in this study

Gene name	Forward primer and reverse primer
rp 49	5′-CTGCTCATGCAGAACCGCGT-3′
	5′-GGACCGACAGCTGCTTGGCG-3′
APP	5′-GCCGTGGCATTCTTTTGGGGC-3′
	5′-GTGGTCAGTCCTCGGTCGGC-3′
BACE-1	5′-GCAGGGCTACTACGTGGAGA-3′
	5′-GTATCCACCAGGATGTTGAGC-3′
GFP	5’-AAGTTCATCTGCACCACCG-3’
	5’-TCCTTGAAGAAGATGGTGCG-3

3.6. Western blot analysis

The *elav<APP/BACE-1* flies were cultured from the egg stage, as described previously. The lysates were obtained from the heads of 50 male flies (20 days old) by placing the heads in 100 μL RIPA buffer (pH 8.0) containing a 1% protease inhibitor cocktail (Chakraborty *et al*., 2011). The controls received 0.1% DMSO. The lysates were centrifuged at 14,000 rpm for 30 min at 4°C. The protein content of the supernatant was determined using a Bradford Protein Assay kit (Sigma-Aldrich) and BSA was used as the standard. The total proteins (30 μg/sample for APP and BACE-1 detection; 70 μg/sample for Aβ detection) were mixed with an equal volume of 5× sample buffer (Bollag *et al*., 1996) containing 40 mM of DL-dithiothreitol, boiled for 10 min, and then loaded onto 8, 10, and 12% sodium dodecyl sulfate-polyacrylamide gels using a Mini-Protean 3

electrophoresis cell (Bio-Rad, Hercules, CA, USA) for APP, APP-CTF (APP-αCTF and APP-βCTF) and AICD, BACE-1, and Aβ detection, respectively. After electrophoresis at 110 V in 2 h, the proteins from the gels were transferred onto a polyvinyl difluoride membrane (Pall Corporation, Pensacola, FL, USA) using an electroblotting apparatus. The membrane was then blocked with 5% skim milk (BD Difco, Flanklin Lakes, NJ, USA) in PBS containing 0.1% (v/v) Tween-20 (0.1% PBS-T) at room temperature for 1 h, and further incubated overnight at 4°C with a 1:4,000 dilution of an anti-APP C-terminal antibody to detect the cleaved APP product, a 1:1,000 dilution of anti-BACE-1, and a 1:1,000 dilution of anti-amyloid (4G8). After washing with 0.1% PBS-T three times at 10 min intervals, the membranes were further incubated for 2 h with a goat anti-rabbit IgG H&L (HRP) secondary antibody at a1:4,000 dilution for APP and BACE-1 and a goat anti-mouse lgG-HRP at a 1:5,000 dilution for Aβ. Finally, after washing with 0.1% PBS-T three times with a 10 min interval between washes, the membranes were developed with an ECL chemiluminescence reagent (Amersham Bioscience, Buckinghamshire, UK) and immediately exposed to a CP-PU X-ray film (AGFA, Mortsel, Belgium). The differences in protein expression were quantified using a Molecular Imager Gel Doc XR system (Bio-Rad, Hercules, CA, USA) and normalized to actin expression on the same membrane.

3.7. Data analysis

The results are expressed as the means ± SEs of duplicate samples from three independent experiments. The significance between means was determined using a one-way or two-way analysis of variance (ANOVA) statistical test (GraphPad Prism 5.1 software).

RESULTS

3.1. Effect of acacetin on the human *APP* and *BACE-1* mRNA levels

Many studies have focused on APP proteolysis and Aβ generation as potential targets for AD therapy (Haass, 2004), and APP inhibitors are also used to lower the Aβ peptide levels, as described previously (Utsuki *et al*., 2006). To investigate whether acacetin affected the transcription of the human *BACE-1* and *APP* genes, the *APP* and *BACE-1* mRNA levels in male *elav<APP/BACE-1* flies (20 days old) was analyzed using real-time qRT-PCR. An active compound could reduce the human *APP* and *BACE-1* mRNA levels by indirectly inhibiting the *elav* promoter. To investigate this, flies with a *UAS-GFP* sequence driven by the *elav* promoter and treated them with acacetin were used. The levels of the *GFP* mRNA were also quantified. There were no significant differences in the *GFP* mRNA levels between the vehicle-fed and acacetin-fed flies (Fig. 62A). However, a significant reduction in the *APP* mRNA levels (69–82%) was observed in the male *elav<APP/BACE-1* flies following treatment with acacetin (100, 300, and 500 μM) compared to the vehicle-treated flies (Fig. 62B). Similarly, the human *BACE-1* mRNA levels were reduced to 82–89% of the control levels following acacetin treatment (Fig. 62C). Taken together, these data indicate that acacetin had no significant effect on the *GFP* mRNA levels, but decreased the human *APP* and *BACE-1* mRNA levels rather than indirectly inhibiting the *elav* promoter.

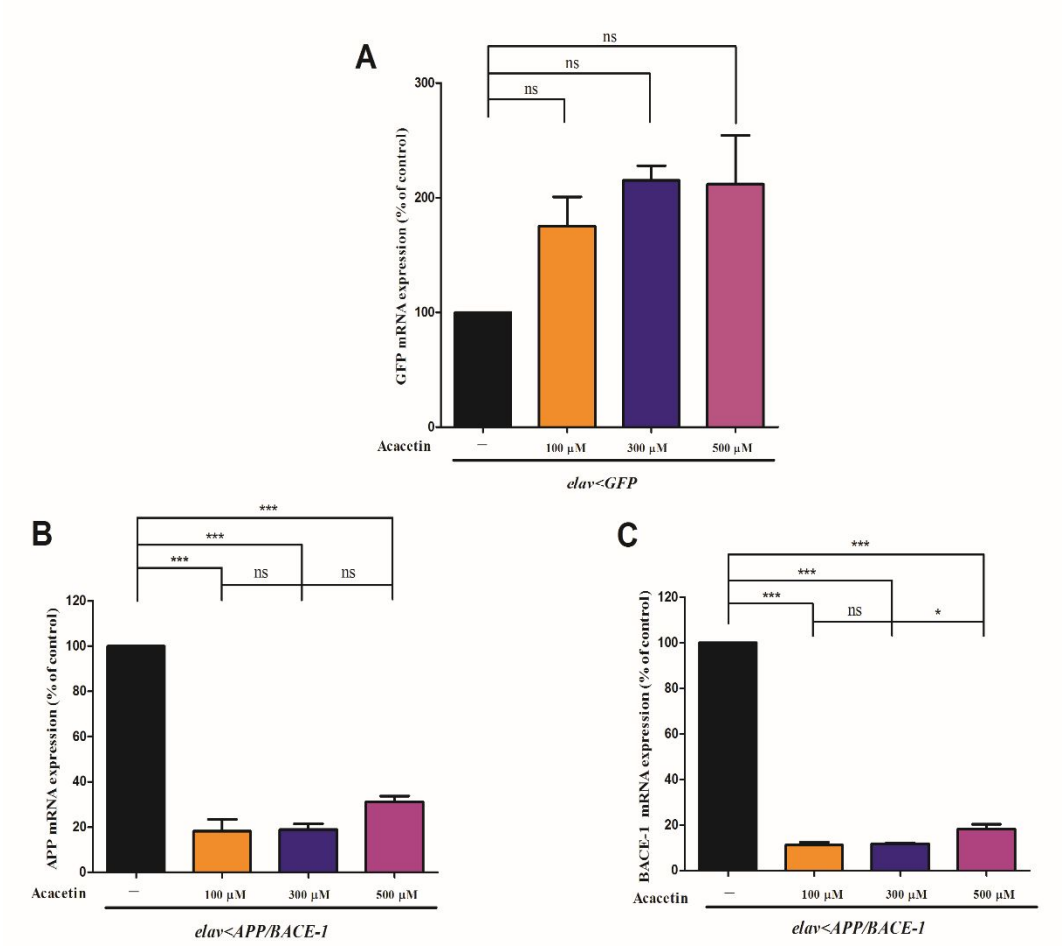

Fig. 62. Effect of acacetin on the expression of the human *BACE-1* and *APP* mRNAs. The total RNA was extracted from 30 heads (30 mg) of *elav<APP/BACE-1* and *elav<GFP* flies (20 days old) cultured from the egg stage in polystyrene vials containing media supplemented with acacetin (100, 300, and 500 µM) in 0.1% dimethyl sulfoxide. Real-time quantitative reverse transcription polymerase chain reaction was performed to determine the levels of the *BACE-1* and *APP* mRNAs. Specific *BACE-1*, *APP*, and *rp 49* coding sequence primers were used to amplify the *BACE-1*, *APP*, and *rp 49* cDNAs, as described in the 'MATERIALS and METHODS' section. (**A**) The *elav<GFP* flies were used as control flies to confirm that the effects of acacetin to reduce the APP and BACE-1 levels were not due to its inhibitory activity toward the Gal4 transcription activator.

Acacetin had no significant effects on *GFP* mRNA expression, irrespective of concentration. (**B**) Acacetin significantly reduced the human *APP* mRNA levels. (**C**) Acacetin significantly reduced human *BACE-1* mRNA expression in 20-day-old male flies. The mRNA expression was normalized to the constitutive expression of the mRNA for the housekeeping gene, *rp 49*, and analyzed by the $2^{-\Delta\Delta CT}$ method. Each bar represents the mean ± SE of duplicate samples run in three independent experiments ($^{***}P<0.001$; $^{*}P<0.05$; ns, no significant difference, using Bonferroni's multiple comparison test).

3.2. Acacetin significantly reduces the Aβ levels by interfering with human APP proteolytic processing and BACE-1 expression

A western blot analysis revealed that acacetin suppressed Aβ expression, although the responses varied according to concentration. Aβ (approximately 4 kDa) was not detected in the control *elav-Gal4/+* flies (Fig. 63A). Quantification of the western blots showed that 100, 300, and 500 μM acacetin decreased the Aβ levels to 71, 72, and 47% of the controls, respectively (Fig. 63B). To determine whether the anti-amyloidogenic effect of acacetin was mediated by modulating APP proteolytic processing or BACE-1 expression, the protein levels of BACE-1 and APP were analyzed. A band corresponding to BACE-1 (approximately 70 kDa) was visible in the transgenic flies, but was not detected in the control *elav-Gal4/+* flies. Treatment with 100, 300, and 500 μM acacetin decreased the expression of BACE-1 (Fig. 63C). Quantification of the western blots indicated that the BACE-1 protein levels were considerably decreased to 81, 75, and 74% of the control levels using 100, 300, and 500 μM acacetin, respectively (Fig. 63D). In this experiment, the APP monomer (approximately 100 kDa) and dimer bands (approximately 200 kDa) were confirmed by the western blots, as described previously (Jung *et al*., 2014), and were also visible in the control *elav-Gal4/+* flies, which is consistent with the previous study (Groth *et al*., 2010) (Fig. 63E). Quantification of the western blots indicated that the APP levels were also significantly reduced to 70 and 69% of the control levels by 300 and 500 μM acacetin, respectively, but 100 μM acacetin reduced the APP levels to 86%, which was not significantly different from the control APP levels (Fig. 63F). The effects

of acacetin on the formation of the APP-alpha C-terminal fragment (αCTF) (14 kDa, marked with the green arrow in Fig. 63G) and APP-βCTF (14.5 kDa, marked with the red arrow in Fig. 63G) were also analyzed, because the level of the APP-CTF is useful for understanding how genetic manipulation of APP processing impacts Aβ generation and accumulation. Acacetin inhibited the generation of the APP-CTF by affecting APP cleavage (approximately 80% of the control levels) (Fig. 63H). The AICD fragment has been shown to be involved in a variety of signaling processing, many of which are potentially relevant to AD pathology, and the AICD levels are elevated in human AD brains, as described previously (Branca *et al*., 2014). Accordingly, the effects of acacetin on the AICD levels were also investigated. A single band was detected in both the control *elav-Gal4/+* and transgenic *elav<APP/BACE-1* flies, and acacetin decreased the AICD levels (approximately 7 kDa) in the transgenic flies (Fig. 63G). Quantification of the western blots revealed that the AICD levels were reduced to 68, 27, and 37% of the control levels following treatment with 100, 300, and 500 μM acacetin, respectively (Fig. 63I).

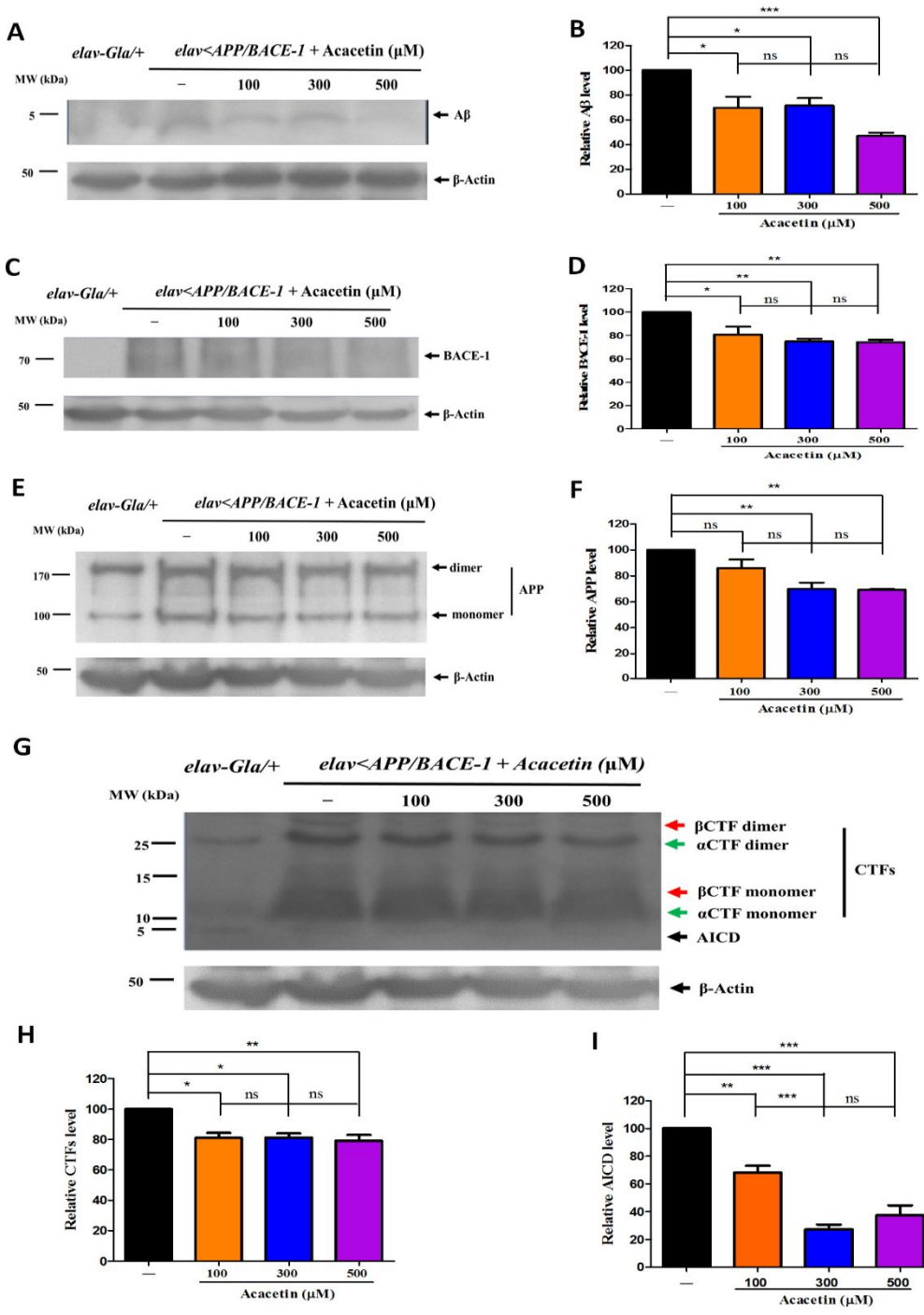
A
elav-Gla/+
elav<APP/BACE-1 + Acacetin (μM)
MW (kDa)
–
100
300
500
5
Aβ
50
β-Actin
B
Relative Aβ level
Acacetin (μM)
C
elav-Gla/+
elav<APP/BACE-1 + Acacetin (μM)
MW (kDa)
70
BACE-1
50
β-Actin
D
Relative BACE-1 level
Acacetin (μM)
E
elav-Gla/+
elav<APP/BACE-1 + Acacetin (μM)
MW (kDa)
170
100
dimer
monomer
APP
50
β-Actin
F
Relative APP level
Acacetin (μM)
G
elav-Gla/+
elav<APP/BACE-1 + Acacetin (μM)
MW (kDa)
25
15
10
5
50
βCTF dimer
αCTF dimer
βCTF monomer
αCTF monomer
AICD
CTFs
β-Actin
H
Relative CTFs level
Acacetin (μM)
I
Relative AICD level
Acacetin (μM)

Fig. 63. Effect of acacetin on Aβ, BACE-1, and APP processing in the transgenic flies. Human APP and BACE-1 transgenic flies (*elav<APP/BACE-1*) were cultured from the egg stage in polystyrene vials containing media supplemented with acacetin (100, 300, and 500 μM) in 0.1% dimethyl sulfoxide. Western blot analyses were performed to determine the levels of the Aβ, BACE-1, APP, APP-CTFs, and AICD proteins, as described in the 'MATERIALS AND METHODS' section. (**A**) Aβ was immunoblotted with an Adβ, 17-24 (4G8) monoclonal antibody, and each lane contained 70 μg of protein. (**B**) The relative amounts of total Aβ were detected by western blotting. (**C**) BACE-1 was probed with an anti-BACE-1 antibody, and each lane contained 30 μg of protein. (**D**) Protein levels of human BACE-1 in the transgenic flies. (**E**) Human APP was detected by western blotting with an anti-APP C-terminal antibody. Each lane contained 30 μg of protein. (**F**) Quantification of the human APP protein levels in the transgenic flies. (**G**) The APP proteolytic processing products βCTF, αCTF, and AICD were detected by western blotting with an anti-APP C-terminal antibody; each lane contained 30 μg of protein. (**H**) The levels of the CTFs resulting from APP processing in the transgenic flies. (**I**) The levels of the AICD fragment resulting from APP processing in the transgenic flies. β-Actin was used as a loading control. The differences in protein expression were quantified using a Molecular Imager Gel Doc XR system and normalized to the actin expression on the same membrane. Each bar represents the mean ± SE of duplicate samples of three independent experiments ($^{***}P<0.001$; $^{**}P<0.01$; $^{*}P<0.05$; ns, no significant difference, using Bonferroni's multiple comparison test).

DISCUSSION

An investigation of the mechanisms of action of naturally occurring anti-AD compounds may provide useful information for the development of selective anti-AD therapeutic alternatives with novel target sites (Caesar *et al*., 2012). The target sites and mechanisms underlying the anti-dementia actions of plant secondary substances have been well documented by Howes and Perry (2011). In the amyloidogenic pathway, APP is cleaved by BACE-1 and releases a large soluble ectodomain of APP and APP-βCTF, which is then further cleaved by γ-secretase to generate toxic Aβ (Cole and Vassar, 2007; Tian *et al*., 2010). The protein levels and enzymatic activity of BACE-1 are elevated in AD brains, suggesting that abnormal BACE-1 regulation may significantly contribute to AD pathogenesis (Chen *et al*., 2009). Utsuki *et al*. (2006) screened 144 analogs of phenserine, a physostigmine analog, to identify small molecules that inhibit APP protein synthesis and the subsequent Aβ production, without possessing potent AChE inhibitory activity, using an enzyme-linked immunosorbent assay. They reported eight analogs, including posiphen, an (–)-enantiomer of phenserine, that were capable of dose-dependently reducing APP and Aβ production without causing cell toxicity. These analogs also inhibited APP synthesis, resulting in a decrease in the number of amyloid plaques (Utsuki *et al*., 2006).

Natural curcumin, catechins, and arctigenin have been suggested possessing the function of AD prevention due to their anti-amyloidogenic, anti-inflammatory, anti-oxidative properties (Kim *et al*., 2010). In particular, curcumin has potential properties for AD prevention in both *in vitro* and *in vivo* (Ringman *et al*., 2005). In *Drosophila* of AD, curcumin has been suggested to reduce neurotoxicity due to promoting amyloid fibril conversion through decreasing the pre-fibrillar/oligomeric

species of Aβ (Caesar *et al*., 2012). NF-κB is believed to play an important role in many chronic disease including AD that can travel into the nuclei and active genes related to inflammation to transcription, and curcumin was reported to suppress NF-κB signaling pathway (Singh and Aggarwal, 1995; Olivera *et al*., 2012). Natural EGCG was reported to reduce Aβ and plaques in Tg2576 AD mice (Rezai-Zadeh *et al*., 2005) and to be able to reduce Aβ levels by inhibition the expression of holo-APP that was consistent with this study (Levites *et al*., 2003). In addition, Lee *et al*. (2009) demonstrated that the compound reduced BACE-1 activity and suppressed the metabolic products of APP via inhibition of ERK and NF-κB pathways in mice. Natural arctigenin was reported to be capable of inhibiting Aβ production by inhibiting BACE-1 expression and accelerate Aβ clearance by promoting autophagy via AKT/mTOR signaling inhibition and AMPK/Raptor pathway activation (Zhu *et al*., 2013). Natural flavonoids, such as myricetin and quercetin, have also been reported to be potent inhibitors of BACE-1 activity and to reduce the Aβ levels in primary cortical neurons (Shimmyo *et al*., 2008). Long-term treatment with the EGb761 *Ginkgo biloba* extract significantly lowered the APP protein levels in a transgenic AD mouse model, suggesting that the potential neuroprotective properties of EGb761 may be, at least in part, related to its APP lowering activity (Augustin *et al*., 2009). In addition, certain flavonoids and their metabolites have been shown to exert beneficial effects on neurological processes through their interaction with neuronal signaling pathways, such as the PI3K/Akt, tyrosine kinase, protein kinase C, and MAPK signing pathways, as well as the NF-κB pathway. Inhibitory or stimulatory effects on these pathways are likely to have a large impact on neuronal function by modulating gene expression (Baptista *et al*., 2014).

In this study, the real-time qRT-PCR analysis revealed that acacetin was able to reduce both the human *APP* and *BACE-1* mRNA levels in a transgenic *Drosophila* AD model, without significantly affecting the *GFP* mRNA levels. This finding suggests that acacetin plays an important role in inhibiting human BACE-1 and APP by regulating gene transcription, and it does not block binding of the transcriptional activator Gal4 to the UAS activation domain. Western blot analysis revealed that acacetin reduced Aβ

production by interfering with BACE-1 activity and APP synthesis, resulting in a decrease in the levels of APP-CTF and AICD. Therefore, the protective effect of acacetin on Aβ production is mediated by transcriptional regulation of the *BACE-1* and *APP* genes, which results in decreased APP levels and BACE-1 activity. Acacetin acts as a direct inhibitor of BACE-1 activity and regulates the expression of both APP and BACE-1. Previous studies (Shimmyo *et al*., 2008; Jung *et al*., 2010) demonstrated that flavonoids exhibited inhibitory activity against BACE-1 in cell-free and cell-based systems. The flavonoids epicatechin and epigallocatechin were reported to be potent inhibitors of APP processing (Cox *et al*., 2015). It has also been reported that the flavonoid icariin possesses the ability to decrease amyloid deposition in a transgenic mouse model by reducing APP and BACE-1 expression (Zhang *et al*., 2014). Acacetin was reported to exert its anti-inflammatory activity by downregulating pro-inflammatory mediators via inhibition of the NF-κB signaling pathways (Kim *et al*., 2012). Furthermore, acacetin enhanced the phosphorylation of p38 mitogen-activated protein kinase (p38 MAPK), which activates the classical Ras/MAPK pathway, to induce neuritogenesis and neuronal differentiation (Nishina *et al*., 2013); therefore, acacetin could be used as a potential therapeutic agent for AD.

In conclusion, the anti-amyloidogenic mechanism of actions of acacetin was realized through the decreased APP and BACE-1 on both protein and mRNA levels. However, the effects of acacetin on the transcriptional and post-transcriptional regulation of APP and BACE-1 and on the factors and signaling pathways involved in genes transcription are needed to be established.

LITERATURE CITED

Adams, M. D., S. E. Celniker, R. A. Holt, C. A. Evans, J. D. Gocayne, *et al.* 2000. The genome sequence of *Drosophila melanogaster*. Science **287,** 2185–2195.

Ali, Y. O., W. Escala, K. Ruan, and R. G. Zhai. 2011. Assaying locomotor, learning, and memory deficits in Drosophila models of neurodegeneration. J. Vis. Exp. **49,** e2504.

Alzheimer's Association. 2014. 2014 Alzheimer's disease facts and figures. Alzheimers Dement. **10,** e47–e92.

Araújo, C. A. C., and L. L. Leon. 2001. Biological Activities of *Curcuma longa* L. Mem. Inst. Oswaldo Cruz. **96,** 723–728.

Augustin, S., G. Rimbach, K. Augustin, R. Schliebs, S. Wolffram, and R. Cermak. 2009. Effect of a short- and long-term treatment with *Ginkgo biloba* extract on amyloid precursor protein levels in a transgenic mouse model relevant to Alzheimer's disease. Arch. Biochem. Biophys. **481,** 177–182.

Bahadorani, S., P. Bahadorani, J. P. Phillips, and A. J. Hilliker. 2008. The effects of vitamin supplementation on Drosophila life span under normoxia and under oxidative stress. J. Gerontol. A Biol. Sci. Med. Sci. **63,** 35–42.

Baptista, F. I., A. G. Henriques, A. M. S. Silva, J. Wiltfang, and O. A. B. da Cruze Silva. 2014. Flavonoids as therapeutic compounds targeting key protein involved in Alzheimer's disease. ACS Chem. Neurosci. **5,** 83–92.

Begum, A. N., M. R. Jones, G. P. Lim, T. Morihara, P. Kim, D. D. Heath, C. L. Rock, M. A. Pruitt, F. Yang, B. Hudspeth, S. Hu, K. F. Faull, B. Teter, G. M. Cole, and S. A. Frautschy. 2008. Curcumin structure-function, bioavailability, and efficacy in models of neuroinflammation and Alzheimer's disease. J. Pharmacol. Exp. Ther. **326,** 196–208.

Binetti, G. 2009. Familial Alzheimer's Disease. Alzheimer Europe. tinyurl.com/lr5ojvy (Accessed: 15th February 2015).

Birks, J. 2006. Cholinesterase inhibitors for Alzheimer's disease (review). Cochrane Database of Systematic Reviews. Art. No.: CD005593. doi:10.1002/14651858.CD005593. Issue **1**.

Bollag, D. M., M. D. Rozycki, and S. J. Edelstein. 1996. Protein Methods; Wiley-Liss Press: New York, US.

Branca, C., I. Sarnico, R. Ruotolo, A. Lanzillotta, A. R. Viscomi, M. Benarese, V. Porrini, L. Lorenzini, L. Calzà, B. P. Imbimbo, S. Ottonello, and M. Pizzi. 2014. Pharmacological targeting of the β-amyloid precursor protein intracellular domain. Sci. Rep. **4,** 4618.

Burns, A., and S. Iliffe. 2009. Alzheimer's disease. BMJ. **338,** b158.

Burock, J., and L. Naqvi. 2014. Practical management of Alzheimer's dementia. R. I. Med .J. 97, 36–40.

Butterfield, D. A., A. Castegna, J. Drake, G. Scapagnini, and V. Calabrese. 2002. Vitamin E and neurodegenerative disorders associated with oxidative stress. Nutr.

Neurosci. **5,** 229–239.

Caesar, I., M. Jonson, K. P. R. Nilsson, S. Thor, and P. Hammarström. 2012. Curcumin promotes A-beta fibrillation and reduces neurotoxicity in transgenic Drosophila. PLoS ONE. **7,** e31424.

Caillé, I., B. Allinquant, E. Dupont, C. Bouillot, A. Langer, U. Muller, and A. Prochiantz. 2004. Soluble form of amyloid precursor protein regulates proliferation of progenitors in the adult subventricular zone. Development **131,** 2173–2181.

Carmine-Simmen, K., T. Proctor, J. Tschape, B. Poeck, T. Triphan, R. Strauss, and D. Kretzschmar. 2009. Neurotoxic effects induced by the Drosophila amyloid-beta peptide suggest a conserved toxic function. Neurobiol. Dis. **33,** 274–281.

Carvalho, G. B., P. Kapahi, and S. Benzer. 2005. Compensatory ingestion upon dietary restriction in Drosophila melanogaster. Nat. Methods. **2,** 813–815.

Castro, D. M., C. Dillon, G. Machnicki, and R. F. Allegr. 2010. The economic cost of Alzheimer's disease. Family or public-health burden? Dement. Neuropsychol. **4,** 262–267.

Chakraborty, R., V. Vepuri, S. D. Mhatre, B. E. Paddock, S. Miller, S. J. Michelson, R. Delvadia, A. Desai, M. Vinokur, D. J. Melicharek, S. Utreja, P. Khandelwal, S. Ansaloni, L. E. Goldstein, R. D. Moir, J. C. Lee, L. P. Tabb, A. J. Saunders, and D. R. Marenda. 2011. Characterization of a Drosophila Alzheimer's disease model: pharmacological rescue of cognitive defects. PLoS ONE. **6,** e20799.

Chen, Y., K. Zhou, R. Wang, Y. Liu, Y. D. Kwak, T. Ma, R. C. Thompson, Y. Zhao, L.

Smith, L. Gasparini, Z. Luo, H. Xu, and F. F. Liao. 2009. Antidiabetic drug metformin (GlucophageR) increases biogenesis of Alzheimer's amyloid peptides via up-regulating BACE1 transcription. Proc. Natl. Acad. Sci. USA. **106,** 3907–3912.

Cheon, M. S., M. Dierssen, S. H. Kim, and G. Lubec. 2008. Protein expression of BACE1, BACE2 and APP in Down syndrome brains. Amino Acids **35,** 339–43.

Choi, C. W., Y. H. Choi, M. R. Cha, Y. S. Kim, G. H. Yon, K. S. Hong, W. K. Park, Y. H. Kim, and S. Y. Ryu. 2011. *In vitro* BACE1 inhibitory activity of resveratrol oligomers from the seed extract of *Paeonia lactiflora*. Planta Med. **77,** 374–376.

Choi, Y. H., G. H. Yon, K. S. Hong, D. S. Yoo, C. W. Choi, W. K. Park, J. Y. Kong, Y. S. Kim, and S. Y. Ryu. 2008. *In vitro* BACE-1 inhibitory phenolic components from the seeds of *Psoralea corylifolia*. Planta Med. **74,** 1405–1408.

Choi, Y. H., M. Y. Yoo, C. W. Choi, M. R. Cha, G. H. Yon, D. Y. Kwon, Y. S. Kim, W. K. Park, and S. Y. Ryu. 2009. A new specific BACE-1 inhibitor from the stembark extract of Vitis vinifera. Planta Med. **75,** 537–540.

Cholbi, M. R., M. Paya, and M. J. Alcaraz. 1991. Inhibitory effects of phenolic compounds on CCl4-induced microsomal lipid peroxidation. Experientia **47,** 195–199.

Çıkrıkçı, S., E. Mozioğlu, and H. Yılmaz. 2008. Biological activity of curcuminoids isolated from *Curcuma longa*. Rec. Nat. Prod. **2,** 19–24.

Citron, M. 2004a. Strategies for disease modification in Alzheimer's disease. Nat. Rev. Neurosci. **5,** 677–685.

Citron, M. 2004b. β-secretase inhibition for the treatment of Alzheimer's disease — promise and challenge. Trends Pharmacol. Sci. **25,** 92-97.

Cleveland, D. W., S. Y. Hwo, and M. W. Kirschner. 1977. Physical and chemical properties of purified tau factor and the role of tau in microtubule assembly. J. Mol. Biol. **116,** 227–247.

Cole, S. L., and R. Vassar. 2007. The Alzheimer's disease β-secretase enzyme, BACE 1. Mol. Neurodegener **2,** 22.

Cox, C. J., F. Choudhry, E. Peacey, M. S. Perkinton, J. C. Richardson, D. R. Howlett, S. F. Lichtenthaler, P. T. Francis, and R. J. Williams. 2015. Dietary (–)-epicatechin as a potent inhibitor of βγ-secretase amyloid precursor protein processing. Neurobiol. Aging **36,** 178–187.

Crowther D. C., K. J. Kinghorn, E. Miranda, R. Page, J. A. Curry, F. A. Duthie, D. C. Gubb, and D. A. Lomas. 2005. Intraneuronal Aβ, non-amyloid aggregates and neurodegeneration in a *Drosophila* model of Alzheimer's disease. Neuroscience **132,** 123–135.

Dam, N. P., T. D. Dung, L. H. Van Long, and N. K. Phi Phung. 2010. Four triterpenoids from *Hedyotis tenelliflora* (Rubiaceae) growing in Vietnam. J. Chem. **48** (4B), 250–254.

Danysz, W., and C. G. Parsons. 2012. Alzheimer's disease, β-amyloid, glutamate, NMDA receptors and memantine – searching for the connections. Br. J. Pharmacol. **167,** 324–352.

de Paula, V. J. R., F. M. Guimarães, B. S. Diniz, and O.V. Forlenza. 2009. Neurobiological pathways to Alzheimer's disease Amyloid-beta, Tau protein or both? Dement. Neuropsychol. **3,** 188–194.

De Strooper, B., R. Vassar, and T. Golde. 2010. The secretases: enzymes with therapeutic potential in Alzheimer disease. Nat. Rev. Neurol. **6,** 99–107.

Deshpande S. A., G. B. Carvalho, A. Amador, A. M. Phillips, S. Hoxha, K. J. Lizotte, and W. W. Ja. 2014. Quantifying *Drosophila* food intake: comparative analysis of current methodology. Nat. Methods **11,** 535–540.

Drubin, D. G., and W. J. Nelson. 1996. Origins of cell polarity. Cell **84,** 335–344.

Duffy, J. B. 2002. GAL4 system in *Drosophila*: a fly geneticist's Swiss army knife. Genesis **34,** 1–15.

Duthey, B. 2013. Background paper 6.11: Alzheimer disease and other dementias. A Public Health Approach to Innovation; Update on 2004 Background Paper. **2013,** 1–74. Available online: http://www.who.int/medicines/areas/priority medicines/BP6 11Alzheimer.pdf (Accessed: 8th March 2014).

Evin, G., G. Lessene, and S. Wilkins. 2011. BACE inhibitors as potential drugs for the treatment of Alzheimer's disease: focus on bioactivity. Recent Pat. CNS Drug Discov. **6,** 91–106.

Evin, G., and Q. X. Li. 2012. Platelets and Alzheimer's disease: potential of APP as a biomarker. World J. Psychiatr. **2,** 102–113.

Fabry, W., P. Okemo, and R. Ansborg. 1996. Activity of East African medicinal plants

against *Helicobacter pylori*. Chemotherapy **42,** 315–317.

Faria, A., M. Meireles, I. Fernandes, C. Santos-Buelga, S. Gonzalez-Manzano, M. Dueñas, V. de Freitas, N. Mateus, and C. Calhau. 2014. Flavonoid metabolites transport across a human BBB model. Food Chem. **149,** 190–196.

Ferri, C., M. Prince, C. Brayne, H. Brodaty, L. Flatiglioni, M. Ganguli, K. Hall, K. Hasegawa, H. Hendrie, Y. Huang, A. Jorm, C. Mathers, P. Menezes, E. Rimmer, and M Scazufca. 2005. Global prevalence of dementia: a Delphi consensus study. Lancet **366,** 2112–2117.

Finder, V. H. 2010. Alzheimer's disease: a general introduction and pathomechanism, J. Alzheimers Dis. **22,** S5–S19.

Finelli, A., A. Kelkar, H. J. Song, H. Yang, and M. Konsolaki. 2004. A model for studying Alzheimer's Abeta42-induced toxicity in Drosophila melanogaster. Mol. Cell Neurosci. **26,** 365–375.

Francis, P. T. A. M. Palmer, M. Snape, and G. K. Wilcock. 1999. The cholinergic hypothesis of Alzheimer's disease: a review of progress. J. Neurol. Neurosurg. Psychiatry **66,** 137–147.

Furukawa, K., B. L. Sopher, R. E. Rydel, J. G. Begley, D. G. Pham, G. M. Martin, M. Fox, and M. P. Mattson. 1996. Increased activity-regulating and neuroprotective efficacy of alpha-secretase-derived secreted amyloid precursor protein conferred by a C-terminal heparin-binding domain. J. Neurochem. **67,** 1882–1896.

Gangwal, A., S. K. Parmar, and N. R. Sheth. 2010. Triterpenoid, flavonoids and sterols

from *Lagenaria siceraria* fruits. Der Pharmacia Lettre **2,** 307–317.

Gao, J., Y. Inagaki, X. Li, N. Kokudo, and W. Tang. 2013. Research progress on natural products from traditional Chinese medicine in treatment of Alzheimer's disease. Drug Discov. Ther. **7,** 46–57.

Ghosh, A. K., S. Gemma, and J. Tang. 2008. beta-Secretase as a therapeutic target for Alzheimer's disease. Neurotherapeutics **5,** 399–408.

Goodson H.V., C. Valetti, and T. E. Kreis. 1997. Motors and membrane traffic. Curr. Opin. Cell Biol. **9,** 18–28.

Greeve, I., D. Kretzschmar, J. A. Tschäpe, A. Beyn, C. Brellinger, M. Schweizer, R. M. Nitsch, and R. Reifegerste. 2004. Age-dependent neurodegeneration and Alzheimer amyloid plaque formation in transgenic Drosophila. J. Neurosci. **24,** 3899–3906.

Groth, C., W. G. Alvord, O. A. Quiñones, and M. E. Fortini. 2010. Pharmacological analysis of *Drosophila melanogaster* γ-secretase with respect to differential proteolysis of Notch and APP. Mol. Pharmacol. **77,** 567–574.

Guzior, N., A. Wieckowska, D. Panek, and B. Malawska. 2015. Recent development of multifunctional agents as potential drug candidates for the treatment of Alzheimer's disease. Curr. Med. Chem. **22,** 373–404.

Haass, C. 2004. Take five—BACE and the gamma-secretase quartet conduct Alzheimer's amyloid beta-peptide generation. EMBO J. **23,** 483–488.

Hardy, J., and D. Allsop. 1991. Amyloid deposition as the central event in the aetiology

of Alzheimer's disease. Trends Pharmacol. Sci. **12,** 383–388.

Hardy, J., and D. J. Selkoe. 2002. The amyloid hypothesis of Alzheimer's disease: progress and problems on the road to therapeutics. Science **297,** 353–356.

Hartman, H., and T. L. Hayes. 1971. Scanning electron microscopy of *Drosophila*. J. Hered. **62,** 41–44.

Herrup, K. 2010. Reimagining Alzheimer's Disease–an age-based hypothesis. J. Neurosci. **30,** 16755–16762.

Hippius, H. 2003. The discovery of Alzheimer's disease. Dialogues Clin. Neurosci. **5,** 101–108.

Hong, L., G. Koelsch, X. Lin, S. Wu, S. Terzyan, A. K. Ghosh, X. C. Zhang, and J. Tang. 2000. Structure of the protease domain of memapsin 2 (beta-secretase) complexed with inhibitor. Science **290,** 150–153.

Hong, Y. K., S. H. Park, S. Lee, S. Hwang, M. J. Lee, D. Kim, J. H. Lee, S. Y. Han, S. T. Kim, Y. K. Kim, S. Jeon, B. S. Koo, and K. S. Cho. 2011. Neuroprotective effect of SuHeXiang Wan in *Drosophila* models of Alzheimer's disease. J. Ethnopharmacol. **134,** 1028–1032.

Hossain, M. A., and Z. Ismail. 2013. Isolation and characterization of triterpenes from the leaves of *Orthosiphon stamineus*. Arabian J. Chem. **6,** 295–298.

Howes, M. J., and E. Perry. 2011. The role of phytochemicals in the treatment and prevention of dementia. Drugs Aging **28,** 439–468.

Iijima, K., H. P. Liu, A. S. Chiang, S. A. Hearn, M. Konsolaki, and Y. Zhong. 2004.

Dissecting the pathological effects of human Abeta40 and Abeta42 in Drosophila: a potential model for Alzheimer's disease. Proc. Natl Acad. Sci. USA **101,** 6623–6628.

Iijima-Ando, K., and K. Iijima. 2010. Transgenic Drosophila models of Alzheimer's disease and tauopathies. Brain Struct. Funct. **214,** 245–262.

Itokawa, H., Q. Shi, T. Akiyama, S. L. Morris-Natschke, and K. H. Lee. 2008. Recent advances in the investigation of curcuminoids. Chinese Med. **3,** 11.

Jäger, A. K., and L. Saaby. 2011. Flavonoids and the CNS. Molecules **16,** 1471–1485.

Jayaprakasha, G. K., L. J. M. Rao, and K. K. Sakariah. 2002. Improved HPLC method for the determination of curcumin, demethoxycurcumin, and bisdemethoxycurcumin. J. Agric. Food Chem. **50,** 3668–3672.

Jeon, S. Y., K. Bae, Y. H. Seong, and K. S. Song. 2003. Green tea catechins as a BACE1 (β-secretase) inhibitor. Bioorg. Med. Chem. Lett. **13,** 3905–3908.

Ji, H., and H. Zhang. 2008. Multipotent natural agents to combat Alzheimer's disease. Functional spectrum and structural features. Acta Pharmacol. Sin. **29,** 143–151.

John, V. 2006. Human beta-secretase (BACE) and BACE inhibitors: progress report. Curr. Top. Med. Chem. **6,** 569–578.

John, V., J. P. Beck, M. J. Bienkowski, S. Sinha, and R. L. Heinrikson. 2003. Human β-secretase (BACE) and BACE inhibitors. J. Med. Chem. **46,** 4625–4630.

Jung, H. A., B. S. Min, T. Yokozawa, J. H. Lee, Y. S. Kim, and J. S. Choi. 2009a. Anti-Alzheimer and antioxidant activities of Coptidis Rhizoma alkaloids. Biol. Pharm. Bull. **32,** 1433–1438.

Jung, H. A., E. J. Lee, J. S. Kim, S. S. Kang, J. H. Lee, B. S. Min, and J. S. Choi. 2009b. Cholinesterase and BACE1 inhibitory diterpenoids from *Aralia cordata*. Arch. Pharm. Res. **32,** 1399–1408.

Jung, H. A., T. Yokozawa, B. W. Kim, J. H. Jung, and J. S. Choi. 2010. Selective inhibition of prenylated flavonoids from *Sophora flavescens* against BACE1 and cholinesterases. AM. J. Chin. Med. **38,** 415–429.

Jung, J. I., S. Premraj, P. E. Cruz, T. B. Ladd, Y. Kwak, E. H. Koo, K. M. Felsenstein, T. E. Golde, and Y Ran. 2014. Independent relationship between amyloid precursor protein (APP) dimerization and γ-secretase processivity. PLoS ONE **9,** e111553.

Kalaria, R., G. E. Maestre, R. Arizaga, R. P. Friedland, D. Galasko, K. Hall, J. A. Luchsinger, A. Ogunniyi, E. K. Perry, F. Potocnik, M. Prince, R. Stewart, A. Wimo, Z. X. Zhang, and P. Antuono. 2008. Alzheimer's disease and vascular dementia in developing countries: prevalence, management, and risk factors. Lancet Neurol. **7,** 812–826.

Kandalepas, P. C, K. R. Sadleir, W. A. Eimer, J. Zhao, D. A. Nicholson, and R. Vassar. 2013. The Alzheimer's beta-secretase BACE1 localizes to normal presynaptic terminals and to dystrophic presynaptic terminals surrounding amyloid plaques. Acta Neuropathol. **126,** 329–352

Karran, E., M. Mercken, and B. De Strooper. 2011. The amyloid cascade hypothesis for Alzheimer's disease: an appraisal for the development of therapeutics. Nat. Rev. Drug Discov. **10,** 698–712.

Kim, H. G., M. S. Ju, S. K. Ha, H. Lee, H. Lee, S. Y. Kim, and M. S. Oh. 2012. Acacetin protects dopaminergic cells against 1-methyl-4-phenyl-1,2,3,6-tetrahydropyridine-induced neuroinflammation *in vitro* and *in vivo*. Biol. Pharm. Bull. **35,** 1287–1294.

Kim, J., H. J. Lee, and K. W. Lee. 2010. Naturally occurring phytochemicals for the prevention of Alzheimer's disease. J. Neurochem. **112,** 1415–1430.

Kim, N. Y., D. S. Park., and H. Y. Lee. 2015. Effect of anti-skin wrinkle and antioxidant of *Agastache rugosa* Kentz through fermentation process of the lactic acid. Korean J. Med. Crop Sci. **23,** 37–42.

Kolarova, M., F. García-Sierra, A. Bartos, J. Ricny, and D. Ripova. 2012. Structure and pathology of tau protein in Alzheimer disease. Int. J. Alzheimers Dis. **2012,** Article ID 731526.

Kramer, J. M., and B. E. Staveley. 2003. GAL4 causes developmental defects and apoptosis when expressed in the developing eye of *Drosophila melanogaster*. Genet. Mol. Res. **2,** 43–47.

Kuhn, M. A., and D. Winston. 2001. Herbal Therapy and Supplements: A Scientific & Traditional Approach, pp. 330–335. Lippincott Williams & Wilkins Press, New York.

Kwak. Y. D., R. Wang, J. J. Li, Y. W. Zhang, H. Xu, and F. F. Liao. 2011. Differential regulation of BACE1 expression by oxidative and nitrosative signals. Mol. Neurodegener. **6,** 17.

Lee, K. S., B. S. Lee, S. Semnari, A. Avanesian, C. Y. Um, H. J. Jeon, K. M. Seong, K.

Yu, K. J. Min, and M. Jafari. 2010. Curcumin extends life span, improves health span, and modulates the expression of age-associated aging genes in Drosophila melanogaster. Rejuvenation Res. **13,** 561–570.

Lemaitre, B., M. Meister, S. Govind, P. Georgel, R. Steward, J. M. Reichhart, and J. A. Hoffmann. 1995. Functional analysis and regulation of nuclear import of dorsal during the immune response in *Drosophila*. EMBO J. **14,** 536–545.

Levites, Y., T. Amit, S. Mandel, and M. B. Youdim. 2003. Neuroprotection and neurorescue against Abeta toxicity and PKC-dependent release of nonamyloidogenic soluble precursor protein by green tea polyphenol (-)-epigallocatechin-3-gallate. FASEB J. **17,** 952–974.

Li, H., B. Wang, Z. Wang, Q. Guo, K. Tabuchi, R. E. Hammer, T. C. Sudhof, and H. Zheng. 2010. Soluble amyloid precursor protein (APP) regulates transthyretin and Klotho gene expression without rescuing the essential function of APP. Proc. Natl. Acad. Sci. USA. **107,** 17362–17367.

Lim, G. P, T. Chu, F. Yang, W. Beech, S. A. Frautschy, and G. M. Cole. 2001. The curry spice curcumin reduces oxidative damage and amyloid pathology in an Alzheimer transgenic mouse. J. Neurosci. **21,** 8370–8377.

Lin, T. Y., W. J. Huang, C. C. Wu, C. W. Lu, and S. J. Wang. 2014. Acacetin inhibits glutamate release and prevents kainic acid-induced neurotoxicity in rats. PLoS ONE. **9,** e88644.

Liu, H., Z. Li, D. Qiu, Q. Gu, Q. Lei, and L. Mao. 2010. The inhibitory effects of different curcuminoids on β-amyloid protein, β-amyloid precursor protein and β-site

amyloid precursor protein cleaving enzyme 1 in swap HEK293 cells. Nuerosci. Lett. **485,** 83–88.

Liu, Y., Y. W. Zhang, X. Wang, H. Zhang, X. You, F. F. Liao, and H. Xu. 2009. Intracellular trafficking of presenilin 1 is regulated by beta-amyloid precursor protein and phospholipase D1. J. Biol. Chem. **284,** 12145–12152.

Luo, L., T. Tully, and K. White. 1992. Human amyloid precursor protein ameliorates behavioral deficit of flies deleted for Appl gene. Neuron **9,** 595–605.

Lv, L., Q. Y. Yang, Y. Zhao, C. S. Yao, Y. Sun, E. J. Yang, K. S. Song, I. Mook-Jung, and W. S. Fang. 2008. BACE1 (beta-secretase) inhibitory chromone glycosides from *Aloe vera* and *Aloe nobilis*. Planta Med. **74,** 540–545.

Mahoney, M. B., C. M. Singh, L. T. Diggins, D. Keefe, E. Lund, P. O'Neil, E. Sigel, J. Symonds, A. Villaluz, M. K. Ahlijanian., and M. G. Palfreyman. 2009. Compound screening in a *Drosophila melanogaster* Alzheimer's disease model using a behavioral readout. Alzheimer. Dement. **5,** e11–e12.

Mancini, F., A. De Simone, and V. Andrisano. 2011. Bata-secretase as a target for Alzheimer's disease drug discovery: an overview of *in vitro* methods for characterization of inhibitors. Anal. Bioanal. Chem. **400,** 1979–1996.

Marques, F., J. C. Sousa, N. Sousa, and J. A. Palha. 2013. Blood–brain-barriers in aging and in Alzheimer's disease. Mol. Neurodegener. **8,** 38.

Marumoto, S., and M. Miyazawa. 2010. beta-secretase inhibitory effects of furanocoumarins from the root of *Angelica dahurica*. Phytother. Res. **24,** 510–513.

McGeer, E. G., and P. L. McGeer. 1998. The importance of inflammatory mechanisms in Alzheimer disease. Exp. Gerontol. **33,** 371–378.

Mhatre, S. D., B. E. Paddock, A. J. Saunders, and D. R. Marenda. 2013. Invertebrate models of Alzheimer's disease. J. Alzheimers Dis. **1,** 3–16.

Min, K. J., and M. Tatar. 2006. *Drosophila* diet restriction in practice: do flies consume fewer nutrients? Mech. Ageing Dev. **127,** 93–96.

Mishra, S., and K. Palanivelu. 2008. The effect of curcumin (turmeric) on Alzheimer's disease: An overview. Ann. Indian. Acad. Neurol. **11,** 13–19.

Miyazawa, M., and M. Hisama. 2003. Antimutagenic activity of flavonoids from *Chrysanthemum morifolium*. Biosci. Biotechnol. Biochem. **67,** 2091–2099.

Mohandas, E., V. Rajmohan, and B. Raghunath. 2009. Neurobiology of Alzheimer's disease. Indian J. Psychiatry **51,** 56–61.

Molinuevo, J. L., A. Lladó, and L. Rami. 2005. Memantine: targeting glutamate excitotoxicity in Alzheimer's disease and other dementias. Am. J. Alzheimers Dis. Other. Demen. **20,** 77–85.

Morgan, T. H. 1910. Sex limited inheritance in *Drosophila*. Science **32,** 120–122.

Mukherjee, P. K., V. Kumar, M. Mal, and P. J. Houghton. 2007. Acetylcholinesterase inhibitors from plants. Phytomedicine **14,** 289–300.

Ng, C. F., C. H. Ko, C. M. Koon, J. W. Xian, P. C. Leung, K. P. Fung, H. Y. E. Chan, and C. B. Lau. 2013. The Aqueous Extract of Rhizome of *Gastrodia elata* Protected Drosophila and PC12 Cells against Beta-Amyloid-Induced Neurotoxicity.

Evidence-Based Complementary and Alternative Medicine. **2013,** Article ID 516741.

Nikolaev, A., T. McLaughlin, D. D. O'Leary, and M. Tessier-Lavigne. 2009. APP binds DR6 to trigger axon pruning and neuron death via distinct caspases. Nature **457,** 981–989.

Nishina, A., H. Kimura, H. Tsukagoshi, K. Kozawa, M. Koketsu, M. Ninomiya, and S. Furukawa. 2013. Neurite outgrowth in PC12 cells stimulated by components from *Dendranthema* × *grandiflorum* cv. "Mottenohoka" is enhanced by suppressing phosphorylation of p38MAPK. Evid. Based Complement Alternat. Med. **2013,** 403503.

Olivera, A., T. W. Moore, F. Hu, A. P. Brown, A. Sun, D. C. Liotta, J. P. Snyder, Y. Yoon, H. Shim, A. I. Marcus, A. H. Miller, and T. W. W. Pacea. 2012. Inhibition of the NF-κB signaling pathway by the curcumin analog, 3,5-Bis(2-pyridinylmethylidene)-4-piperidone (EF31): anti-inflammatory and anti-cancer properties. Int. Immunopharmacol. **12,** 368–377.

Orhan, I. E. 2012. Current concepts on selected plant secondary metabolites with promising inhibitory effects against enzymes linked to Alzheimer's disease. Curr. Med. Chem. **19,** 2252–2261.

Pan, M. H., C. S. Lai, Y. J. Wang, and C. T. Ho. 2006. Acacetin suppressed LPS-induced up-expression of iNOS and COX-2 in murine macrophages and TPA-induced tumor promotion in mice. Biochem. Pharmacol. **72,** 1293–1303.

Pandey, U. B., and C. D. Nichols. 2011. Human disease models in *Drosophila melanogaster* and the role of the fly in therapeutic drug discovery. Pharmacol. Rev. **63,**

411–436.

Paris, D., V. Mathura, G. Ait-Ghezala, D. Beaulieu-Abdelahad, N. Patel, C. Bachmeier, and M. Mullan. 2011. Flavonoids lower Alzheimer's Aβ production via an NFκB dependent mechanism. Bioinformation **6,** 229–236.

Park, J. H., J. W. Jung, Y. J. Ahn, and H. W. Kwon. 2012. Neuroprotective properties of phytochemicals against paraquat-induced oxidative stress and neurotoxicity in *Drosophila melanogaster*. Pestic. Biochem. Physiol. **104,** 118–125.

Park, Y. T., J.Y. Jeong, M. J. Lee, K. I. Kim, T. H. Kim, Y. D. Kwon, C. Lee, O. J. Kim, and H. J. An. 2013. MicroRNAs overexpressed in ovarian ALDH1-positive cells are associated with chemoresistance. J. Ovarian Res. **6,** 18.

Parsons, C. G., W. Danysz, A. Dekundy, and I. Pulte. 2013. Memantine and cholinesterase inhibitors: complementary mechanisms in the treatment of Alzheimer's disease. Neurotox. Res. **24,** 358–369.

Patel, S., L. Vuillard, A. Cleasby, C. W. Murray, and J. Yon. 2004. Apo and inhibitor complex structures of BACE (beta-secretase). J. Mol. Biol. **343,** 407–416.

Periz, G., and M. E. Fortini. 2004. Functional reconstitution of gamma-secretase through coordinated expression of presenilin, nicastrin, Aph-1, and Pen-2. J. Neurosci. Res. **77,** 309–322.

Perumalsamy, H., J. R. Kim, S. M. Oh, J. W. Jung, Y. J. Ahn, and H. W. Kwon. 2013. Novel histopathological and molecular effects of natural compound pellitorine on larval midgut epithelium and anal gills of *Aedes aegypti*. PLoS ONE. **8,** e80226.

Phelps, C. B., and A. H. Brand. 1998. Ectopic gene expression in *Drosophila* using GAL4 system. Methods **14,** 367–379.

Pirooznia S. K., J. Sarthi, A. A. Johnson, M. S. Toth, K. Chiu, S. Koduri, and F. Elefant. 2012. Tip60 HAT activity mediates APP induced lethality and apoptotic cell death in the CNS of a *Drosophila* Alzheimer's disease model. PLoS ONE **7,** e41776.

Prince, M., J. Jackson., and Alzheimer's Disease International. 2009. World Alzheimer Report 2009. Available at https://www.alz.co.uk/research/files/WorldAlzheimerReport.pdf (Accessed: 20th February 2015).

Probst, G., and Y. Z. Xu. 2012. Small-molecule BACE1 inhibitors: a patent literature review (2006–2011). Expert. Opin. Ther. Pat. **22,** 511–540.

Prüßing, K., A. Voigt, and J. B. Schulz. 2013. *Drosophila melanogaster* as a model organism for Alzheimer's disease. Mol. Neurodegener. **8,** 35.

Qiu, C., M. Kivipelto, and E. von Strauss. 2009. Epidemiology of Alzheimer's disease: occurrence, determinants, and strategies toward intervention. Dialogues Clin. Neurosci. **11,** 111–128.

Raskin, I., D. M. Ribnicky, S. Komarnytsky, N. Ilic, A. Poulev, N. Borisjuk, A. Brinker, D. A. Moreno, C. Ripoll, N. Yakoby, J. M. O'Neal, T. Cornwell, I. Pastor, and B. Fridlender. 2002. Plants and human health in the twenty-first century. Trends Biotechnol. **20,** 522–531.

Rates, S. M. K. 2001. Plants as source of drugs. Toxicon **39,** 603–613.

Reitz1, C. 2012. Alzheimer's disease and the amyloid cascade hypothesis: a critical

review. Int. J. Alzheimers Dis. **2012** (2012), Article ID 369808.

Ren, C., S. E. Finkel, and J. Tower. 2009. Conditional inhibition of autophagy genes in adult *Drosophila* impairs immunity without compromising longevity. Exp. Gerontol. **44,** 228–235.

Rezai-Zadeh, K., D, Shytle, N, Sun, T, Mori, H, Hou, D, Jeanniton, J. Ehrhart, K. Townsend, J. Zeng, D. Morgan, J. Hardy, T. Town, and J. Tan. 2005. Green tea epigallocatechin-3-gallate (EGCG) modulates amyloid precursor protein cleavage and reduces cerebral amyloidosis in Alzheimer transgenic mice. J. Neurosci. **25,** 8807–8814.

Ringman, J. M., S. A. Frautschy, E. Teng, A. N. Begum, J. Bardens, M. Beigi, K. H. Gylys, V. Badmaev, D. D. Heath, L. G. Apostolova, V. Porter, Z.a Vanek, G. A. Marshall, G. Hellemann, C. Sugar, D. L. Masterman, T. J. Montine, J. L. Cummings and G. M. Cole. 2012. Oral curcumin for Alzheimer's disease: tolerability and efficacy in a 24-week randomized, double blind, placebo-controlled study. Alzheimers Res. Ther. **4,** 43.

Ringman, J. M., S. A. Frautschy, G. M. Cole, D. L. Masterman, and J. L. Cummings. 2005. A potential role of the curry spice curcumin in Alzheimer's disease. Curr. Alzheimer Res. **200,** 131–136.

Rizzi, L., I. Rosset and M. Roriz-Cruz. 2014. Global epidemiology of dementia: Alzheimer's and vascular types. BioMed Res. Int. **2014,** Article ID 908915.

Sasaki, H., K. Miki, K. Kinoshita, K. Koyama, L. D. Juliawaty, S. A. Achmad, E. H. Hakim, M. Kaneda, and K Takahashi. 2010. β-Secretase (BACE-1) inhibitory

effect of biflavonoids. Bioorg. Med. Chem. Lett. **20,** 4558–4560.

Sarantseva, S., S. Timoshenko, O. Bolshakova, E. Karaseva, D. Rodin, A. L. Schwarzman, and M. P. Vitek. 2009. Apolipoprotein E-Mimetics Inhibit Neurodegeneration and Restore Cognitive Functions in a Transgenic Drosophila Model of Alzheimer's Disease. PLoS One. **4,** e8191.

Scarmeas, N., Y. Stern, R. Mayeux, J.J. Manly, N. Schupf, and J. A. Luchsinger. 2009. Mediterranean diet and mild cognitive impairment. Arch. Neurol. **66,** 216–225.

Schneider, L. S. 2013. Alzheimer disease pharmacologic treatment and treatment research. Continuum (Minneap Minn). **19** (2 Dementia), 339–357.

Selkoe, D. J. 1991. The molecular pathology of Alzheimer's disease. Neuron **6,** 403–409.

Shen, K. H., S. H. Hung, L. T. Yin, C. S. Huang, C. H. Chao, C. L. Liu, and Y. W. Shih. 2010. Acacetin, a flavonoid, inhibits the invasion and migration of human prostate cancer DU145 cells via inactivation of the p38 MAPK signaling pathway. Mol. Cell. Biochem. **333,** 279–291.

Shimizu, H., A. Tosaki, K. Kaneko, T. Hisano, T. Sakurai, and N. Nukina. 2008. Crystal structure of an active form of BACE1, an enzyme responsible for amyloid beta protein production. Mol. Cell Biol. **28,** 3663–3671.

Shimmyo, Y., T. Kihara, A. Akaike, T. Niidome, and H. Sugimoto. 2008. Flavonols and flavones as BACE-1 inhibitors: structure-activity relationship in cell-free, cell-based and in silico studies reveal novel pharmacophore features. Biochim. Biophys. Acta. **1780,** 819–825.

Silbert, L. C. 2007. Does statin use decrease the amount of Alzheimer disease pathology in the brain? Neurology.**69,** E8–11.

Silvestri, R. 2009. Boom in the development of non-peptidic beta-secretase (BACE1) inhibitors for the treatment of Alzheimer's disease. Med. Res. Rev. **29,** 295–338.

Singh, S., and B. B. Aggarwal. 1995. Activation of transcription factor NF-kappa B is suppressed by curcumin (diferuloylmethane) [corrected]. J. Biol. Chem. **270,** 24995–25000.

Stachel, S. J., C. A. Coburn, T. G. Steele, K. G. Jones, E. F. Loutzenhiser, and A. R. Gregro. 2004. Structure-based design of potent and selective cell-permeable inhibitors of human β-secretase (BACE-1). J. Med. Chem. **47,** 6447–6450.

Sun, X, Y. Wang, H. Qing, M. A. Christensen, Y. Liu, W. Zhou, Y. Tong, C. Xiao, Y. Huang, S. Zhang, X. Liu, and W. Song. 2005. Distinct transcriptional regulation and function of the human BACE2 and BACE1 genes. FASEB J. **19,** 739–49.

Tamura, T., M. Sone, T. Iwatsubo, K. Tagawa, E. E. Wanker, and H. Okazawa. 2011. Ku70 alleviates neurodegeneration in *Drosophila* models of Huntington's disease. PLoS ONE **6,** e27408.

Tanaka, J. C. A., G. J. Vidotti, and C. C. da Silva. 2003. A new tormentic acid derivative from *Luehea divaricata* Mart. (Tiliaceae). J. Braz. Chem. Soc. **14,** 475–478.

Tang, E., and G. Eisenbrand. 1992. Chinese Drugs of Plant Origin, pp. 613–619. Springer-Verlag Press, New York.

Terry, A.V Jr, and J. J. Buccafusco. 2003. The cholinergic hypothesis of age and Alzheimer's disease-related cognitive deficits: recent challenges and their implications for novel drug development. J. Pharmacol. Exp. Ther. **306,** 821–827.

Thompson, L. A., J. J. Bronson, and F. C. Zusi. 2005. Progress in the discovery of BACE inhibitors. Curr. Pharm. Des. **11,** 3383–3404.

Thompson, S., K. L. Lanctôt, and N. Herrmann. 2004. The benefits and risks associated with cholinesterase inhibitor therapy in Alzheimer's disease. Expert Opin. Drug Saf. **3,** 425–440.

Tian, Y., B. Bassit, D. Chau, and Y. M. Li. 2010. An APP inhibitory domain containing the Flemish mutation residue modulates γ-secretase activity for Aβ production. Nat. Struct. Mol. Biol. **17,** 151–158.

Utsuki, T., Q. S. Yu, D. Davidson, D. Chen, H. W. Holloway, A. Brossi, K. Sambamurti, D. K. Lahiri, N. H. Greig, and T. Giordano. 2006. Identification of novel small molecule inhibitors of amyloid precursor protein synthesis as a route to lower Alzheimer's disease amyloid-beta peptide. J. Pharmacol. Exp. Ther. **318,** 855–862.

Vassar, R. 2014. BACE1 inhibitor drugs in clinical trials for Alzheimer's disease. Alzheimers Res. Ther. **6,** 89.

Viña, J. and A. Lloret. 2010. Why women have more Alzheimer's disease than men: gender and mitochondrial toxicity of amyloid-beta peptide. J. Alzheimers Dis. **2,** S527–S533.

Wang, X., J. R. Kim, S. B. Lee, Y. J. Kim, M. Y. Jung, H. W. Kwon, and Y. J. Ahn. 2014. Effects of curcuminoids identified in rhizomes of Curcuma longa on BACE-1 inhibitory and behavioral activity and lifespan of Alzheimer's disease Drosophila models. BMC Complement. Altern. Med. **14,** 88. doi: 10.1186/1472-6882-14-88.

Wang, X., H. Perumalsamy, H. W. Kwon, Y. E. Na, and Y. J. Ahn. 2015. Effects and possible mechanisms of action of acacetin on the behavior and eye morphology of Drosophila models of Alzheimer's disease. Sci. Rep. **5,** 16127. doi: 10.1038/srep16127.

Wawer, I., and A. Zielinska. 2001. ^{13}C CP/MAS NMR studies of flavonoids. Magn. Reson. Chem. **39,** 374–380.

Wimo, A., L. Jonsson, J. Bond, M. Prince, and B. Winblad. 2013. The worldwide economic impact of dementia 2010. Alzheimers Dement. **9,** 1–11.

Wimo, A., M. Prince, and Alzheimer's Disease International. 2010. World Alzheimer Report. 2010: The global economic impact of dementia. Available at http://www.alz.org/documents/national/world_alzheimer_report_2010.pdf (Accessed: 25th February 2015).

World Health Organization. 2015. Dementia Fact sheet Nº362. Available at http://www.who.int/mediacentre/factsheets/fs362/en/ (Accessed: 5th March 2015).

Yagi, Y., S. Tomita, M. Nakamura, and T. Suzuki. 2000. Overexpression of human amyloid precursor protein in *Drosophila*. Mol. Cell Biol. Res. Commun. **4,** 43–49.

Yankner, B. A., L. R. Dawes, S. Fisher, L. Villa-Komaroff, M. L. Oster-Granite, and R. L. Neve. 1989. Neurotoxicity of a fragment of the amyloid precursor associated with Alzheimer's disease. Science **245,** 417–420.

Youn, K., and M. Jun. 2012. Inhibitory effects of key compounds isolated from *Corni fructus* on BACE1 activity. Phytother. Res. **26,** 1714–1718.

Youn, K., and M. Jun. 2013. *In vitro* BACE1 inhibitory activity of geraniin and corilagin from *Geranium thunbergii*. Planta Med. **79,** 1038–1042.

Zhang C. 2012. Natural compounds that modulate BACE1-processing of amyloid-beta precursor protein in Alzheimer's disease. Discov. Med. **14,** 189–197.

Zhang, H., Q. Ma, Y.W. Zhang, and H. Xu. 2012. Proteolytic processing of Alzheimer's β-amyloid precursor protein. J. Neurochem. **1,** 9–21.

Zhang, L., C. Shen, J. Chu, R. Zhang, Y. Li, and L. Li. 2014. Icariin decreases the expression of APP and BACE-1 and reduces the β-amyloid burden in an APP transgenic mouse model of Alzheimer's disease. Int. J. Biol. Sci. **10,** 181–191.

Zhang, Y. W., R. Thompson, H. Zhang, and H. Xu. 2011. APP processing in Alzheimer's disease. Mol. Brain **4,** 3.

Zheng, H., C. Quan, C. Y. Hyeon, S. C. Kang, D. U. Lee, O. P. Zee, and J. H. Kwak. 2013. Terpenes and phenolic compounds from *Agastache rugosa* and their inhibitory effect on the release of β-hexosaminidase in RBL-2H3 cells. Planta Med. **79**–PN93.

Zhu, Z., J. Yan, W. Jiang, X. G. Yao, J. Chen, L. Chen, C. Li, L. Hu, H. Jiang, and X. Shen. 2013. Arctigenin effectively ameliorates memory impairment in Alzheimer's

disease model mice targeting both β-amyloid production and clearance. J. Neurosci. **33,** 13138–13149.

Zielińska, S., and A. Matkowski. 2014. Phytochemistry and bioactivity of aromatic and medicinal plants from the genus *Agastache* (Lamiaceae). Phytochem. Rev. **13,** 391–416.

CONCLUSIONS

The U.S. FDA has approved two types of medication for AD treatment. They are AChE inhibitors including donepezil (Aricept), galantamine (Razadyne), rivastigmine (Exelon), and tacrine (Cognex) and NMDA receptor antagonist memantine (Namenda) (Parsons *et al*., 2013). Tacrine, the first AChE inhibitor approved in 1993, is rarely used because of the associated side effects, such as nausea, vomiting and possible liver damage (Schneider, 2013). However, these medications for AD cannot cure or stop the progressing of AD and may take a role in lessen or stabilize symptoms of AD. Therefore, much attention has been focused on BACE-1, a crucial enzyme responsible for amyloid plaque formation. Natural products, particularly traditional Chinese medicine, have been used to isolate and identify BACE-1 inhibitors with good pharmacological characteristics. In this study, BACE-1 inhibitory curcuminoids CCN, DMCCN, and BDMCCN from *C. longa* (IC_{50}, 340, 217, and 17 μM) and acacetin, oleanolic acid, and maslinic acid from *A. rugosa* (IC_{50}, 88, 355, and 488 μM) were identified. Although the isolated compounds were less potent in inhibiting BACE-1 than the human BACE-1 inhibitor IV, they may have better pharmacological characteristics, such as small molecular weight and better plasma membrane permeability through BBB than peptide-based inhibitors.

Gal4-UAS system was used widely for target genes expression in *Drosophila* specific tissue (Duffy, 2002). Based on this, the *Drosophila* models of AD were constructed. The *elav-Gal4* and *GMR-Gal4* drove co-expression of target genes human *APP* and *BACE-1* in *Drosophila* nervous system and photoreceptor compound eyes, respectively. The isolated compounds CCN, BDMCCN, and acacetin showed neuroprotective effects on

human APP and BACE-1 co-expression induced climbing defects, abnormal phenotypes of compound eyes, and reduced median life time of *Drosophila*. It has been reported that CCN could decrease elimination pre-fibrillar/oligomeric species of Aβ, reduce levels of Aβ in *Drosophila* or mice models of AD (Lim *et al*., 2001; Begum *et al*., 2008; Caesar *et al*., 2012). However, clinical or biochemical evidence of efficacy of AD was not observed when CCN was orally taken by AD patients (Ringman *et al*., 2012). That may be due to the differences of metabolism of CCN in rodent, *Drosophila*, and human or bioavailability of CCN. In this study, the possible mechanisms of action of acacetin in *Drosophila* models of AD were demonstrated. It can reduce Aβ production mediated by transcription regulation of *BACE-1* and *APP* genes, interfering with BACE-1 activity and APP processing. Nishina *et al*. (2013) reported that acacetin can induce neuritogenesis and neuronal differentiation by enhancing the phosphorylation of p38 MAPK that can active the classical Ras/MAPK pathway. However, animal models should be taken into consideration for anti-AD mechanism of action of acacetin. Further study is also need on the bioavailability and effects of acaetin on neuroprotective signaling pathway.

AD is a complex and progressive neurodegenerative disorder, development of multifunctional agents as potential drug candidates for AD treatment is emerging (Guzior *et al*., 2015). For practical use of *C. longa* rhizome- and whole *A. rugosa* plant-derived materials as novel potential anti-AD agents to processed, further more research is need to establish their human safety and improve their pharmacological characteristics.